Solvation Dynamics of Concentrated Aqueous Polymer Mixtures: A Two Dimensional Infrared Spectroscopy Study

by

Kimberly Rose Daley

A dissertation submitted in partial fulfillment
of the requirements for the degree of
Doctor of Philosophy
(Chemistry)
in the University of Michigan
2018

Doctoral Committee:

Professor Kevin Kubarych, Chair
Associate Professor Julie Biteen
Associate Professor Vanessa Sih
Assistant Professor Dominika Zgid

Kimberly R. Daley
krdaley@umich.edu
ORCID iD: 0000-0002-7818-3113

Dedication

To my family (Mom, Dad, Katie, and Rachel)

Acknowledgements

There are so many people, experiences, and events to acknowledge that have helped me get to where I am and to complete this dissertation. First, I would like to acknowledge **Kevin Kubarych** for allowing me to join his research group. Thank you to my committee (**Julie Biteen, Dominika Zgid, and Vanessa Sih**) for your guidance and support over the years. Thank you to my parents Cyndi and Patrick Daley for birthing me and raising me in a very loving and encouraging household. Both of you have taught me love, patience, strength, and survival. You both also cared a great deal about my education and provided a great one. Thank you to my sisters **Katie and Rachel Daley** for being my first mentees and teaching me how to listen, support, and show love even during frustrating times, and **Boss and Ji Woon.** Thank you to **Aunt Debbie, Uncle Rich, Alexis, Kayla, and Sammy** for supporting and showing me love whenever I come back to Cleveland. Thank you to **Uncle David, Uncle Harold, Aunt Sue, Uncle Don, and Grandma Daley** for finding interest and caring about my education. I want to thank my very encouraging teachers from St. Leo the Great and Trinity High School. You all help contribute to who I am today and taught very important skills, even outside of school. I want to acknowledge in particular **Mr. Lit, Mrs. Whener, Ms. Barile, Mr. Gorby, Mr. Tenney**. Acknowledgement of my longest friendship with **Alex Notoro**. We have known each other for over 20 years, and we still have a loving and wonderful friendship. Thank you for all of the wonderful experiences we have shared together. You are great <3 I want to acknowledge my research, educational, international, and social justice experiences from college that helped mold the path that led me to where I am now. In particular I want to acknowledge **Dr. Aitken, Dr. Madura, Dr. Evanseck, L.J. DiMaggio, Matt Walsh, and Kate Lecci.** Also to my college friends for all of your support: **Jared Romeo, Matt Orlowski, John Stepansky, Colin**

Schmucker, Ralph McFerson, Rachael Ross, Corey Bisbal, Michael Jarrett, and Rachel Van Campenhout. A very special shout out to my college roommate **Elizabeth Day** for introducing me to LOTR and other (gay) media, sharing our mutual love of Harry Potter, and helping me get through college science classes. Thank you for your consistent encouragement and amazing friendship. Thank you to my Fair Food family. I have learned SO much from you all, and there is just so much love in my relationships with you all. **Natali Rodriguez, Yaissy Solis, Angel Morales, Sarita Ahmed, Joe Deras, Amanda Ferguson, Ben Wibking, and Anna Hankins. Jessica Bray and Micka Peck** are friends I met while studying abroad when I was 19, and we still remain in supportive contact. Jessica, you have been an amazing support and I love and appreciate your perspective. Micka, thank you for sharing with me your experiences with science <3

All of the people I met and experiences I had while in grad school truly transformed me. I have learned SO MANY THINGS it is UNBELIEVABLE. I would not be finishing this dissertation without the patience and support of Kevin. Kevin supported me and provided a really great work environment the past 6 years. Through a variety of mental health, physical health, and personal struggles, Kevin gave me the space to make sure I was still a healthy and a well rounded human while in grad school. He at one point met with me multiple times a week so he could help me learn quantum chemistry. I would like to acknowledge past (**John King, Aaron White, Evan Arthur, Laura Kiefer, Derek Osborne, Josef Dunbar, Peter Eckert) and present (Ved Roy, Lindsay Michocki, Joe Meadows, Rong Duan**) lab mates. Laura was an amazing mentor and I learned so much from her. I want to acknowledge the amazing experiences I had traveling to various conferences while in graduate school. I was able to attend conferences in Canada, the Netherlands, Illinois, Oregon, Wisconsin, and New Mexico (Thanks to Kevin and Rackham Travel Grants). Thank you to the Chemistry department for accepting me into the program, for the teaching opportunities, and for investing in my future. Thank you to Rackham for the Rackham Merit Fellowship (I also met super rad people, and my first grad

school friends, through the RMF, including **Stephen Molldrem, Max Alvarez, and Liz Mosley)**. Thank you to the staff in 1500 for holding the department together, especially **Margarita Bekiares, Cornelius Wright, and Liz Oxford.** I want to acknowledge my experiences organizing the Vaughan/Karle Symposium and with the chemistry graduate student council. Thank you to RELATE for teaching me more and peaking my interest in science communication. I want to acknowledge **Linda Van Blaircum** from across the hall for wonderful and thoughtful conversations through the years, especially about ancestry. Thanks to members of the **Bartlett, Ogilvie, and Sension** lab from 2012 to now for your support over the years. Thank you to all of the women scientists who came before me. A shoutout to that one woman in my career development seminar who was the first woman PhD student in science I had ever met. I had never even considered that I could get a PhD before that moment.

I appreciate that my loans from undergrad have been deferred while in grad school (though the interest is exploding). Thank you to GEO for my benefits and allowing me to see the following amazing health care professionals: **Hsiao-Wen Lo, Monique Steele, Jane McCort, and Joseph Myers**. Also, thank you to whoever told me, “B’s get PhDs.” I appreciate all of my animal friends (mel, honey, paige, willow, nomi).

Finally, Thank you and SO MUCH LOVE AND APPRECIATION to the following people: **Stephanie Sim from ScholarSpace**, **Laura Herbert, Andrea Holther-Cruz, Andrew Molina, Bjorn, Oleg, Aaron Proctor, Ariana Hall, Sydonie Schimler, Veronica Policht, Jimmy Brancho, Anna Hansen, Jim Mogensen, Sarah Sherburne, Mikey Norman, Austin McCoy, Morgan Whitcomb, Denise Bailey, Nicky Hentrich, Blair Ellis, Persphon Hernandez-Vigt, Vidhya Aravind, Jean Bunn, Erin Grimm, John Ware, Drew Nowak, Katy Clark, Missy Herskowitz, Payton Alexandre, Taylor Field, Zach Storey, Jordan Adams, Brynne Curtis, and Shane McParland <3**

Table of Contents

List of Figures

List of Tables

List of Abbreviations

1D: one-dimensional

2D: two-dimensional

2DIR: two-dimensional infrared (spectroscopy)

BBO: beta-barium borate

CCD: charged coupled device

cm^{-1}: wavenumber

CORM: carbon monoxide releasing molecule

DFG: difference frequency generation

DLS: depolarized light scattering

DR: dielectric relaxation (spectroscopy)

FFCF: frequency-fluctuation correlation function

fs: femtosecond

FT: fourier transform

FTIR: Fourier Transform Infrared (Spectroscopy)

FWHM: full width half max

GaSe: Gallium Selenide

H-bond: hydrogen bond

INS: inelastic neutron scattering

IR: infrared radiation

IVR: intramolecular vibrational redistribution

LO: local oscillator

MD: molecular dynamics

MRD: magnetic relaxation dispersion

Nm: nanometer

NMR: nuclear magnetic resonance

NOE: nuclear overhauser effect

ODNP: Overhauser Dynamics Nuclear Polarization

OH: water hydroxyl

OKE: optical Kerr-effect (spectroscopy)

OPA: optical parametric amplification

PEG-X: polyethylene glycol - molecular weight

PEO: Poly ethylene oxide

ps: picosecond

QENS: quasi-elastic neutron scattering

SFG: sum-frequency generation

TDSS: time-dependent stokes shift spectroscopy

Thz: terahertz

Ti:sapph: Titanium:sapphire

Vis: visible

ω1: excitation axis

ω3: detection axis

ABSTRACT

Water-solute interactions still remain a challenge to study experimentally, though they are critical to protein and biomacromolecule stability, structure, and function. Hydration dynamics at interfaces are generally slower than bulk water. While many investigations into the dynamics of water using advanced spectroscopy methods have occurred, considerably less specific attention has been paid to biologically relevant highly crowded solutions. Macromolecular crowding is the result of both steric and chemical interactions of the crowding agent with the targeted molecule of study. Considering steric effects of crowding agents is not enough, and studies of chemical interactions are increasingly being done. Crowding agents typically are polymers, proteins, reverse micelles, or hydrogels, and in this study, we focus on polymers. We seek to understand how polymer crowders affect hydration dynamics. Using ultrafast two-dimensional infrared (2D-IR) spectroscopy of a new water-soluble transition metal complex acting as a vibrational probe, we look at a range of polymers at various lengths, concentrations, and temperatures. We find that PEG, which exhibits unusual structural and thermodynamic trends, has a very stable hydration shell at room temperature. The stable hydration shell promotes bulk like hydration dynamics even at high concentrations and viscosities. From temperature variance experiments, we calculate activation energies and find that the results are similar to activation energies of water. Our studies provide fundamental information about the hydration dynamics of concentrated polymer solutions and we find evidence for distinct dynamics sensed by the probe depending on the crowding agent.

Chapter 1 Introduction

1.1 PRESERVATION OF HYDRATION SHELL DYNAMICS

Water makes up 71% of the earth's surface, and makes up on average 60% of a human body. Though water is vital to life on earth, there is still much to learn, especially regarding how water interacts with proteins and other biomacromolecules within organisms.[1] The most important aspect of water-solute interactions is the hydration shell, which remains a challenge to investigate experimentally. An intuitive definition that includes all of the water molecules within the first layer of water around a biomolecule, which is typically 3.5 angstroms, is commonly denoted "biological water" by the biochemical and structural biology communities, largely due to the presence of these water molecules in x-ray crystal structures. For computational studies, one can be very specific as to which molecules will be interrogated, though it can be difficult to link aspects of arbitrary water shells to experimental measurements.[2] Often, the water molecules in the hydration shell behave differently from the bulk, which is why there is an interest in studying aspects of hydration dynamics of both bulk and interfacial water molecules on timescales ranging from ultrafast (fs-ps) to much slower dynamics. Hydration dynamics arise from time-dependent fluctuations of the complex structural network of water molecules reflecting cooperative and directional hydrogen bonding. Processes that can be studied by various experimental techniques included in water dynamics are vibrational lifetimes, hydrogen bond (H-bond) lifetimes, structural fluctuations, energy transfer, and energy dissipation, which occur on a picosecond timescale.[3]

This work focuses on the hydration dynamics of various aqueous polymer solutions. Aqueous polymer solutions and hydrogels have a wide variety of applications in modern society. The food industry uses polymers as stabilizers,

thickeners, and gelling agents for texture and taste,[4-6] while the pharmaceutical and biomedical industries use polymer solutions and hydrogels for clinical applications, drug delivery, tissue engineering, and much more.[7, 8] Hydraulic fracturing liquid is an effective substance used to extract natural gas from shales, and this liquid uses guar gum to increase viscosity.[9-11]

In particular, we focus primarily on a remarkable polymer—poly ethylene glycol (PEG)—that is one of the most widely used biocompatible molecular materials. PEG is a polyether that is used in a wide range of applications, from improving bioavailability of drugs and other payloads, to serving as a coating for medical devices. [12, 13] In basic science research, PEG is used as a chemically neutral macromolecule for studies of crowding[14] as well as a promoter of protein crystallization. [15] PEG's water solubility largely arises from the favorable spacing of the oxygen atoms in the $–O(CH_2)_2–O(CH_2)_2–$ chain, which matches geometrically the natural spacing of oxygens in water's hydrogen bonded network.[16] Chemically very similar polyethers $–O(CH_2)–O(CH_2)–$ [(poly(methylene oxide)] and $–O(CH_2)_3–O(CH)_3–$ [(poly(trimethylene oxide)] are insoluble in water. Although the thermodynamics of PEG hydration are well understood, there is little known about the dynamical nature of PEG hydration. In light of recent work to probe interfacial water in the vicinity of biological macromolecules, this work aims to characterize the nature of PEG hydration dynamics in a range of concentrations, molecular mass, and temperature.

There are many reviews that have been published that discuss hydration water: examining the dynamics of water itself, how various solutes, such as proteins or macromolecules, in dilute concentration influence the dynamical aspects of water, and how more concentrated solutes influence water by studying crowding and confinement of water molecules using macromolecules such as proteins and polymers. [1-3, 17-71] Key aspects of the current understanding of hydration dynamics are summarized here.

1.1.1 Water Dynamics

While much work has been done to understand the dynamics of water, there is still much to learn due to its importance in many biological processes and to life on earth.[1, 72] Studies of OH/OD stretch of liquid, supercooled, and crystalline water has revealed that vibrational spectroscopies are able to extract information about local interactions, stability, and rearrangement dynamics of the H-bond network of water because vibrational frequencies are very sensitive to local environments. Comparing the time-dependent fluctuations measured to MD simulations can help determine structural information of water H-bond networks.[17-21]

The hydrogen bond network of water is constantly experiencing the breaking and forming of h-bonds due to water molecule reorientation, and adapts to solute inclusion. The extended jump model developed by Laage and Hynes describes this mechanism of water reorientation, and it is consistent with experimental results. In this mechanism, the reorienting water molecules experiences concerted H-bond breaking and forming through a large angular jump. [30, 31, 73]

Studies of molecular structure of water at air and biological interfaces seek to determine, compared to bulk water, how water structure and dynamics are influenced by the H-bond network interruption. The hydration shells of proteins have been increasingly studied in the past couple of decades. However, interest in understanding protein hydration goes further back.[32, 33] Since the development of ultrafast spectroscopy, we have been able to significantly build on these studies of the interactions between water and macromolecules. There are a number of reviews detailing work relating to the interactions of proteins and water. [1, 3, 34-46] These interfaces can be studied using Overhauser dynamics nuclear polarization (ODNP) enhanced NMR spectroscopy, interface specific SFG spectroscopy, dynamic stokes shift spectroscopy, pump-probe spectroscopy, 2DIR, and MD simulations. While much work has been done, different timescale results from these experimental methods for interfacial studies still need to be addressed.[22-24]

Similarly to studies of water at interfaces, studies of confined and crowded water seek to determine how dynamics are different from water in the bulk. Reverse micelles, hydrogels, and other macromolecules have been used as confining and crowding agents, and have found that depending on the crowding agent and size of confinement, there are various affects on the water dynamics timescales, generally a slowing of dynamics. [2, 25-27, 29, 74]

1.1.2 Macromolecular Crowding and Concentrated Aqueous Polymer Solutions

Understanding the dynamics of water and water interacting with macromolecules aid us in our quest to understand how water and solute interactions change as solute concentration increases. Traditionally, mechanisms, equilibria, rates, and dynamics of biochemical solutions have been studied containing concentrations of less than 1 mg/mL of total macromolecule, DNA, or protein, when living systems exist in crowded environments of 50-400 mg/mL.[47-52, 75] In response to this, studies of how macromolecular crowding and confinement affect the dynamics of biological and non-biological solutions have increased.

There are several reviews that describe the principles and importance of considering macromolecular crowding.[47-53] To take into account physiological conditions and confined spaces, artificial crowding agents are being used to create more realistic environments for experiments. Macromolecular crowding creates an excluded volume effect, where a crowding agent takes up space that can no longer be occupied by another molecule, which doesn't necessarily occur in dilute conditions. Excluded volume is made up of both steric effects and soft interactions, which are chemical interactions.[64, 76] There has been much work done that only consider the steric effects, without considering possible chemical interactions in studying protein aggregation[54], protein stability and folding[56], nucleic acid structure and function[60-63], and MD simulations[65, 66].

Challenges to crowding studies include: can studies that utilize supposedly inert crowding agents an accurate imitate in vivo crowded environments? Are there any crowding agents that are actually inert, or will there

always be chemical interactions to keep in mind? While PEG is not necessarily inert, because it is used in so often in industries, it is good to try to understand its interactions with biological media.[64] Crowding agents should be inert to what is being studied, where only steric interactions occur and not chemical interactions.[51]

Research has started to examine how other aspects of macromolecular crowding must be taken into account for a more complete picture, such as viscosity, soft interactions, perturbed diffusion, and crowder shape, confinement, and concentration, all of which affect the crowded solution. [55, 57-59, 64, 67-71] In order to think about the whole picture, both hard and soft interactions must be considered individually. Hard core repulsions, or steric interactions, are entropic in nature because it involves molecular arrangement. Using the lens of the equilibrium principle, these steric interactions favor compact arrangements. Soft interactions, chemical in nature, are repulsive or attractive. Favorable attractive (nonspecific) interactions with proteins can lead to unfolding, which has an enthalpic part. Repulsive soft interactions are stabilizing, similar to steric repulsions.[77] In a crowding study done comparing the effects of Ficoll-70 and its monomer, sucrose, by Pielak and coworkers, it was determined that sucrose and Ficoll had almost the same enthalpy-driven stabilization effect on a chymotrypsin inhibitor.[78] There have also been studies that explicitly show crowding agents destabilizing proteins rather than stabilize and that soft interactions can help regulate protein interactions with other proteins.[79, 80] These results indicate that soft interactions are important phenomena to consider, and sometimes are of a greater influence than excluded volume. It is in this direction we taken this dissertation.

1.2 HOW DO WE STUDY SOLUTE HYDRATION?

The water hydration shell has been studied by many methods, all which give us different pieces to this puzzle of understanding water dynamics. There are several reviews that detail the variety of methods used to study hydration

dynamics.[2, 20, 23, 29, 81] Briefly, I will go through other techniques and how they are used to study hydration dynamics.

Linear spectroscopies such as FTIR and Raman are commercially available, and used for characterization of dynamics and structure of water of water molecules directly. However, the line shapes are broadened by both homogeneous and inhomogeneous broadening, without being able to distinguish between the two.[20] Sum frequency generation (SFG) spectroscopy can provide much information about water's interactions at interfaces because it is a surface specific technique.[23] It is possible to gain spectral diffusion information similarly to 2DIR with the 2D extension of SFG.[20] Pump probe spectroscopy is a one dimensional nonlinear ultrafast spectroscopy and directly probes water molecules. Pump-probe can provide information on vibrational population relaxation and anisotropy decay.[20, 23] Photon echo spectroscopy is the predecessor to 2DIR and measures water molecules directly by vibrational dephasing time and can separate inhomogeneous and homogeneous broadening.[20] NMR directly probes water dynamics and measures water reorientation times, however, the signal is averaged over all water molecules.[2, 29, 81] However, Overhauser dynamics nuclear polarization (ODNP) enhanced NMR can report on interfaces by attaching a radical spin probe attached to an interface. To enhance the NMR signal, the probe transfers spin polarization to the area water protons.[23, 81] Optical Kerr-effect (OKE) spectroscopy is a one-dimensional nonlinear time-resolved spectroscopy that is able to measure collective and intermolecular dynamics of water. The response function measured by OKE is the same as depolarized light scattering, but in the time domain.[20, 29, 81] Depolarized light scattering (DLS) probes collective water dynamics, measuring structural dynamics of water.[29, 81] Quasi-elastic and inelastic neutron scattering (QENS, INS) directly probe water molecules, providing collective water information. QENS and INS both can study ultrafast translational and rotational motions.[2, 29, 81] Dielectric relaxation (DR) spectroscopy studies collective reorientation of water by measuring the electric dipole

relaxation.[29, 81] Terahertz (Thz) spectroscopy probes collective motion of water molecules and intermolecular vibrations of the hydrogen bond network.[2, 29, 81] Time-Dependent Stoke stokes shift spectroscopy (TDSS) uses a probe to study water dynamics instead of studying the water molecules directly. TDSS excites a chromophore within the biomolecule of interest, and this chromophore has a radiative lifetime much longer than probes used in 2DIR.[2, 23, 81]

In this dissertation, we use two-dimensional infrared (2DIR) spectroscopy to examine the hydration dynamics of aqueous solutions of various shapes and lengths of polymers.

1.3 INTRODUCTION TO VIBRATIONAL SPECTROSCOPY

The molecular environment is sensitive to vibrational spectroscopy, which makes it a useful technique to study the dynamics and structure of molecules in the condensed phase. Linear IR spectroscopy can provide information about the chemical groups of an unknown molecule, but spectral congestion and a lack of significant spectral differentiation causes spectral overlap and interference that makes assignment of complex heterogeneous systems nearly impossible. Further complicating the use of linear IR spectroscopy, is its inherent time-averaging, and the fact that it is impossible to differentiate between inhomogenous and homogeneous broadening.[82] These qualitatively different broadening mechanisms are described in detail below.

1.3.1 Nonlinear and Multidimensional Spectroscopy

Absorption, reflection, light propagation, and refraction from a weak light field are related to the creation of a linear polarization in a medium. Nonlinear spectroscopies are related to nonlinear polarization induced by multiple field-matter interactions (multi-wave mixing). As typically implemented, multi-wave mixing results from the interaction of more than one laser field with a system, generating a coherent signal field, often in a unique, background-free direction.[83] Nonlinear spectroscopies can be one-dimensional or multidimensional. One-

dimensional nonlinear spectroscopies include pump-probe, photon echo, and optical Kerr effect spectroscopy.[20] To make a spectroscopy multidimensional, two or more excitation pulses separated by time are combined along with a probe pulse, where the pump pulse and probe pulse frequencies are resolved.[82] More formally, a multidimensional spectroscopy method should give access to a multi-time interval correlation function. For example 2DIR, a third-order technique, is governed by the three-point (two-interval) time correlation function of the dipole moment: $C(t_1,t_2,t_3) = \langle\mu(t_1+t_2+t_3)\mu(t_1+t_2)\mu(t_1)\rangle$.

1.4 TWO-DIMENSIONAL INFRARED SPECTROSCOPY

Two-dimensional infrared spectroscopy (2DIR) is a multidimensional nonlinear optical technique. Nonlinear multidimensional spectroscopies have been reviewed previously.[82, 84-93] 2DIR is able to directly probe water molecules. However, it is also possible to use transition metal carbonyl complexes, as they are powerful probes of solution environments.[94-99]

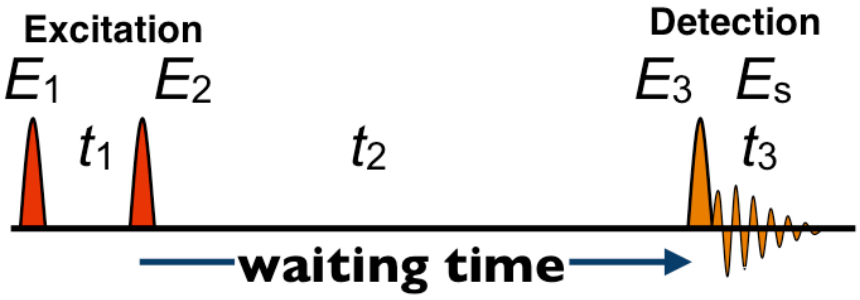

Figure 1.1 2DIR pulse sequence

In its current implementation, an output centered around 800 nm from a regeneratvely amplified Ti:sapphire laser is used. This output has a 1 KHz repetition rate and uses a dual optical parametric amplifier with beta barium borate crystals to generate near IR pulses. These pulses are then used to generate two mid-IR pulses by difference frequency generation in separate GaSe crystals. The mid IR pulses are centered around 2000 cm^{-1} with about 100 cm^{-1} FWHM bandwidth. Using beam splitters, these two beams are split into three IR pulses, the tracer, and the local oscillator.[95]

The three infrared femtosecond laser pulses interact with the sample and create a third-order nonlinear signal (**Figure 1.1**). The three fields are E_1, E_2, or E_3 with corresponding wave vectors k_1, k_2, and k_3. The fields are separated by time delays t_1, t_2 (the so-called "waiting time"), and t_3. The pulses interact with the sample in a noncollinear box geometry in order to generate a signal in a background free direction during t_3. The two directions are $k_R = -k_1 + k_2 + k_3$ and $k_N = k_1 - k_2 + k_3$ which are the "rephasing" and "nonrephasing" signals, respectively. By interchanging the pulse ordering with delay stages, it is possible to generate the rephasing and nonrephasing signals in the same physical direction in the space (though not at the same time). The phase and amplitude of the signal field (with wavevector k_R or k_N) are measured directly with a spectrometer via optical heterodyne detection by interference with the local oscillator. [86, 89]

During the experiment, the waiting time is incrementally stepped over a range of picoseconds. At each waiting time, the time delay between the first two pulses is scanned continuously. The complex electric field that is collected during this delay is Fourier transformed with respect to the first the time delay to yield the excitation frequency axis (ω_1). The spectrometer measures the signal field emitted during t_3 directly in the frequency domain, creating the detection axis directly. The IR signal, the local oscillator, and a chirped 800 nm pulse are combined and upconverted by sum frequency generation to roughly 690 nm and detected using a silicon CCD.[95]

Increasing the waiting time between excitation and detection reveals dynamical changes in the 2D spectral features, which can be related to processes such as solvation dynamics, vibrational energy transfer, and vibrational energy relaxation. A recent review summarizes several of the observables from 2DIR.[93] Here we will provide a brief overview of spectral diffusion as the major observable discussed in this work.

1.4.1 Spectral Diffusion

In linear FTIR spectroscopy, homogeneous and inhomogeneous broadening cannot be separated, and provides time averaged spectra.

Inhomogeneous broadening results when different microscopic environments in the solvent are sampled, and it leads to a variation of transition energies. Homogeneous broadening is a result from rapid fluctuations, whereas inhomogeneous broadening is from slower fluctuations. Using 2DIR, it is possible to separate inhomogeneous broadening from homogeneous broadening and extract information about solvent-solute interactions, vibrational dynamics, and molecular structure.[89]

During the incrementally increasing waiting times, the probe molecule is able to sample these microscopically distinct environments because of stochastic fluctuations of the system, causing their frequencies to evolve. At early waiting times, the excitation and detection frequencies are well correlated, with an inhomogenously broadened peak shape, because the probe has not had the chance to sample many microscopic environments. As the waiting time increases, correlation is lost as the probe samples more solvent environments, causing the peak shape to become more homogeneously broadened. The timescale for this loss in correlation can be related to characteristic timescales of the solvent dynamics. This process is known as spectral diffusion. Spectral diffusion reports on the chemical dynamics of the system of study. 2DIR is able to directly measure the timescales for spectral diffusion.

The frequency fluctuation correlation function (FFCF), which is often interpreted as arising from spectral diffusion, is denoted as $C(\tau)=\langle\delta\omega(\tau)\delta\omega(0)\rangle$, where $\delta\omega(\tau)$ is the instantaneous fluctuation from the average frequency.[83] The inhomogeneous index, I(t), which is directly proportional to the FFCF, is extracted from 2DIR spectra as the amplitude difference of the rephasing and nonrephasing signals: $I(t_2) = (A_r - A_n)/(A_r + A_n)$, where A_r is the rephasing signal amplitude, and A_n is the nonrephasing signal amplitude.[100] The function that transforms the inhomogeneity index to the FFCF is: $C(t_2) = \sin[(\pi * I(t_2))/2]$.

1.5 THESIS OUTLINE

This dissertation is organized as follows: **Chapter 2** describes the 2DIR experiments of a new water-soluble transition metal complex acting as a vibrational probe. These experiments show that over a range of concentration

and polyethylene glycol (PEG) molecular mass (2000, 8000, and 20,000 Da), the time scale of the sensed hydration dynamics has the signature of bulk-like water, even where there are slower time scale dynamics. A notable exception is PEG-400, where we observe a sharp dynamical slowdown near the critical overlap concentration, indicating that chain interactions and possibly collective hydration alters the water dynamics in a manner similar to previous observations in crowded protein solutions. PEG is well known to establish a highly stable hydration shell because the spacing between adjacent ethereal oxygens nearly matches water's hydrogen bonding network. Although these first-shell water molecules are likely significantly retarded, they present an interface to subsequent hydration shells, and thus diminish the largely entropic perturbation to water's orientational dynamics. Comparison between these dynamical results and previously reported steady-state infrared spectroscopy of aqueous PEG-1000 solutions reveals a strikingly identical dependence on number of water molecules per ethylene oxide monomer, scaled according to the critical overlap concentration.

Chapter 3 describes temperature variation experiments that follow up the work of chapter 2, where it was found that over a wide range of concentration and molecular weights of PEG, the time scale of sensed hydration dynamics differed negligibly from bulk water with an exception of PEG-400, where a dynamical slowdown was observed. The time scale was attributed to the stability of the hydration shell around the long chain PEGs. By looking at thermodynamic trends of aqueous PEG, it was concluded that shorter PEGs promote a less stable hydration shell than do the longer chain polymers, which in turn enables a collective slowdown of hydration dynamics. Building on that study, temperature variation was done to observe how thermodynamics of aqueous PEG solutions may change, and how that might affect the hydration dynamics measured. Using two-dimensional infrared spectroscopy of a water-soluble transition metal complex acting as a vibrational probe, we will report on the hydration dynamics of PEG 400 at low and high concentrations from 283 K to 325 K.

Chapter 4 describes studies of concentrated aqueous polysaccharide polymer solutions of guar and Ficoll. We investigate how structural properties, such as branching and size, affect the hydration dynamics. Guar, a linear polymer, and Ficoll, a hard, spherical polymer, serve as model macromolecular crowders, while their monomer units serve as control solutes and allow us to isolate the effects of polymer size and shape. By studying the fundamental properties of these mixtures, we learn how crowding and confinement affects the structural and dynamical properties of liquids on both a micro- and a macroscale. We explore how hydration dynamics depend on connectivity of the monomer units (i.e. polymerized vs. discrete) and how polymer shape (i.e. linear vs. spherical) affects hydration dynamics of heterogeneous mixtures.

Chapter 5 summarizes the content of this dissertation and provides future directions for this research.

1.6 REFERENCES

1. Ball, P., Water as an active constituent in cell biology. *Chemical Reviews* **2008,** *108* (1), 74-108.

2. Fogarty, A. C.; Duboué-Dijon, E.; Sterpone, F.; Hynes, J. T.; Laage, D., Biomolecular hydration dynamics: A jump model perspective. *Chemical Society Reviews* **2013,** *42* (13), 5672-5683.

3. Laage, D.; Elsaesser, T.; Hynes, J. T., Water Dynamics in the Hydration Shells of Biomolecules. *Chemical Reviews* **2017**, DOI: 10.1021/acs.chemrev.6b00765.

4. Chang, Y.-Y.; Li, D.; Wang, L.-J.; Bi, C.-H.; Adhikari, B., Effect of gums on the rheological characteristics and microstructure of acid-induced SPI-gum mixed gels. *Carbohydrate polymers* **2014,** *108*, 183-91.

5. Rosell, C. M.; Collar, C.; Haros, M., Assessment of hydrocolloid effects on the thermo-mechanical properties of wheat using the Mixolab. *Food Hydrocolloids* **2007,** *21* (3), 452-462.

6. Torres, M. D.; Hallmark, B.; Wilson, D. I., Effect of concentration on shear and extensional rheology of guar gum solutions. *Food Hydrocolloids* **2014,** *40*, 85-95.

7. Coviello, T.; Matricardi, P.; Marianecci, C.; Alhaique, F., Polysaccharide hydrogels for modified release formulations. *Journal of controlled release : official journal of the Controlled Release Society* **2007,** *119* (1), 5-24.

8. Van Thienen, T. G.; Horkay, F.; Braeckmans, K.; Stubbe, B. G.; Demeester, J.; De Smedt, S. C., Influence of free chains on the swelling pressure of PEG-HEMA and dex-HEMA hydrogels. *International Journal of Pharmaceutics* **2007,** *337* (1-2), 31-39.

9. Vidic, R. D.; Brantley, S. L.; Vandenbossche, J. M.; Yoxtheimer, D.; Abad, J. D., Impact of shale gas development on regional water quality. *Science (New York, N.Y.)* **2013,** *340*, 1235009.

10. Xu, B.; Hill, A. D.; Zhu, D.; Wang, L., Experimental Evaluation of Guar-Fracture-Fluid Filter-Cake Behavior. **2011**.

11. Zhang, J.; Chen, G., Improve the Temperature Resistance of Guar Gum by Silanization. *Advanced Materials Research* **2012,** *415-417*, 652-655.

12. Harris, J. M.; Chess, R. B., Effect of pegylation on pharmaceuticals. *Nature Reviews Drug Discovery* **2003,** *2* (3), 214-221.

13. Veronese, F. M.; Pasut, G., PEGylation, successful approach to drug delivery. *Drug Discovery Today* **2005,** *10* (21), 1451-1458.

14. Hirano, A.; Shiraki, K.; Arakawa, T., Polyethylene Glycol Behaves Like Weak Organic Solvent Polyethylene Glycol Behaves Like Weak Organic Solvent. *Biopolymers* **2011,** *97*.

15. McPherson, A., Crystallization of Proteins from Polyethylene-Glycol. *Journal of Biological Chemistry* **1976,** *251* (20), 6300-6303.

16. Kjellander, R. F., Ebba, Water structure and changes in thermal stability of the system poly(ethylene oxide)-water. *Journal of the Chemical Society, Faraday Transactions 1: Phyiscal Chemistry in Condensed Phases* **1981,** *77* (9), 2053-2077.

17. Nibbering, E. T. J.; Elsaesser, T., Ultrafast Vibrational Dynamics of Hydrogen Bonds in the Condensed Phase. *Chemical Reviews* **2004,** *104* (4), 1887-1914.

18. Roberts, S. T.; Ramasesha, K.; Tokmakoff, A., Structural Rearrangements in Water Viewed Through Two-Dimensional Infrared Spectroscopy. *ACCOUNTS OF CHEMICAL RESEARCH* **2009,** *42* (9), 1239-1249.

19. Skinner, J. L.; Auer, B. M.; Lin, Y.-S., Vibrational Line Shapes, Spectral Diffusion, and Hydrogen Bonding in Liquid Water. *Advances in Chemical Physics* **2009,** *142*, 59-103.

20. Perakis, F.; de Marco, L.; Shalit, A.; Tang, F.; Kann, Z. R.; Kühne, T. D.; Torre, R.; Bonn, M.; Nagata, Y., Vibrational Spectroscopy and Dynamics of Water. *Chemical Reviews* **2016,** *116*, 7590-7607.

21. Bakker, H.; Skinner, J., Vibrational spectroscopy as a probe of structure and dynamics in liquid water. *Chemical reviews* **2010,** *110*, 1498-1517.

22. Bonn, M.; Nagata, Y.; Backus, E. H. G., Molecular structure and dynamics of water at the water-air interface studied with surface-specific vibrational

spectroscopy. *Angewandte Chemie - International Edition* **2015,** *54* (19), 5560-5576.

23. Kubarych, K. J.; Roy, V. P.; Daley, K. R., *Interfacial Water Dynamics*. 1 ed.; Elsevier: 2018; p 443-461.

24. Buntkowsky, G.; Vogel, M.; Winter, R., Properties of Hydrogen-Bonded Liquids at Interfaces. *Zeitschrift fur Physikalische Chemie* **2018,** *232* (7-8), 937-972.

25. Fayer, M. D.; Levinger, N. E., Analysis of water in confined geometries and at interfaces. *Annual review of analytical chemistry* **2010,** *3*, 89-107.

26. Park, S.; Moilanen, D. E.; Fayer, M. D., Water Dynamics - The Effects of Ions and Nanoconfinement. *Journal of Physical Chemistry B* **2008,** *112*, 5279-5290.

27. Fayer, M. D., Water in a Crowd. *Physiology* **2011,** *26*, 381-392.

28. Bakker, H. J., Structural Dynamics of Aqueous Salt Solutions. *Chem. Rev.* **2008,** *108* (4), 1456-1473.

29. Comez, L.; Paolantoni, M.; Sassi, P.; Corezzi, S.; Morresi, A.; Fioretto, D., Molecular properties of aqueous solutions: A focus on the collective dynamics of hydration water. *Soft Matter* **2016,** *12* (25), 5501-5514.

30. Laage, D.; Stirnemann, G.; Hynes, J. T., Why Water Reorientation Slows without Iceberg Formation around Hydrophobic Solutes. *Journal of Physical Chemistry B* **2009,** *113* (8), 2428-2435.

31. Laage, D.; Hynes, J. T., A molecular jump mechanism of water reorientation. *SCIENCE* **2006,** *311* (5762), 832-835.

32. Kuntz, I. D., Jr.; Kauzmann, W. , Hydration of Proteins and Polypeptides. *Advances in Protein Chemistry* **1974,** *28* (C), 239-345.

33. Rupley, J. A.; Careri, G., Advances in Protein Chemistry Volume 41. *Advances in Protein Chemistry* **1991,** *41*, 37-172.

34. Fayer, M. D., Fast Protein Dynamics Probes with Infrared Vibrational Echo Experiments. *Annual review of physical chemistry* **2001,** *52* (12), 315-356.

35. Fayer, D., Dynamics of Liquids, Molecules, and Proteins Measured with Ultrafast 2D IR Vibrational Echo Chemical Exchange Spectroscopy. *Annual review of physical chemistry* **2009,** *60*, 21-38.

36. Zhuang, W.; Hayashi, T.; Mukamel, S., Coherent multidimensional vibrational spectroscopy of biomolecules: Concepts, simulations, and challenges. *Angewandte Chemie - International Edition* **2009,** *48* (21), 3750-3781.

37. Bellissent-Funel, M. C.; Hassanali, A.; Havenith, M.; Henchman, R.; Pohl, P.; Sterpone, F.; van der Spoel, D.; Xu, Y.; Garcia, A. E., Water Determines the Structure and Dynamics of Proteins. *Chemical Reviews* **2016,** *116* (13), 7673-7697.

38. Smith, J. C.; Merzel, F.; Bondar, A. N.; Tournier, A.; Fischer, S., Structure, dynamics and reactions of protein hydration water. *Philosophical Transactions of the Royal Society B: Biological Sciences* **2004,** *359* (1448), 1181-1190.

39. Bagchi, B., Water Dynamics in the Hydration Layer Around Proteins and Micelles. *Chemical Reviews* **2005,** *105* (9), 3197-3219.

40. Halle, B., Protein hydration dynamics in solution: a critical survey. *Philosophical Transactions of the Royal Society of London Series B-Biological Sciences* **2004,** *359* (1448), 1207-1223.

41. Pal, S. K.; Zewail, A. H., Dynamics of water in biological recognition. *Chemical Reviews* **2004,** *104* (4), 2099-2123.

42. Levy, Y.; Onuchic, J. N., Water mediation in protein folding and molecular recognition. *Annual review of biophysics and biomolecular structure* **2006,** *35*, 389-415.

43. Berkowitz, M. L.; Bostick, D. L.; Pandit, S., Aqueous solutions next to phospholipid membrane surfaces: Insights from simulations. *Chemical Reviews* **2006,** *106* (4), 1527-1539.

44. Jungwirth, P., Biological Water or Rather Water in Biology? *Journal of Physical Chemistry Letters* **2015,** *6* (13), 2449-2451.

45. Helms, V., Protein dynamics tightly connected to the dynamics of surrounding and internal water molecules. *ChemPhysChem* **2007,** *8* (1), 23-33.

46. Zhong, D.; Pal, S. K.; Zewail, A. H., Biological water: A critique. *Chemical Physics Letters* **2011,** *503* (1-3), 1-11.

47. Zimmerman, S. B.; Minton, A. P., MACROMOLECULAR CROWDING: Biochemical, Biophysical, and Physiological Consequences. *Annual review of biophysics and biomolecular structure* **1993,** *22*, 27-65.

48. Ellis, R. J., Macromolecular crowding : obvious but under appreciated. *TRENDS in Biochemical Sciences* **2001,** *26*, 597-604.

49. Minton, A. P., The Influence of Macromolecular Crowding and Macromolecular Confinement on Biochemical Reactions in Physiological Media. *Journal of Biological Chemistry* **2001,** *276*, 10577-10580.

50. Minton, A. P., Macromolecular crowding. *Curr Biol* **2006,** *16* (8), R269-71.

51. Zhou, H.-X.; Rivas, G.; Minton, A. P., Macromolecular crowding and confinement: biochemical, biophysical, and potential physiological consequences. *Annual review of biophysics* **2008,** *37*, 375-397.

52. Rivas, G.; Minton, A. P., Macromolecular Crowding In Vitro, In Vivo, and In Between. *Trends in Biochemical Sciences* **2016,** *41* (11), 970-981.

53. Gnutt, D.; Ebbinghaus, S., The macromolecular crowding effect - From in vitro into the cell. *Biological Chemistry* **2016,** *397* (1), 37-44.

54. Ellis, R. J.; Minton, A. P., Protein aggregation in crowded environments. *Biological Chemistry* **2006,** *387*, 485-497.

55. Musiani, F.; Giorgetti, A., *Protein Aggregation and Molecular Crowding: Perspectives From Multiscale Simulations*. 1 ed.; Elsevier Inc.: 2017; Vol. 329, p 49-77.

56. Samiotakis, A.; Wittung-Stafshede, P.; Cheung, M. S., Folding, stability and shape of proteins in crowded Environments: Experimental and computational approaches. *International Journal of Molecular Sciences* **2009,** *10* (2), 572-588.

57. Zhou, H. X., Influence of crowded cellular environments on protein folding, binding, and oligomerization: Biological consequences and potentials of atomistic modeling. *FEBS Letters* **2013,** *587* (8), 1053-1061.

58. Spitzer, J., From Water and Ions to Crowded Biomacromolecules: In Vivo Structuring of a Prokaryotic Cell. *Microbiology and Molecular Biology Reviews* **2011,** *75* (3), 491-506.

59. Theillet, F.-x.; Binol, A.; Frembgen-kesner, T.; Hingorani, K.; Sarkar, M.; Kyne, C.; Li, C.; Crowley, P. B.; Gierasch, L.; Pielak, G. J.; Elcock, A. H.; Gershenson, A.; Selenko, P., Physicochemical Properties of Cells and Their Effects on Intrinsically Disordered Proteins (IDPs). *Chem. Rev* **2014,** *114*, 6661-6714.

60. Nakano, S. I.; Miyoshi, D.; Sugimoto, N., Effects of molecular crowding on the structures, interactions, and functions of nucleic acids. *Chemical Reviews* **2014,** *114* (5), 2733-2758.

61. Miyoshi, D.; Fujimoto, T.; Sugimoto, N., Molecular Crowding and Hydration Regulating of G-Quadruplex Formation. *Topics in Current Chemistry* **2013,** *330*, 87-110.

62. Huet, S.; Lavelle, C.; Ranchon, H.; Carrivain, P.; Victor, J. M.; Bancaud, A., *Relevance and limitations of crowding, fractal, and polymer models to describe nuclear architecture*. 1 ed.; Elsevier Inc.: 2014; Vol. 307, p 443-479.

63. Yanagisawa, M.; Sakaue, T.; Yoshikawa, K., *Characteristic behavior of crowding macromolecules confined in cell-sized droplets*. 1 ed.; Elsevier Inc.: 2014; Vol. 307, p 175-204.

64. Elcock, A. H., Models of macromolecular crowding effects and the need for quantitative comparisons with experiment. *Current Opinion in Structural Biology* **2010,** *20* (2), 196-206.

65. Długosz, M.; Trylska, J., Diffusion in crowded biological environments: Applications of Brownian dynamics. *BMC Biophysics* **2011,** *4* (1).

66. Kim, J. S.; Szleifer, I., *Crowding-induced formation and structural alteration of nuclear compartments: Insights from computer simulations*. 1 ed.; Elsevier Inc.: 2014; Vol. 307, p 73-108.

67. Weiss, M., *Crowding, diffusion, and biochemical reactions*. 1 ed.; Elsevier Inc.: 2014; Vol. 307, p 383-417.

68. Dix, J. A.; Verkman, A. S., Crowding Effects on Diffusion in Solutions and Cells. *Annual Review of Biophysics* **2008,** *37* (1), 247-263.

69. Giesa, T.; Buehler, M. J., Nanoconfinement and the Strength of Biopolymers. *Annual Review of Biophysics* **2013,** *42* (1), 651-673.

70. Kuznetsova, I. M.; Zaslavsky, B. Y.; Breydo, L.; Turoverov, K. K.; Uversky, V. N., Beyond the excluded volume effects: Mechanistic complexity of the crowded milieu. *Molecules* **2015,** *20* (1), 1377-1409.

71. Shahid, S.; Hassan, M. I.; Islam, A.; Ahmad, F., Size-dependent studies of macromolecular crowding on the thermodynamic stability, structure and functional activity of proteins: in vitro and in silico approaches. *Biochimica et Biophysica Acta - General Subjects* **2017,** *1861* (2), 178-197.

72. Ball, P., Water is an active matrix of life for cell and molecular biology. *Proceedings of the National Academy of Sciences* **2017,** *114* (51), 13327-13335.

73. Laage, D.; Hynes, J. T., On the molecular mechanism of water reorientation. *The Journal of Physical Chemistry B* **2008,** *112* (45), 14230-14242.

74. Yan, C.; Kramer, P. L.; Yuan, R.; Fayer, M. D., Water Dynamics in Polyacrylamide Hydrogels. *Journal of the American Chemical Society* **2018,** *140* (30), 9466-9477.

75. Minton, A. P., How can biochemical reactions within cells differ from those in test tubes? *Journal of cell science* **2006,** *119*, 2863-9.

76. Sarkar, M.; Li, C.; Pielak, G. J., Soft interactions and crowding. *Biophysical Reviews* **2013,** *5* (2), 187-194.

77. Wang, Y.; Sarkar, M.; Smith, A. E.; Krois, A. S.; Pielak, G. J., Macromolecular Crowding and Protein Stability. *Journal of the American Chemical Society* **2012,** *134* (40), 16614-16618.

78. Benton, L. A.; Smith, A. E.; Young, G. B.; Pielak, G. J., Unexpected effects of macromolecular crowding on protein stability. *Biochemistry* **2012,** *51* (49), 9773-9775.

79. Sarkar, M.; Lu, J.; Pielak, G. J., Protein crowder charge and protein stability. *Biochemistry* **2014,** *53* (10), 1601-1606.

80. Guseman, A. J.; Speer, S. L.; Perez Goncalves, G. M.; Pielak, G. J., Surface Charge Modulates Protein-Protein Interactions in Physiologically Relevant Environments. *Biochemistry* **2018,** *57* (11), 1681-1684.

81. Laage, D.; Elsaesser, T.; Hynes, J. T., Water Dynamics in the Hydration Shells of Biomolecules. *Chemical Reviews* **2016,** *117* (16), 10694-10725.

82. Cho, M. H., Coherent two-dimensional optical spectroscopy. *Chemical Reviews* **2008,** *108* (4), 1331-1418.

83. Mukamel, S., *Principles of Nonlinear Optical Spectroscopy*. Oxford University Press: Oxford, U.K., 1995.

84. Hamm, P.; Zanni, M., *Concepts and methods of 2D Infrared Spectroscopy*. Cambridge University Press: New York, 2011.

85. Ogilvie, J. P.; Kubarych, K. J., *Multidimensional Electronic and Vibrational Spectroscopy: An Ultrafast Probe of Molecular Relaxation and Reaction Dynamics*. 2009; Vol. 57, p 249-321.

86. Mukamel, S., Multidimensional Femtosecond Correlation Spectroscopies of Electrionic and Vibrational Excitations. *Annual Review of Physical Chemistry* **2000,** *51*, 691-729.

87. Wright, J. C., *Coherent multidimensional vibrational spectroscopy*. 2002; Vol. 21, p 185-255.

88. Jonas, D. M., Two-dimensional Femtosecond Spectroscopy. *Annual Review of Physical Chemistry* **2003,** *54*, 425-63.

89. Khalil, M.; Demirdöven, N.; Tokmakoff, a., Coherent 2D IR Spectroscopy: Molecular Structure and Dynamics in Solution. *The Journal of Physical Chemistry A* **2003,** *107*, 5258-5279.

90. Park, S.; Kwak, K.; Fayer, M. D., Ultrafast 2D-IR vibrational echo spectroscopy: A probe of molecular dynamics. *Laser Physics Letters* **2007,** *4*, 704-718.

91. Zheng, J.; Kwak, K.; Fayer, M. D., Ultrafasf 2D IR Vibrational Echo Spectroscopy. *Accounts of Chemical Research* **2007,** *40*, 75-83.

92. Anna, J. M.; Baiz, C. R.; Ross, M. R.; McCanne, R.; Kubarych, K. J., Ultrafast equilibrium and non-equilibrium chemical reaction dynamics probed with multidimensional infrared spectroscopy. *International Reviews in Physical Chemistry* **2012,** *31*, 367-419.

93. Kiefer, L. M.; Kubarych, K. J., Two-dimensional infrared spectroscopy of coordination complexes: From solvent dynamics to photocatalysis. *Coordination Chemistry Reviews* **2018,** *372*, 153-178.

94. Treuffet, J.; Kubarych, K. J.; Lambry, J.-C.; Pilet, E.; Masson, J.-B.; Martin, J.-L.; Vos, M. H.; Joffre, M.; Alexandrou, A., Direct observation of ligand transfer and bond formation in cytochrome c oxidase by using mid-infrared chirped-pulse upconversion. *Proceedings of the National Academy of Sciences of the United States of America* **2007,** *104*, 15705-10.

95. Nee, M. J.; McCanne, R.; Kubarych, K. J.; Joffre, M., Two-dimensional infrared spectroscopy detected by chirped pulse upconversion. *Optics letters* **2007,** *32*, 713-5.

96. Baiz, C. R.; Nee, M. J.; McCanne, R.; Kubarych, K. J., Ultrafast nonequilibrium Fourier-transform two-dimensional infrared spectroscopy. *Optics letters* **2008,** *33*, 2533-5.

97. Anna, J. M.; Ross, M. R.; Kubarych, K. J., Dissecting enthalpic and entropic barriers to ultrafast equilibrium isomerization of a flexible molecule using 2DIR chemical exchange spectroscopy. *The journal of physical chemistry. A* **2009,** *113*, 6544-7.

98. King, J. T.; Ross, M. R.; Kubarych, K. J., Water-assisted vibrational relaxation of a metal carbonyl complex studied with ultrafast 2D-IR. *The journal of physical chemistry. B* **2012,** *116*, 3754-9.

99. Osborne, D. G.; King, J. T.; Dunbar, J. a.; White, A. M.; Kubarych, K. J., Ultrafast 2DIR probe of a host-guest inclusion complex: Structural and dynamical constraints of nanoconfinement. *The Journal of Chemical Physics* **2013,** *138*, 144501.

100. Roberts, S. T.; Loparo, J. J.; Tokmakoff, A., Characterization of spectral diffusion from two-dimensional line shapes. *The Journal of chemical physics* **2006,** *125*, 084502.

Chapter 2 An "Iceberg" Coating Preserves Bulk Hydration Dynamics in Aqueous PEG Solutions

The work in this chapter has been published in the following paper:
Daley, K. R.; Kubarych, K. J., An "Iceberg" Coating Preserves Bulk Hydration Dynamics in Aqueous PEG Solutions. *The Journal of Physical Chemistry B* **2017,** *121* (46), 10574-10582.

2.1 INTRODUCTION

Macromolecular hydration is central to biomolecule structure and function.[1] Agents that alter hydration have applications ranging from practical methods to increasing solubility or shielding payloads from immune response, to enabling fundamental studies of cell-like environments and crowding.[2-11] Polyethylene glycol (PEG) is a widely used polymer due to its water solubility, biocompatibility, and ready availability over a wide range of molecular masses. For example, pegylation of proteins protects them from immune response, and pegylation of therapeutics can enhance solubility of typically hydrophobic molecules.[12-13] In biochemistry, PEG is a common additive to concentrated protein solutions facilitating protein crystallization,[14] an effect attributed to the differential affinity for water between PEG and the protein.[10] In biophysical investigations of macromolecular crowding PEG often plays the role of a chemically inert species that mimics the highly concentrated environment of cells.[15] In our own work, we used a short PEG (PEG-400) as a crowding agent, investigating the role of crowding on the perturbation of protein hydration water dynamics.[16] PEG's appeal in protein crowding studies derives from its apparent inertness to proteins, high solubility, and lack of charges.[11, 15, 17]

There is ample evidence, however, from biochemical and biophysical studies that PEG is actually rather unusual, and is likely not an ideal model for universal macromolecular interactions.[18-19] In addition to the structured hydration shell discussed in detail below, PEG tends to aggregate in solution, rather than forming a homogeneous mixture.[20] In the present work, we find that even in highly concentrated and viscous PEG solutions, the water dynamics sensed with a vibrational probe differ negligibly, if at all, from bulk water. Complementary ultrafast IR spectroscopy measurements by Cho *et al*.[21] and by Fayer *et al*.[75] have reached similar conclusions, though using different spectroscopic observables. Inspired by the NMR approach taken by Han *et al*.,[22] we can rationalize the experimental results found here, as well as those recently reported by Cho *et al*., using a picture based on a structured hydration shell combined with the entropic hydrogen bond jumping framework developed by Laage *et al.*[23-24] We find that for PEGs with molecular masses greater than ~400 Dalton, the hydration dynamics is essentially bulk-like, even in concentrated solutions. In contrast, in low molecular mass PEG-400, we find strongly concentration dependent dynamics.

The influence of solutes on the dynamical aspects of water has been investigated using several experimental approaches. Considerable progress has been made using NMR, both ^{17}O spin relaxation and Overhauser dynamic nuclear polarization (ODNP) employing radical probes, providing complementary views of interfacial hydration. ^{17}O spin relaxation probes directly the orientational dynamics of the water molecules in the vicinity of macromolecules such as proteins, yielding a dynamical readout that averages over the whole hydration shell.[25-26] ODNP provides site-specific translational dynamics of the hydration water.[27-28] Ultrafast IR pump-probe and 2D-IR spectroscopy have been used to study water in concentrated solute solutions, or within micelles.[29-32] 2D-IR has also been used to study solute transitions under dilute conditions avoiding the effects of crowding.[33-36] In the case of these small molecule probes, whether neutral or ionic, the spectral dynamics obtained with 2D-IR correspond to the same time scales measured for neat water using 2D-IR without a probe. Ultrafast

dynamic fluorescence Stokes shift spectroscopy has been applied to protein hydration using tryptophan mutations that permit site-specific solvation dynamics.[37-40] THz spectroscopy of various aqueous solutions can isolate concentration dependent interfacial water dipole relaxation, and provided a notable observation of long-range hydration perturbation in protein solutions.[41-44] Optical Kerr effect (OKE) spectroscopy can provide dynamical information that is complementary to the THz studies, though due to water's nearly isotropic polarizability, OKE is sensitive to the collective intermolecular motions rather than to the dipolar reorientation.[45-47] The aspect of hydration dynamics perturbation that we address here is that which arises from macromolecular crowding or confinement. Based on previous work on proteins,[16, 43, 48] polymers,[21, 44] micelles,[32, 49-50] and carbohydrates,[51] it would be reasonable to expect that the extended networks macromolecular polymers have would create pools of water similar to micelles, and thus collectively slow the hydration water dynamics. As detailed in the following, we find both expected and unexpected trends, though we propose a unifying explanation based on the thermodynamics of PEG hydration[52] as well as the extended jump model for hydrogen bond reorientation.[23, 53-55]

2.2 EXPERIMENTAL METHODS

2.2.1 Equilibrium 2DIR Spectroscopy

2DIR spectroscopy uses three infrared femtosecond laser pulses to interact with the sample and create a third-order nonlinear signal that is proportional to the material response function.[56] There are three time delays in the experiment, which include the coherence evolution period (t_1), the waiting time delay (t_2), and the detection coherence period (t_3). Each delay follows the corresponding pulse of E_1, E_2, or E_3. The pulses interact with the sample in the noncollinear box[57] geometry in order to generate the signal in a background-free direction. Based on the possible field interactions, the responses can be divided into rephasing and nonrephasing responses, which are easily isolated experimentally.[58] In the rephasing pathway, the coherences produced during t_1

have phases that are conjugates of those generated during the detection period.[59] In the nonrephasing pathway, coherences evolve with the same phases during t_1 and t_3.[60]

During the experiments, t_1 is scanned using an optical delay line and the signal at each detection frequency ω_3 via a grating-based spectrometer is Fourier transformed to yield the ω_1 frequency axis. The phase and amplitude of the signal are measured directly in a spectrometer[61] via heterodyne detection and spectral interference with a local oscillator field.[57] Increasing the waiting time (t_2) between excitation and detection steps reveals dynamical changes in the 2D spectral features, which can be related to processes such as solvation dynamics, vibrational energy transfer, and vibrational energy relaxation.[62] Using 2D-IR, it is possible to extract information about solvent-solute interactions, vibrational dynamics, and molecular structure.[58] We have previously shown that transition metal carbonyl complexes are powerful probes of solution environments.[63-68]

A 2D-IR spectrum correlates an excited and detected frequency and spectral inhomogeneity is manifested in the 2D peak shape as a slant along the frequency diagonal. As the solute probe vibrations sample new environments, the correlation between the excited and detected frequencies is lost—a process known as spectral diffusion—and the peak shape becomes more symmetric. Spectral diffusion is an observable linked to the solvent environment of the probe used in experiments.[69] It has been shown by numerous studies that a variety of measures of the peak shape asymmetry can be related to the correlation function of frequency fluctuations.[70] The frequency-fluctuation correlation function (FFCF) is denoted as $C(t) = \langle \delta\omega(0)\delta\omega(t) \rangle$, where $\delta\omega(t)$ is the instantaneous fluctuation from the average frequency.[70] The inhomogeneous index, $I(t)$, which is directly proportional to the FFCF,[71] is extracted from 2DIR spectra as the amplitude difference of the rephasing and nonrephasing signals: $I(t) = (A_r - A_n)/(A_r + A_n)$,[71] where A_r is the rephasing signal amplitude, and A_n is the nonrephasing signal amplitude.

At early waiting times (t_2), the excitation and detection frequencies are well correlated because the probe has not had the chance to sample many

microscopic environments. As the waiting time (t_2) increases, correlation is lost as the probe samples more solvent environments. The timescale for this loss in correlation can be related to characteristic timescales of the solvent dynamics.[56]

2.2.2 Molecular Dynamics Simulation

The MD simulation of a short six-mer of PEG was done simply to investigate reasonable structural models for PEG hydration geometries. Similarly to a previously reported simulation by Oelmeier *et al.*,[72] we employed YASARA 14.6.5 using the Amber03 force field (TIP3P for the water), and the built-in function AutoSMILES to generate force field parameters for the PEG atoms. The simulation was run for more than 500 ps, and the figure in the main text is the final snapshot of that simulation. The simulation box had dimensions of 42 x 26 x 26 Å. Future work will investigate the structure and dynamics of hydrated PEG in more detail.

2.2.3 Sample Preparation

A water-soluble variant of $[Ru(CO)_3]_2(\mu\text{-}Cl)_2$ (Strem Chemicals), a carbon monoxide releasing molecule (CORM) commonly referred to as CORM-2, was synthesized for use in these studies. To create the water-soluble variant, the CORM-2 was sonicated in D_2O and heated up to 62°C for 24 minutes until no changes were observed in the FTIR spectrum. CORM-2 has the following IR-active carbonyl stretches: 1972, 2004, 2051, and 2075 cm^{-1}, whereas the water-soluble variant only has 2 observed bands at 1972 and 2051 cm^{-1}. We denote this water-soluble variant as Ru3C.

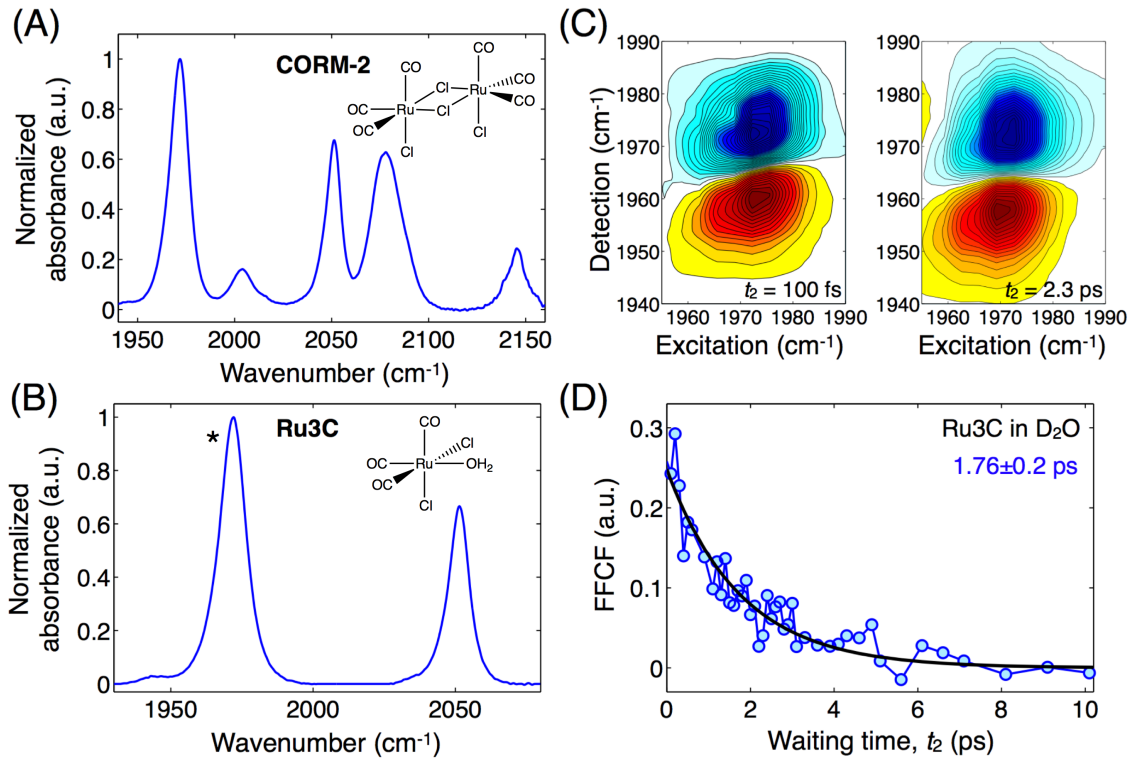

Figure 2.1 A new vibrational probe Ru3C is generated by reacting CORM-2 with water. This probe is water soluble and reports bulk water dynamics (1.76±0.2 ps) through the decay of the frequency-fluctuation correlation function in neat D_2O. Ru3C is the probe used to determine the hydration dynamics in aqueous solutions of poly(ethylene) glycol. (A) Linear FT-IR spectrum of CORM-2 in D_2O with its molecule structure; there are numerous carbonyl stretching bands due to a heterogeneity of structures. (B) The FT-IR of Ru3C in D_2O has two simple peaks consistent with a single tricarbonyl coordination. The asterisk denotes the band shown in (C) and analyzed in (D). (C) 2D-IR spectra of Ru3C at early (t_2 = 100 fs) and later (t_2 = 2.3 ps) waiting times. The slight diagonal elongation indicates a mild degree of inhomogeneous broadening, which disappears due to spectral diffusion. (D) The frequency-fluctuation correlation function of Ru3C in D_2O gives a single exponential time constant of 1.76±0.2 ps, which is consistent with bulk D_2O solvation dynamics.

PEG 400 (FW 400) is a linear macromolecule and an 8-9mer. PEG 2000 is a 45-mer, PEG 8000 is a 181-mer, and PEG 20000 is a 450-mer. Ru3C was combined with each of PEG 2000, PEG 8000, and PEG 20000 in concentrations ranging from 1% to saturation in D_2O. The number following PEG refers to the number of monomer units. PEG 400, a liquid, was dissolved in D_2O at increasing concentrations as separate samples with Ru3C. The specific concentrations used for this series of experiments were 0-90% PEG 400 by volume.

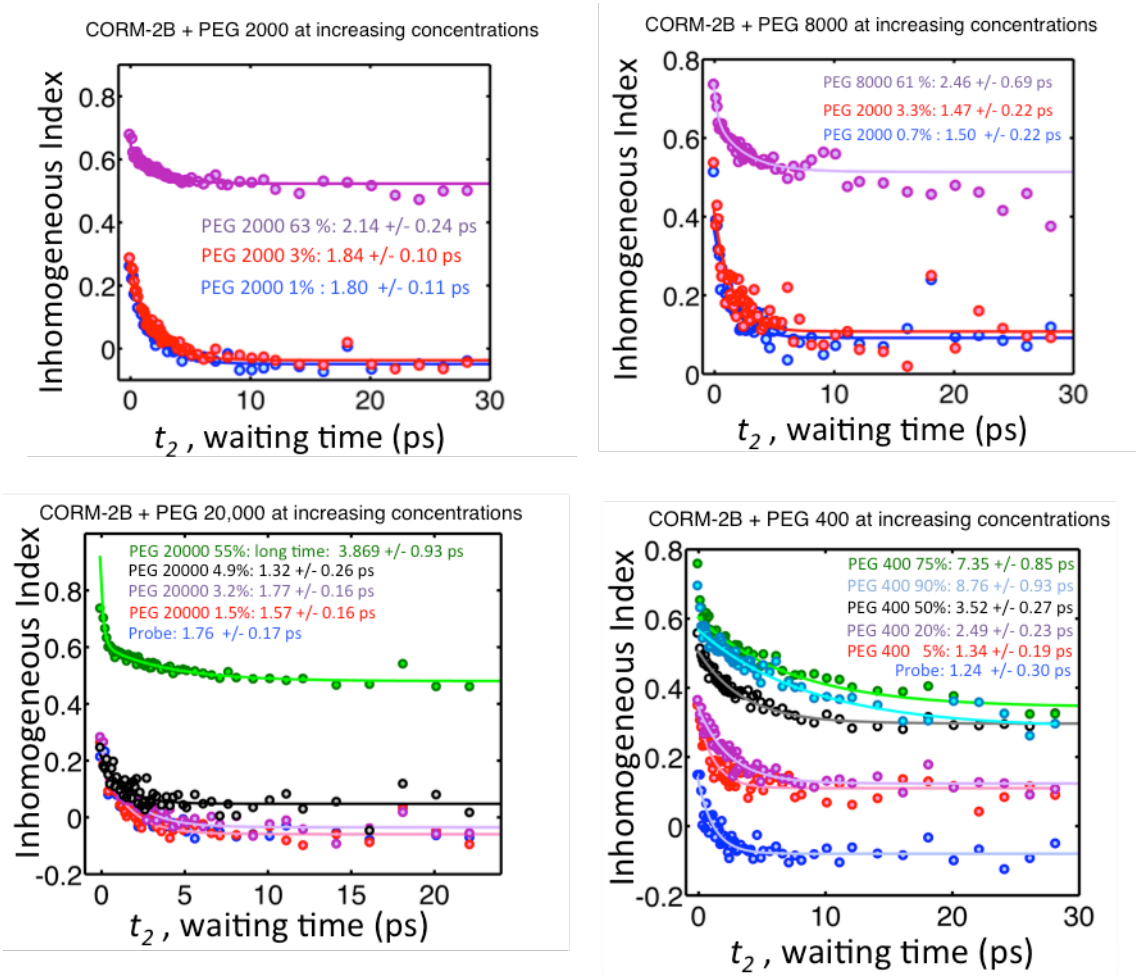

Figure 2.2 Hydration dynamics probed with the 1972 cm^{-1} band of Ru3C in D_2O/PEG mixtures The maximum t_2 delay collected for all spectra is 30 ps. For the high polymer concentrations the FFCF decays become biexponential; the slower component for each case is reported in the figure.

2.3 RESULTS

2.3.1 Water Soluble Transition Metal Complex Senses Bulk Water Dynamics

Previous studies have found that the hydration dynamics of water can be probed using the carbonyl stretch of transition metal carbonyl complexes, and that the frequency-fluctuation correlation function (FFCF) decays of the carbonyl stretch agree quantitatively with the spectral diffusion time scales of the OH stretch of water determined with 2D-IR spectroscopy of neat water.[16, 36] We use metal carbonyls because they provide an intense signal in an isolated region of the IR spectrum. The FTIR spectrum in D_2O (**Fig. 2.1 A**) of $[Ru(CO)_3]_2(\mu\text{-}Cl)_2$, a carbon monoxide releasing molecule (CORM) commonly referred to as CORM-

2,[73] shows several bands in the CO stretching region near 2000 cm^{-1}. CORM-2 is sparingly soluble in polar solvents, and reacts on a relatively slow time scale under ambient conditions, enabling 2D-IR measurements in water and methanol.[36, 74] The community that uses CORMs to deliver CO in biological contexts, however, typically employs the more soluble gycinate derivative, known as CORM-3, which is a mononuclear Ru complex with three carbonyl ligands.

Table 2.1 Fitting results for PEG 400 data

PEG 400 5%	PEG 400 20%	PEG 400 50%	PEG 400 75%	PEG 400 90%
General model: f(x) = a*exp(-x/b)+c Coefficients (with 95% confidence bounds): a = 0.2041 (0.1737, 0.2344) b = 1.304 (0.9283, 1.68) c = 0.1097 (0.097, 0.1224) Goodness of fit: SSE: 0.04648 R-square: 0.7915 Adjusted R-square: 0.7838 RMSE: 0.02934	General model: f(x) = a*exp(-x/b)+c Coefficients (with 95% confidence bounds): a = 0.2145 (0.1963, 0.2328) b = 2.485 (2.027, 2.943) c = 0.1231 (0.1124, 0.1339) Goodness of fit: SSE: 0.02254 R-square: 0.9128 Adjusted R-square: 0.9096 RMSE: 0.02025	General model: f(x) = a*exp(-x/b)+c Coefficients (with 95% confidence bounds): a = 0.2075 (0.194, 0.2209) b = 3.518 (2.976, 4.059) c = 0.2964 (0.2869, 0.306) Goodness of fit: SSE: 0.01347 R-square: 0.9472 Adjusted R-square: 0.9453 RMSE: 0.01565	General model: f(x) = a*exp(-x/b)+c Coefficients (with 95% confidence bounds): a = 0.2588 (0.2373, 0.2804) b = 7.345 (5.648, 9.043) c = 0.3434 (0.3213, 0.3655) Goodness of fit: SSE: 0.0278 R-square: 0.936 Adjusted R-square: 0.9337 RMSE: 0.02248	General model: f(x) = a*exp(-x/b)+c Coefficients (with 95% confidence bounds): a = 0.2824 (0.2599, 0.3048) b = 8.763 (6.904, 10.62) c = 0.2835 (0.2589, 0.3081) Goodness of fit: SSE: 0.01907 R-square: 0.9498 Adjusted R-square: 0.9479 RMSE: 0.01879

Table 2.2 Fitting results for PEG-2000 data

PEG 2000 1%	PEG 2000 3%	PEG 2000 63%
General model: f(x) = a*exp(-x/b)+c Coefficients (with 95% confidence bounds): a = 0.2751 (0.2577, 0.2926) b = 1.843 (1.613, 2.073) c = -0.04929 (-0.05786, -0.04072) Goodness of fit: SSE: 0.01615 R-square: 0.9538 Adjusted R-square: 0.9521 RMSE: 0.01762	General model: f(x) = a*exp(-x/b)+c Coefficients (with 95% confidence bounds): a = 0.2937 (0.2768, 0.3106) b = 1.842 (1.633, 2.051) c = -0.03723 (-0.04554, -0.02891) Goodness of fit: SSE: 0.01521 R-square: 0.9616 Adjusted R-square: 0.9601 RMSE: 0.0171	General model: f(x) = a*exp(-x/b)+c*exp(-x/d)+e Coefficients (with 95% confidence bounds): a = 0.1073 (0.09643, 0.1181) b = 2.137 (1.651, 2.623) c = 0.006689 (-0.0636, 0.07698) d = 0.05312 (-0.2388, 0.3451) e = 0.523 (0.5164, 0.5295) Goodness of fit: SSE: 0.003595 R-square: 0.9478 Adjusted R-square: 0.9431 RMSE: 0.008938

When heated in water, CORM-2 reacts with water rapidly to form a stable complex. CORM-2 is not stable in water, and according to previous work, we hypothesize that it reacts to form $RuCl_2(CO)_3(OH_2)$, which we denote "Ru3C" (**Fig. 2.1 B**).[75-78] Ru3C is water soluble with two simple CO stretching bands. The 2D-IR spectrum of Ru3C in D_2O (**Fig. 2.1 C**) shows moderate inhomogeneous broadening indicated by the elongated line shape at early waiting time (t_2 = 100 fs), which becomes more homogeneously broadened with increased waiting time delay. The asymmetry is due to slight reabsorption. The emitted field can be reabsorbed as it propagates through an optically dense sample; subsequent signal absorption can cause spectral distortion.[79] The exponential spectral diffusion (**Fig. 2.1 D**) time constant for Ru3C in D_2O is 1.76±0.2 ps, which is consistent with the time scale determined directly using 2D-IR spectroscopy of HOD in D_2O.[80] Tables of fitting functions of all FFCFs are located in **Tables 2.1-2.4**. The maximum t_2 delay collected for all spectra is 30 ps, and we do not see appreciable decay on that timescale (**Fig. 2.2**).

Table 2.3 Fitting results for PEG 8000 data

PEG 8000 1%	PEG 8000 3.30%	PEG 8000 61%
General model: f(x) = a*exp(-x/b)+c Coefficients (with 95% confidence bounds): a = 0.2675 (0.2264, 0.3086) b = 1.496 (1.053, 1.939) c = 0.09139 (0.07323, 0.1096) Goodness of fit: SSE: 0.08319 R-square: 0.8189 Adjusted R-square: 0.8119 RMSE: 0.04	General model: f(x) = a*exp(-x/b)+c Coefficients (with 95% confidence bounds): a = 0.2964 (0.2512, 0.3415) b = 1.465 (1.035, 1.895) c = 0.1078 (0.08801, 0.1275) Goodness of fit: SSE: 0.09973 R-square: 0.8001 Adjusted R-square: 0.7924 RMSE: 0.04379	General model: f(x) = a*exp(-x/b)+c*exp(-x/d)+e Coefficients (with 95% confidence bounds): a = 0.1339 (0.1001, 0.1676) b = 2.462 (1.075, 3.849) c = 0.06244 (0.01265, 0.1122) d = 0.2839 (0.02201, 0.5458) e = 0.5137 (0.4954, 0.532) Goodness of fit: SSE: 0.007602 R-square: 0.9357 Adjusted R-square: 0.9294 RMSE: 0.01362

Table 2.4 Fitting results for PEG 20000 data

PEG 20000 1.50%	PEG 20000 3.20%	PEG 20000 4.90%	PEG 20000 55%
General model: f(x) = a*exp(-x/b)+c Coefficients (with 95% confidence bounds): a = 0.2639 (0.2361, 0.2918) b = 1.567 (1.247, 1.887) c = -0.05921 (-0.07183, -0.04659) Goodness of fit: SSE: 0.03896 R-square: 0.8818 Adjusted R-square: 0.8773 RMSE: 0.02737	General model: f(x) = a*exp(-x/b)+c Coefficients (with 95% confidence bounds): a = 0.2654 (0.2412, 0.2895) b = 1.766 (1.452, 2.081) c = -0.03496 (-0.04657, -0.02334) Goodness of fit: SSE: 0.03051 R-square: 0.9125 Adjusted R-square: 0.9091 RMSE: 0.02422	General model: f(x) = a*exp(-x/b)+c Coefficients (with 95% confidence bounds): a = 0.1842 (0.1491, 0.2192) b = 1.32 (0.8239, 1.817) c = -0.1012 (-0.1167, -0.08564) Goodness of fit: SSE: 0.05969 R-square: 0.6866 Adjusted R-square: 0.6746 RMSE: 0.03388	General model: f(x) = a*exp(-x/b)+c*exp(-x/d)+e Coefficients (with 95% confidence bounds): a = 0.1259 (0.1081, 0.1437) b = 3.869 (2.003, 5.735) c = 0.1795 (0.1541, 0.2048) d = 0.1804 (0.1493, 0.2114) e = 0.4802 (0.456, 0.5044) Goodness of fit: SSE: 0.003939 R-square: 0.9663 Adjusted R-square: 0.963 RMSE: 0.009802

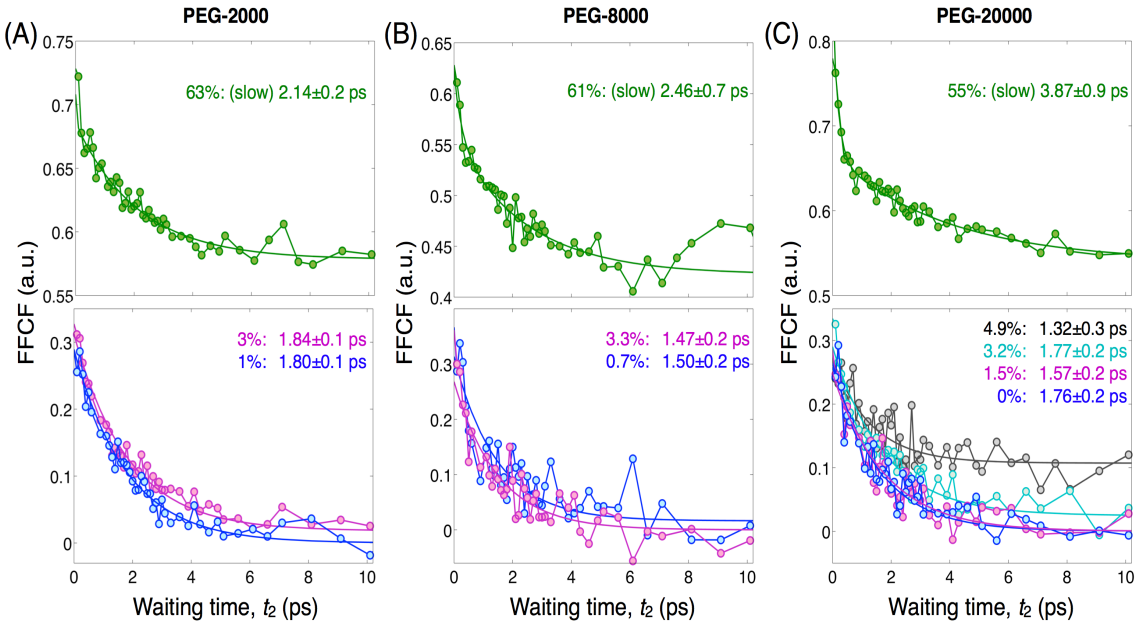

Figure 2.3 Hydration dynamics probed with the 1972 cm^{-1} band of Ru3C in D_2O/PEG mixtures. For the high polymer concentrations the FFCF decays become biexponential; the slower component for each case is reported in the figure. (A) FFCFs for Ru3C in D_2O/PEG-2000 mixtures, ranging from 1% PEG concentration to saturation at 63% PEG concentration. (B) FFCFs for Ru3C in D_2O/PEG-8000 mixtures, ranging from 0.7% PEG concentration to saturation at 61% PEG concentration. (C) FFCFs for Ru3C in D_2O/PEG-20000 mixtures, ranging from pure D_2O (0% PEG) to saturation at 55% PEG concentration. At the high concentrations, the decays appear biexponential, and the time constants quoted are the slow component. Despite some variations with concentration, the overall trend is that the probed solvation dynamics are weakly dependent on concentration, if at all.

2.3.2 Solutions of PEG-2000, PEG-8000, and PEG-20000 Exhibit Bulk-like Hydration Dynamics

Using the Ru3C probe, we studied the ultrafast spectral dynamics using 2D-IR in a series of PEG solutions, varying both the molecular mass of the polymer and its concentration in D_2O. In contrast to our previous studies of covalently labeled proteins in crowded solutions, for all of the concentrations of each mixture (**Fig. 2.3**) we find that the timescales of spectral diffusion do not significantly vary between 1-5 wt% for all lengths of PEG examined. The spectral diffusion time constant for each mixture of each polymer yields a similar value to that of Ru3C in D_2O, within error. This finding is somewhat unexpected since the viscosities of the solutions, though molecular mass dependent, are very high. For example, a 3% solution of PEG-2000 has a viscosity of 1197 cP, and a 3% solution of PEG-20000 has a viscosity of 2593 cP.[81] It is nevertheless not uncommon that dynamical processes slip from a simple hydrodynamic (i.e. viscosity dependent)

behavior.[82-83] Linear FT-IR Spectra of Ru3C in D2O/PEG-2000, D2O/PEG-8000, and D2O/PEG-20000 mixtures of increasing concentrations are shown in **Fig 2.4-2.6**.

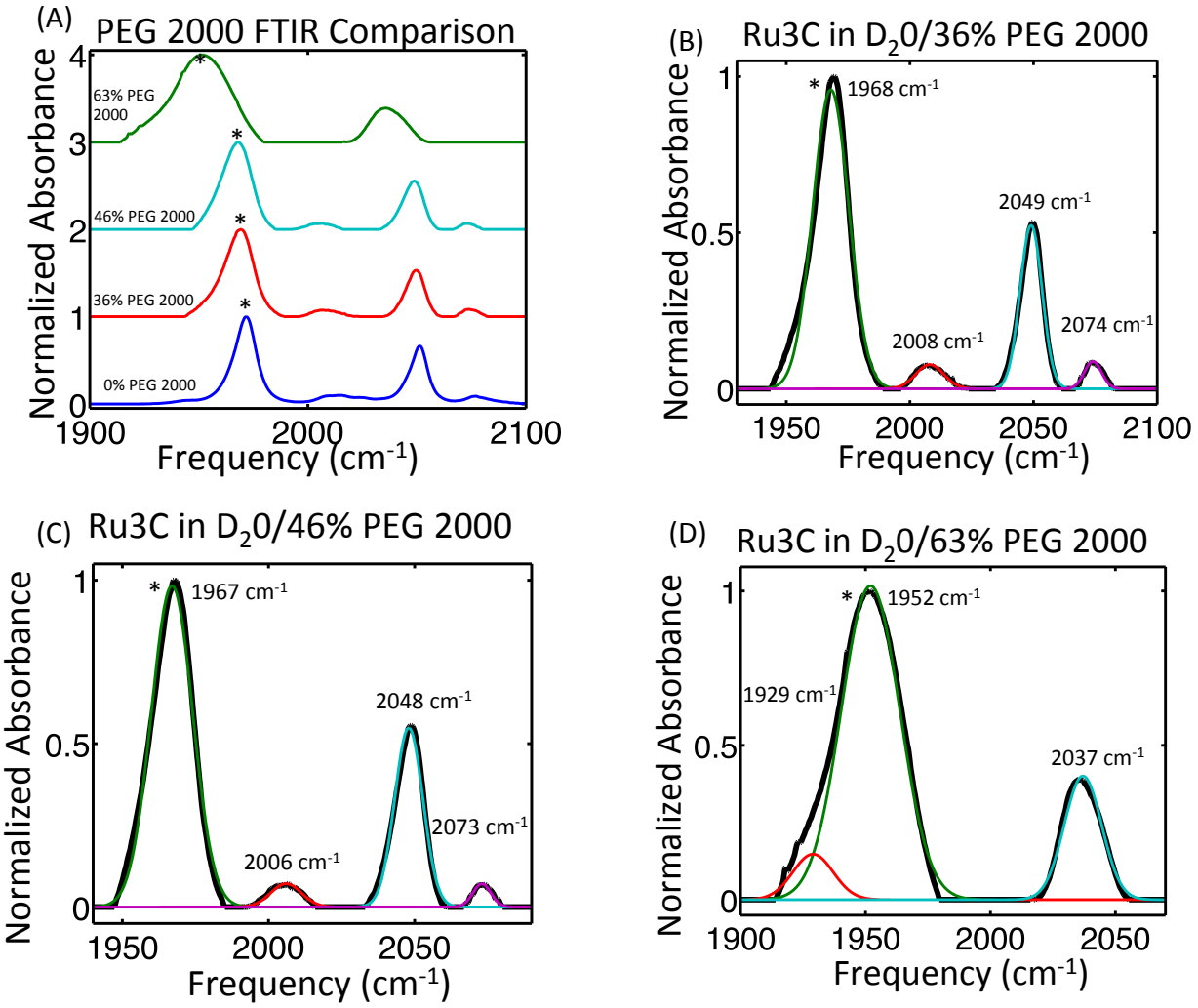

Figure 2.4 Linear FT-IR Spectra of Ru3C in D_2O/PEG-2000 mixtures of increasing concentrations. The asterisks denote the mode analyzed. (A) Linear FT-IR of Ru3C in increasing concentrations of PEG-2000 in D_2O; the peaks show some shifts and changes in intensity. (B) Fitted linear FT-IR spectra of Ru3C in D_2O/36% PEG 2000 (C) Fitted linear FT-IR spectra of Ru3C in D_2O/46% PEG 2000 (D) Fitted linear FT-IR spectra of Ru3C in D_2O/63% PEG 2000

Even at very high polymer concentration, we observe either a bulk-like or only slightly slowed spectral diffusion time constant in PEG-2000, 8000, and 20000. The higher concentrations appear to exhibit biexponential decays, though fitting with single exponentials yields similar time scales for PEG-2000 and 8000. The fast component may arise from a wobbling-in-cone motion, as has been observed in studies of other vibrational chromophores under confinement.[84-85]

We also note that the saturated samples are more highly scattering, which may add a spurious fast component. Since we cannot distinguish these two origins, we choose to focus on the clear slower component of the correlation function decay. At saturation, 63% PEG-2000 yields a very similar time scale (2.14±0.2 ps slow and 0.053 ps fast) compared with the more dilute solutions, but this FFCF does not decay to zero, implying a significant contribution due to dynamics on time scales longer than can be accessed with the finite probe lifetime of 11.5±0.3 ps. We would anticipate that the structural heterogeneity and associated motion of the polymer chains, as well as water-mediated cross-linking is responsible for the slower time scale.[86-87]

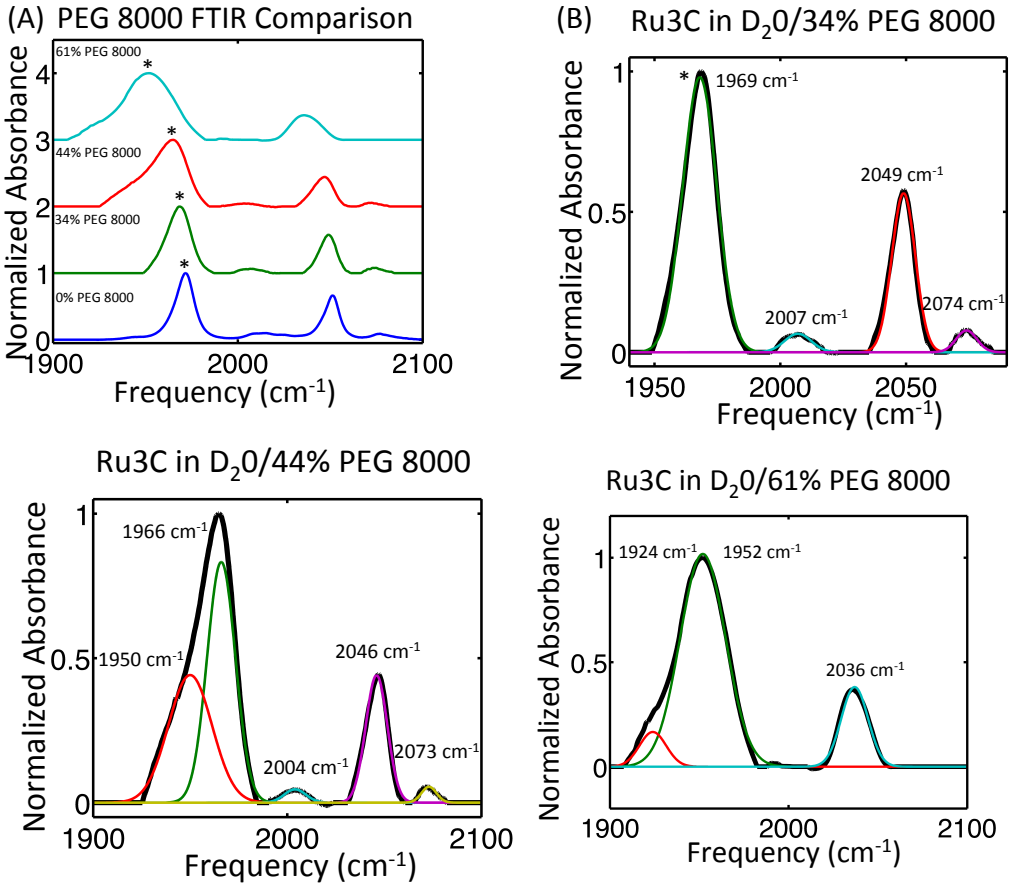

Figure 2.5 Linear FT-IR Spectra of Ru3C in D_2O/PEG-8000 mixtures of increasing concentrations. The asterisks denote the mode analyzed. **(A)** Linear FT-IR of Ru3C in increasing concentrations of PEG-8000 in D_2O; the peaks show some shifts and changes in intensity. **(B)** Fitted linear FT-IR spectra of Ru3C in D_2O/34% PEG 8000 **(C)** Fitted linear FT-IR spectra of Ru3C in D_2O/44% PEG 8000 **(D)** Fitted linear FT-IR spectra of Ru3C in D_2O/61% PEG 8000

Both high concentration PEG-8000 and 20000 exhibit the same general features seen in PEG-2000, though we do note that the saturated (55%) PEG-20000 solution shows a slower time scale. The spectral diffusion time constants are 0.18±0.02 ps (fast) and 3.87±0.9 ps (slow). A significant offset is also present in the lower 4.9% concentration of PEG-20000, which indicates the contribution from the slow phase of chain motion.

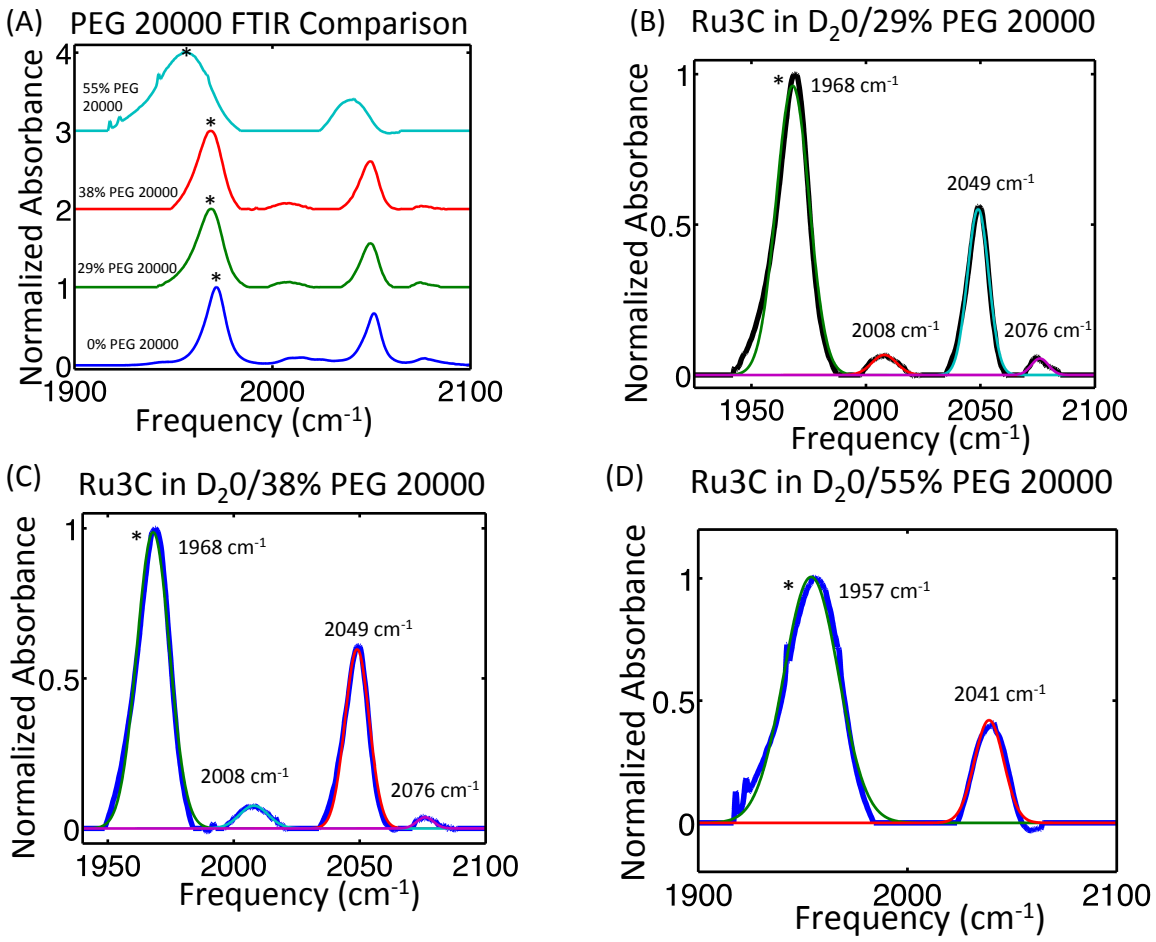

Figure 2.6 Linear FT-IR Spectra of Ru3C in D_2O/PEG-20000 mixtures of increasing concentrations. The asterisks denote the mode analyzed. (A) Linear FT-IR of Ru3C in increasing concentrations of PEG-20000 in D_2O; the peaks show some shifts and changes in intensity. (B) Fitted linear FT-IR spectra of Ru3C in D_2O/29% PEG 20000 (C) Fitted linear FT-IR spectra of Ru3C in D_2O/38% PEG 20000 (D) Fitted linear FT-IR spectra of Ru3C in D_2O/55% PEG 20000

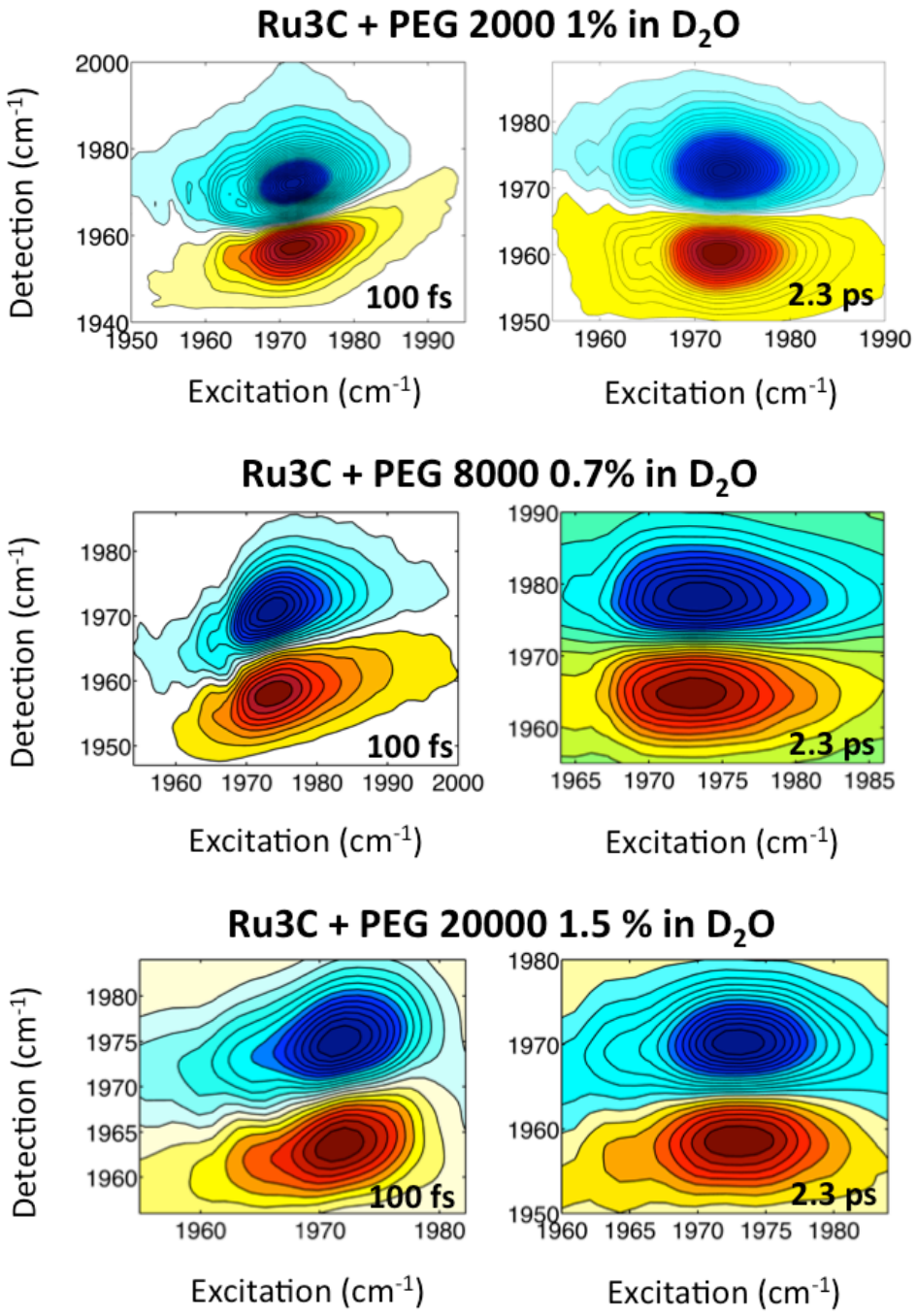

Figure 2.7 2D-IR spectra of Ru3C + PEG at various lengths and concentrations at early (t_2 = 100 fs) and later (t_2 = 2.3 ps) waiting times. The slight diagonal elongation indicates a mild degree of inhomogeneous broadening, which disappears due to spectral diffusion.

2.3.3 A Dynamical Transition in PEG-400 at the Overlap Concentration (*c**)

Our earlier work on protein crowding used the lower molecular mass PEG-400 primarily because its radius of gyration (~2 nm) is similar in size to a protein.[16] It is also a liquid, and is more soluble in water than the higher

molecular mass PEGs discussed so far. FTIR spectra of Ru3C in a range of PEG-400 solutions in D_2O (**Fig 2.7)** clearly indicate that multiple species are present at higher PEG-400 concentration. At high concentrations, Ru3C is possibly binding, or tightly associating, to PEG-400, which could lead to the new peaks in the spectrum (**Fig. 2.8 A**). Similarly to how crown ethers act as ionophores, linear PEGs have also been found to associate with cations.[88-89]

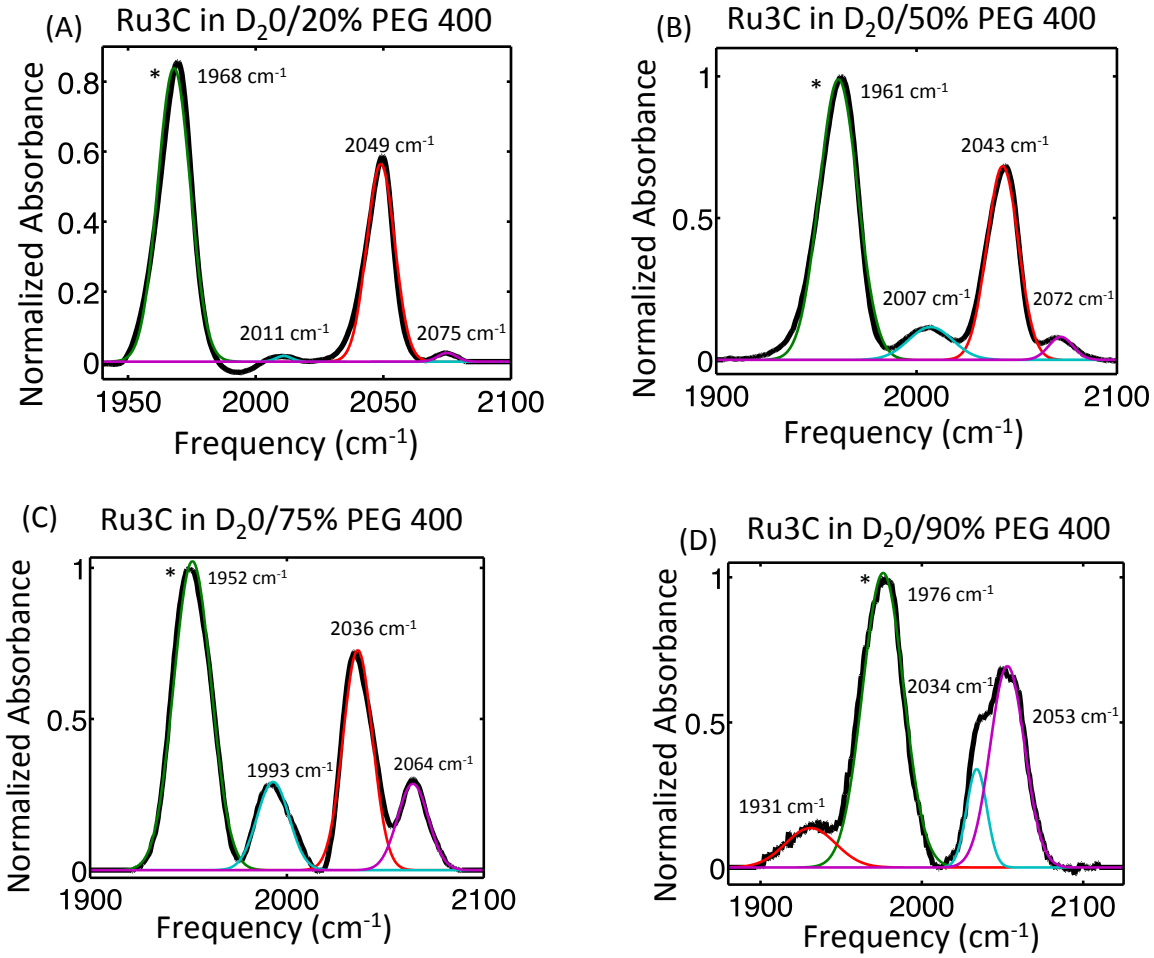

Figure 2.8 Linear FT-IR Spectra of Ru3C in D_2O/PEG-400 mixtures of increasing concentrations. The asterisks denote the mode analyzed. (A) Fitted linear FT-IR spectra of Ru3C in D_2O/20% PEG 400 (B) Fitted linear FT-IR spectra of Ru3C in D_2O/50% PEG 400 (C) Fitted linear FT-IR spectra of Ru3C in D_2O/75% PEG 400 (D) Fitted linear FT-IR spectra of Ru3C in D_2O/90% PEG 400

The shift of the spectrum back to the blue at high PEG-400 concentration is qualitatively distinct from what we observe in the longer PEGs (see **Fig 2.4-2.6**), where we do not see the non-monotonic band shifting. Because the maximum

concentration is limited by saturation, it is not known what the spectrum would be for very high concentrations of the longer chains.

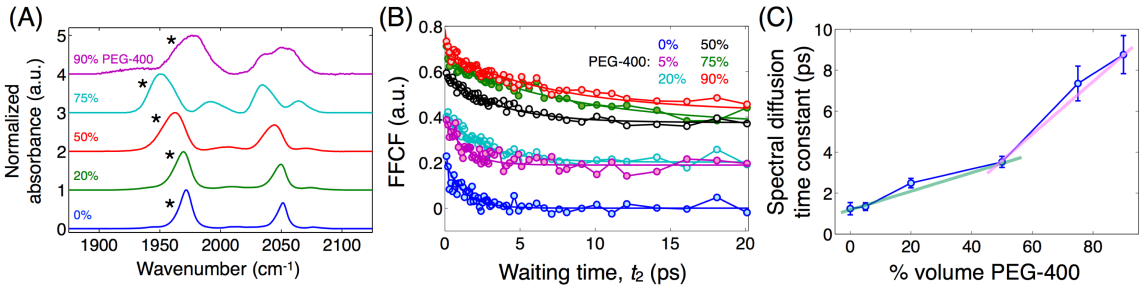

Figure 2.9 Linear FTIR Spectra, FFCFs and hydration dynamics of Ru3C in D_2O/PEG-400 mixtures. (A) Linear FT-IR of Ru3C in increasing concentrations of PEG-400 in D_2O; the peaks show some shifts and changes in intensity. The asterisks denote the mode analyzed in (B). (B) FFCFs for the lowest frequency CO stretching mode of Ru3C in D_2O/PEG-400 mixtures, ranging from pure D_2O to 90% PEG by volume. (C) Spectral diffusion timescale plotted as a function of mixture composition (% v/v). There appear to be two roughly linear regimes, with a slight transition around 50%. The lines are guides to the eye.

With increasing concentrations of PEG-400, the spectral dynamics (**Fig. 2.8 B**) do exhibit a monotonic and gradual slowdown, as well as an offset increase. As the concentration is increased to 90% (v/v), the spectral diffusion time constant slows to 8.76±0.9 ps. Plotting the spectral diffusion time constant versus the volume % of PEG-400 shows a gradual dependence (**Fig. 2.8 C**), and two lines drawn to guide the eye hint at a transition near 50%. This concentration is very close to the critical overlap concentration, where chains from different PEG molecules begin to overlap in a good solvent. We discuss this point in greater detail below.

2.3.4 Spectral Analysis

The homogeneous and inhomogeneous contributions to the total line width were extracted using a procedure introduced by Kwak et al. where the homogeneous widths are taken to be Lorentzian and the inhomogeneous widths are Gaussian.[90] For any given PEG, increasing the concentration causes increases in both the homogeneous and inhomogeneous contributions to the total line width (see **Table 2.5** and **Fig 2.9**). At low concentration, increasing molecular mass leads to decreased inhomogeneous line widths, whereas at high concentration, the trend appears to be reversed, and the inhomogeneity grows with greater chain length. The homogeneous widths, with the exception of PEG-

400, increase with chain length at low concentration. At high concentration all of the solutions show decreased homogeneous width with chain length.

Table 2.5 Line shape contributions for low and high concentration solutions.

		PEG 400	PEG 2000	PEG 8000	PEG 20000
low %	W_G	7.4	7.1	6.6	4.9
	W_L	12.6	6.9	8.0	9.2
high %	W_G	11.9	10.3	14.3	17.0
	W_L	17.3	27.0	25.9	21.3

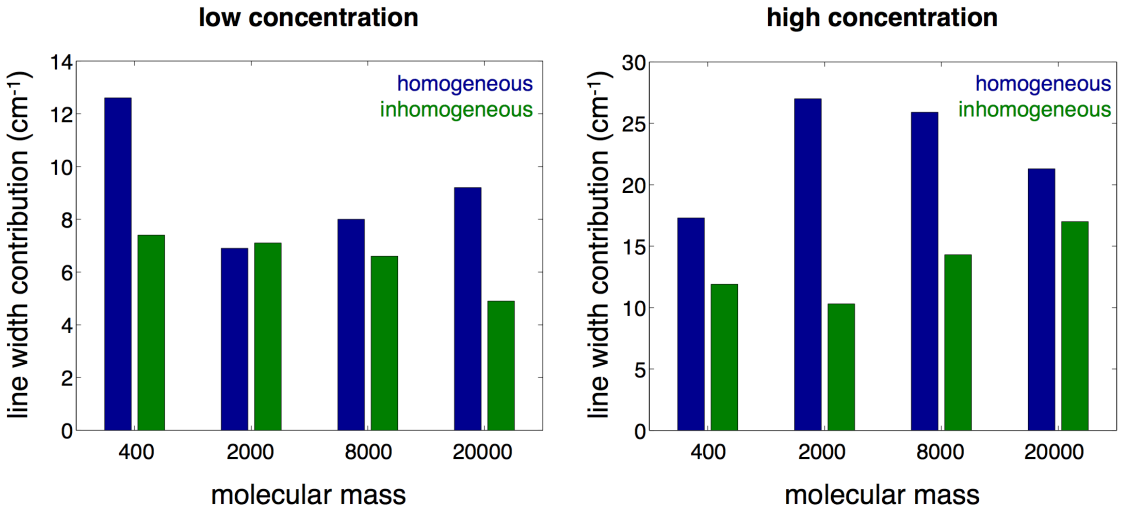

Figure 2.10 Bar plots of the line shape data shown in Table S7.

2.4 DISCUSSION

2.4.1 PEG's Stable Water Shell Templates a Bulk-like Iceberg

In the case of the longer PEGs, we find that the water dynamics of concentrated solutions sensed with the Ru3C vibrational probe differ very little,

with the main difference apparent as an offset reflecting slow chain dynamics. We note that work by Cho *et al.* has found orientational and population relaxation dynamics of three different probes in PEG-1000 solutions to exhibit a similar weak concentration dependence, except at concentrations where the conformation of the polymer is thought to change.[21] Rubinson et al. have conducted several small angle neutron scattering and vibrational spectroscopy measurements of a wide range of PEGs, finding some support for a collective hydration picture from a structural perspective.[91-93]

There are other studies of macromolecular crowding where despite very high protein concentrations, in some cases only a bulk-like water signature emerges. For example, Han *et a*l., used NMR Overhauser dynamic nuclear polarization to probe the hydration dynamics at the protein surface of wild-type human γS-crystallin (γS-WT) and the G18V mutant (γS-G18V), which leads to aggregation and cataracts.[22] The wild-type protein was found to be associated with bulk-like water dynamics, whereas the mutant protein induced a slowdown of the water dynamics. These differences were interpreted as being due to a more stable hydration shell around the wild-type protein, which somehow becomes disrupted by the mutation.

Fayer *et al*. used IR pump-probe spectroscopy to measure vibrational and orientational relaxation of water hydrating a short tetramer of PEO (tetraethylene glycol dimethyl ether).[94] They found two time scales corresponding, respectively, to the tightly associated water molecules, and to the bulk. The reported time scales were not found to be strongly dependent on the solute concentration. Due to the small size of the tetramer it is likely that collective crowding does not occur, which explains the lack of a concentration dependence. Similar results have been found for protein hydration in water-glycerol solutions.[36]

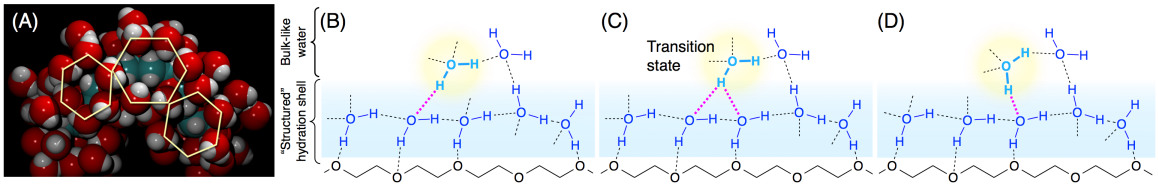

Figure 2.11 Clathrate structure and extended angular jump model. (A) MD simulations shows that water adopts constrained clathrate like packing to avoid the hydrophobic ethylene units, but is nevertheless able to maintain much of its hydrogen bonding network due to the favorable O–O spacings, which effectively template a bulk water structure. (B)-(D) Within the extended angular jump model describing hydrogen bond rearrangements,[54] a highly stable first hydration layer presents a bulk water like surface to subsequent hydration layers. A water molecule (highlighted in yellow) attempting to switch hydrogen bonding partners is unimpeded due to the availability of the three-body transition state structure. The highly stable first hydration shell cloaks the polymer's presence from the other water, and lacking the entropic reduction typically induced by extended interfaces, most of the water behaves like the bulk liquid.

The question that remains to be addressed is: why would a "stable" hydration shell promote bulk-like hydration dynamics? For the case of PEG, we can rationalize this finding by combining the current picture of hydrogen bond reorientation with the specific thermodynamics of aqueous PEG. With the identification by Laage and Hynes of extended angular jumps as the major contribution to hydrogen bond rearrangements,[95] a solute's inhibition of these jumps hinges on its ability to alter the availability of hydrogen bonding partners (**Fig. 2.10 B-D**).[23, 96] With this entropic origin of the interface's influence, for extended interfaces it is straightforward to predict the slowdown of angular jumps to be roughly a factor of two because the surface depletes half of the potential hydrogen bonding partners for interfacial water molecules.[23] Our prior experiments are consistent with this excluded volume explanation, where we find hydration dynamics to slow by roughly a factor of two in the vicinity of proteins and membranes.[36, 97] Simulations by Laage *et al*. of several different proteins support the theoretical prediction as well.[53] It would seem obvious that a large polymer would also slow the dynamics of water since it is likely to present an extended interface, or to create water pools similar to reverse micelles, where slowed water is also found.[49]

There is an aspect of PEG hydration that has been known for decades, but now assumes added importance in PEG's preservation of bulk water dynamics. It is well established that PEG exhibits somewhat unusual solution thermodynamics. The enthalpy of solution of PEG in water is negative, indicating

that there are more favorable interactions in the solution than in the separated species.[52] Since the primary energetic contribution is hydrogen bonding, the exothermicity of solution indicates that water loses very few hydrogen bonds, since it can form them with PEG's oxygen atoms. The entropy of solution is also negative, indicating that despite the intrinsic entropy increase associated with mixing, and the potentially increased configurational flexibility of the polymer, the constraints on the water overwhelm the net entropy balance. It is worth noting that a *trans-gauche-trans* helical conformation in solution, which is similar to the PEG crystal structure, does not contribute as much entropy as would be expected for a random coil polymer. The water becomes constrained specifically so that it can make the new hydrogen bonds with the polymer. In other words, both the entropy and enthalpy are driven by the same underlying microscopic structural origin of maintaining water's hydrogen bonding network.

Within the framework of the Lum-Chandler-Weeks picture of hydration, the preservation of hydrogen bonds suggests that PEG of any molecular mass functions practically as a "small" solute.[98-99] Of course, it is not small. Rather, it can preserve the network due to the particular arrangement of oxygen atoms. Although the CH_2–O–CH_2–CH_2– units are chemically inert,[11, 17] the specific structural arrangement of the oxygen atoms, coupled with the hydration shell, imparts remarkable activity to the PEG.[52] This peculiar aspect of PEG is further magnified when compared to the apparently similar polyethers poly(methylene)glycol (–OCH_2–O–) and poly(trimethylene)glycol (–O$CH_2CH_2CH_2$–O–), neither of which is soluble in water to any extent because the oxygen spacings are incommensurate with the water network.

When PEG is dissolved in water, the water network is extended because of the incorporation of the PEG ether oxygens. The interstitial methylene units decidedly restrict hydrogen-bonding opportunities and become surrounded by local water cages. In those regions the water adopts a clathrate hydrate like packing that enhances the water structure templated by the polymer. In the clathrate structure (**Fig. 2.10 A**), water voids provide free volume to accommodate temporary solvent repacking without suffering high-energy density

increases. A simple molecular dynamics simulation illustrates that the stable water molecules form hexagonally arranged water structures connecting adjacent oxygens.[72] This hexagonal motif is the primitive building block of an ice 1_h structure, though clearly lacking a long-range ice structure due to the twisted conformation of the underlying polymer.

Because PEG's oxygens are geometrically compatible with the bulk liquid water network, the tight integration of the PEG/water interface results in a highly "structured" hydration layer. Although those hydration shell water molecules are excessively constrained dynamically,[94] they are nevertheless fully capable of participating passively in the hydrogen bond rearrangements of the second hydration shell. In other words, except for the water molecules directly in contact with the PEG, there should be little, if any, dynamical perturbation to the majority of hydrogen bond rearrangements. It is interesting to consider the case of DNA, which also has been found to cause tight association of water using 2D-IR spectroscopy,[100] but appears to promote mobile water signatures when viewed using ODNP NMR spectroscopy.[27]

Absent an increased entropic barrier, there is no excluded volume effect for PEG-2000, 8000, and 20000. Here, the idiosyncratic structure of PEG imposes a new contribution that lies in between these two regimes. Because of the periodic and fortuitous placement of the oxygen atoms, hydrogen bond acceptors constructively support a bulk water hydration interface. An entropic penalty must ultimately be paid in creating iceberg-like structures.

2.4.2 Degree of Monomer Hydration (water/EO) Reveals a Sharp Transition Near the Overlap Concentration

Clearly, PEG-400 alters the hydration dynamics more than the longer chain polymers. It is therefore possible that PEG-400 has a less stable hydration shell. Because it is a short 8-9-mer, the end groups of PEG-400 have the potential to contribute significantly to the concentration dependent hydration dynamics.[52]

Several aspects of PEG's solution thermodynamics have been shown to be chain length and concentration dependent. Diluting PEG/water solutions is

exothermic. A study of PEG-6000 found that heats of dilution become less exothermic at increasing concentrations.[101] Similarly, the heat of solution of PEG-20000 in water at increasing concentration becomes less exothermic.[102] In general, heats of dilution and solution increase in exothermicity with decreased molecular mass,[102-104] which is consistent with the high solubility of PEG 400 and with the decreased saturation concentrations of larger chain PEGs. As molecular mass increases, the exothermicity of solution is unable to compensate the entropic cost of constraining the hydration water, and the solubility limit decreases.[105]

The Flory-Huggins theory provides a framework to decompose solution thermodynamics into polymer-polymer, polymer-solvent and solvent-solvent interactions using the interaction parameter χ. $\chi>0$ corresponds to polymer-solvent contacts being less favored than polymer-polymer or solvent-solvent contacts. $\chi<0$ corresponds to polymer-solvent contacts being more favored, promoting solvation of the polymer. Kagemoto *et al*. found the interaction parameter χ to decrease with decreasing molecular mass of the PEG polymer chain.[103] Also, short chain PEGs have more negative χ, which correlates to PEG's solubility increases as chain length decreases.[106] In addition to chain length trends, it has been found that for increasing concentrations, the χ value becomes less negative,[102] indicating that polymer-polymer and solvent-solvent contacts are more preferred at higher concentrations. Combining these thermodynamic trends (increased concentrations creating less exothermic solutions and trends in χ), we feel it is reasonable to conclude that the shorter PEGs do indeed promote a less stable hydration shell than do the longer chain polymers, which in turn enables a collective slowdown of hydration dynamics leading to a crowding transition.

It is possible to compare our findings with structural information obtained using neutron scattering. Modeling the structure factor with an ansatz based on the formation of planar sheets in solution, Rubinson et al.[92] propose that molecule-thick sheets are separated by water on length scales (10-40 Å) comparable to what we[16] and others[41, 44, 107-108] have found in the context of

collective hydration of biomolecules. Within this picture, one would expect a pronounced slowdown due to the extended interface, coupled with the collective influence of two or more such interfaces. The observed lack of a pronounced concentration-dependent slowdown is, nevertheless, compatible with the stable hydration shell PEG establishes because water molecules beyond the first shell see a bulk-water-like interface. The inter-sheet water molecules are effectively masked from the PEG by the highly constrained first hydration shell. Although our experiments are unable to address the nature or existence of the hypothesized sheets, future simulation studies should be able to test these models.[109]

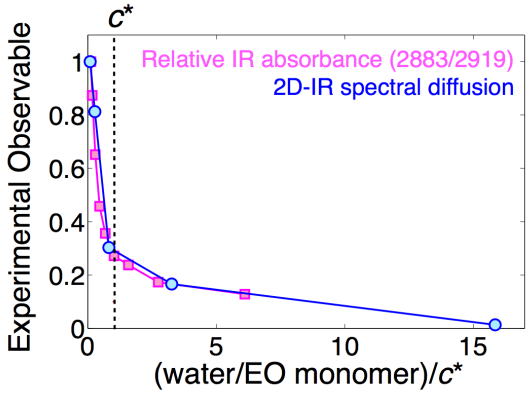

Figure 2.12 A comparison between D_2O/PEGME-1000 mixtures and D_2O/PEG-400 mixtures showing identical hydration dependence when concentrations are scaled to the overlap concentrations of the different molecular mass polymers. A detailed explanation of how this comparison was constructed is given in the SI. The magenta data are from FT-IR spectroscopy by Cho *et al.* (Ref. 21), reported as the ratio of absorbance at two different CH stretching bands (2883 and 2919 cm^{-1}). The blue data are spectral diffusion time constants using the Ru3C probe in this work. The only arbitrary scaling for these two distinct data sets is the vertical scale. The critical overlap concentration *c is denoted by the vertical dashed line.**

Finally, we compare our dynamical measurements with steady-state spectroscopy results of a similar molecular weight PEG derivative. A comparison between the results of Cho *et al.*, who studied poly(ethylene glycol) methyl ester (PEGME) as PEGME-1000, and the present work with PEG-400 shows the nearly identical dependence of the distinct experimental observables on the degree of hydration (**Fig 2.11 and 2.12**). Using a common basis for quantifying PEG hydration, namely, the number of water molecules per ethylene oxide unit, we find a striking universality by analyzing previous infrared spectroscopy studies of PEG-1000.[21] Both our ultrafast dynamics measurements and the previous ratio

of conformation specific CH band amplitudes show identical hydration dependence when concentrations are appropriately scaled to the overlap concentrations of the different molecular mass polymers, detailed below.

2.4.3 Determination of Water Molecules Per EO Monomer and the Critical Overlap Concentrations for PEG-400 and PEG-1000

From the concentration values, we determine the mole fraction. Since the average number of monomer units per PEG-400 is 8.5,[110] we multiply the mole fraction of PEG by 8.5 to get mole fraction of EO units. The number of water molecules per EO unit is the ratio of x_{D2O} to x_{EO}. For our PEG-400 results these are the relevant values:

Table 2.6 Values for mole fraction (xPEG) and water molecules per ethylene oxide units for PEG-400.

v/v (%)	x_{PEG}	D_2O/EO	**D_2O/EO*(400/342)**
0	0	–	
5	0.0026	45.1	52.8
20	0.0125	9.29	10.9
50	0.048	2.33	2.73
75	0.131	0.78	0.912
90	0.312	0.26	0.303

We note that we have scaled the number of water molecules per EO unit by the ratio of the average formula mass (400) and the effective mass accounting for the hydration. The same scaling was used by Cho et al., and we use it below in considering the water per EO unit in PEG-1000.

Values for Cho's study of PEG-1000 are given in weight percent due to the fact that PEG-1000 is a solid at room temperature. The determination of the water per EO unit is similar, except that PEG-1000 has an average number of EO units of 21.[21] To compute the mole fraction, we must use the molecular

weight of the PEG-1000, which although the chemical mass has an average of 1000 g/mol, the effective mass from the point of view of hydration is actually less, so we use the cited value of 699 g/mol.[17]

Table 2.7 Values for mole fraction (xPEG) and water molecules per ethylene oxide units for PEG-1000 from Cho's study.

w/w (%)	x_{PEG}	D_2O/EO
10.046	0.0029	16.56
19.941	0.0064	7.42
30.140	0.0110	4.29
40.031	0.0169	2.77
50.072	0.0252	1.84
59.893	0.0370	1.24
70.070	0.0569	0.790
80.013	0.0935	0.462
85.031	0.1276	0.325

Next we need to determine the critical overlap concentration c^*. A simple definition is the following from polymer theory, where c^* is the polymer chain concentration:

$$c^*\left(\frac{4}{3}R_g^3\right) = \frac{M}{N_A}$$

where M is the mass of a polymer chain, and N_A is Avogadro's number. The radius of gyration (R_g) has been determined for aqueous PEG to be:[111]

$$R_g = 0.0215\left(M_W\right)^{0.583}$$

(in units of nm). There are alternative relationships in the literature, but the exponent is generally similar to 0.5. We can take the ratio of two different overlap concentrations to be:

$$\frac{c^*_{1000}}{c^*_{400}} = \frac{\frac{3}{4}\frac{M_{1000}}{N_A}\frac{1}{R^3_{g,1000}}}{\frac{3}{4}\frac{M_{400}}{N_A}\frac{1}{R^3_{g,400}}} = \frac{M_{1000}R^3_{g,400}}{M_{400}R^3_{g,1000}} = \frac{1000}{400}\frac{R^3_{g,400}}{R^3_{g,1000}} = 2.5\frac{R^3_{g,400}}{R^3_{g,1000}}$$

The ratio of the radii of gyration is

$$\frac{R_{g,400}}{R_{g,1000}} = \frac{0.0215(400)^{0.583}}{0.0215(1000)^{0.583}} = \frac{(400)^{0.583}}{(1000)^{0.583}} = 0.586$$

$$\left(\frac{R_{g,400}}{R_{g,1000}}\right)^3 = 0.201$$

and we note that only the exponent and the molecular weight part of the R_g is retained, since the prefactors cancel.

So we have

$$c^*_{1000} = (2.5)(0.2)c^*_{400} = 0.5c^*_{400}$$

In other words, for case of the longer polymer, the chains begin to come into contact at a lower chain concentration.

From the work of Jora *et al.*[112] the overlap concentration of PEG-400 occurs at an EO/water ratio of 0.3 (i.e. 3.33 water/EO). Scaling this result for the longer polymer, we would expect that PEG-1000 critical overlap occurs at a concentration that 50% of the concentration of PEG-400 at its c*. The concentration of PEG-1000 polymer chains is 50% that of PEG-400, but the longer polymer contains more EO units, so in terms of EO/water, there will be about 23% more EO units (0.5*21/8.5 = 1.23) in the overlap concentration solution of PEG-1000 than there will be in the PEG-400 solution. So, if there are

3.33 waters per EO in the PEG-400 solution, there will be (3.33/1.23 = 2.71) waters per EO in the PEG-1000 solution.

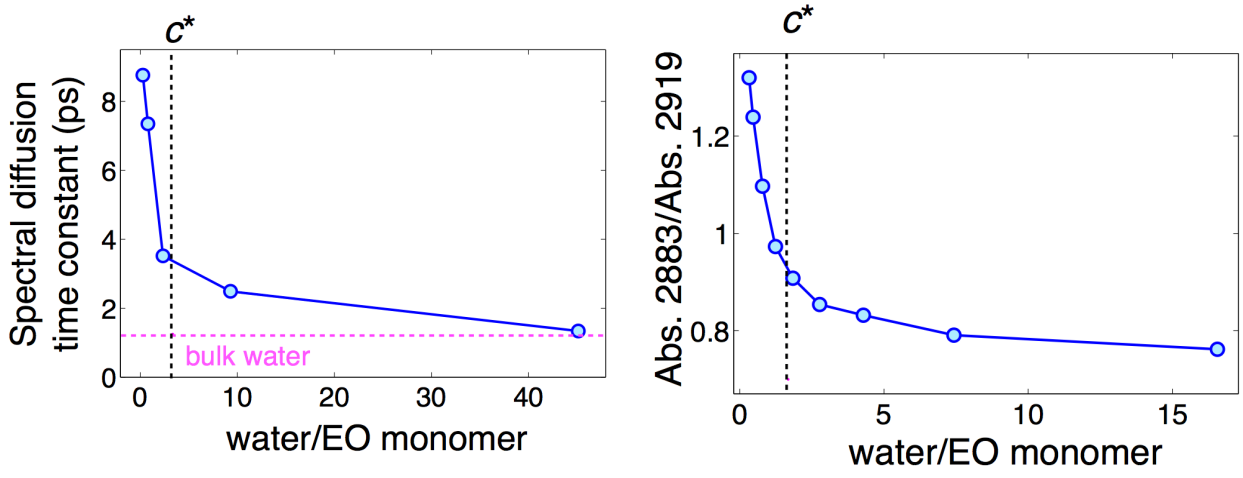

Figure 2.13 . (Left) Spectral diffusion decay times for PEG-400 as a function of the number of water molecules per ethylene oxide unit. (Right) Relative absorption of PEG-1000 at two bands that report different chain conformation as a function of the number of water molecules per ethyelene oxide unit.[21]

Cho's work compares the C-H stretching vibrations of PEGME at 2883 (random-coil conformation) and 2919 cm^{-1} (includes both random-coil and trans-gauche-trans conformations). They note that increased hydration leads to a reduced band ratio, suggesting a reduction in random coil segments.[21] We also observe a transition that is evident in the pronounced changes in the FTIR spectra, which may also be attributable to a structural transition. The spectral diffusion results, however, add a key dynamical signature to this conformational change, and likely provide evidence for a crowding transition similar to what we observed in the protein case.[16] This perspective highlights the importance of chain overlap, and potentially collective hydration, on the structure and dynamics of aqueous PEG solutions.

2.5 CONCLUSIONS

Using 2D-IR, we find clear evidence for qualitatively distinct dynamics sensed by the probe depending on the crowding agent. For PEG-2000, 8000, and 20000, there is extreme decoupling between the solvent and the solute: viscosity is high but we see bulk-like hydration dynamics. We attribute the lack of a pronounced slowdown to the stability of the hydration shell around these long

chain PEGs, and explain how a small-scale iceberg-like structure that preserves the stability is also able to maintain the extended hydrogen bond jump dynamics of bulk water. Thus aqueous PEG solutions may be viewed as being composite materials from the perspective of dynamics.[91] This finding also adds a new aspect to PEG's biocompatibility, not only does PEG preserve water's hydrogen bond network, it also facilitates the maintenance of water's motional dynamics. For PEG-400, however, the spectral diffusion depends on polymer concentration, and exhibits a sharp slowdown in dynamics. Using the number of water molecules per ethylene oxide to quantify PEG hydration, we find that our results from PEG-400 are consistent with recent results by Cho *et al*. of PEG-1000. This comparison highlights the effects of chain overlap on the dynamics and structure of PEG mixtures. By perturbing the local water dynamics, the collective slowdown originally observed in crowded protein solutions is possible once the PEG-400 chains are able to overlap.[93]

2.6 REFERENCES

1. Ball, P., Water as an active constituent in cell biology. *Chem Rev* **2008,** *108* (1), 74-108.

2. Minton, A. P., The Influence of Macromolecular Crowding and Macromolecular Confinement on Biochemical Reactions in Physiological Media. *Journal of Biological Chemistry* **2001,** *276*, 10577-10580.

3. Minton, A. P., Models for excluded volume interaction between an unfolded protein and rigid macromolecular cosolutes: macromolecular crowding and protein stability revisited. *Biophysical journal* **2005,** *88* (2), 971-85.

4. Minton, A. P., Macromolecular crowding. *Current biology : CB* **2006,** *16* (8), R269-71.

5. Minton, A. P., How can biochemical reactions within cells differ from those in test tubes? *Journal of cell science* **2006,** *119*, 2863-9.

6. Ellis, P. R., Protein misassembly: macromolecular crowding and molecular chaperones. *Adv.Exp.Med.Biol.* **2007,** *594*, 1-13.

7. Zhou, H. X.; Dill, K. A., Stabilization of Proteins in Confined Spaces. *Biochemistry* **2001,** *40* (38), 11289-93.

8. Huan-Xiang, Z., Effect of Mixed Macromolecular Crowding Agents on Protein Folding. *Proteins* **2008,** *72* (4), 1109-1113.

9. Ravindra, R.; Zhao, S.; Gies, H.; Winter, R., Protein encapsulation in mesoporous silicate: The effects of confinement on protein stability, hydration, and volumetric properties. *Journal of the American Chemical Society* **2004,** *126*, 12224-12225.

10. Bhat, R.; Timasheff, S. N., Steric exclusion is the principal source of the preferential hydration of proteins in the presence of polyethylene glycols *Protein Science* **1992,** *1*, 1133-1143.

11. Ellis, R. J., Macromolecular crowding : obvious but under appreciated. *TRENDS in Biochemical Sciences* **2001,** *26*, 597-604.

12. Harris, J. M.; Chess, R. B., Effect of pegylation on pharmaceuticals. *Nature Reviews Drug Discovery* **2003,** *2* (3), 214-221.

13. Veronese, F. M.; Pasut, G., PEGylation, successful approach to drug delivery. *Drug Discovery Today* **2005,** *10* (21), 1451-1458.

14. McPherson, A., Crystallization of Proteins from Polyethylene-Glycol. *Journal of Biological Chemistry* **1976,** *251* (20), 6300-6303.

15. Hirano, A.; Shiraki, K.; Arakawa, T., Polyethylene Glycol Behaves Like Weak Organic Solvent Polyethylene Glycol Behaves Like Weak Organic Solvent. *Biopolymers* **2011,** *97*.

16. King, J. T.; Arthur, E. J.; Brooks, C. L.; Kubarych, K. J., Crowding induced collective hydration of biological macromolecules over extended distances. *Journal of the American Chemical Society* **2014,** *136*, 188-194.

17. Reid, C.; Rand, R. P., Probing protein hydration and conformational states in solution. *Biophysical journal* **1997,** *72* (3), 1022-1030.

18. Tyrrell, J.; Weeks, K. M.; Pielak, G. J., Challenge of Mimicking the Influences of the Cellular Environment on RNA Structure by PEG-Induced Macromolecular Crowding. *Biochemistry* **2015,** *54* (42), 6447-6453.

19. Israelachvili, J., The different faces of poly(ethylene glycol). *P Natl Acad Sci USA* **1997,** *94* (16), 8378-8379.

20. Ozdemir, C.; Guner, A., Solubility profiles of poly(ethylene glycol)/solvent systems, I: Qualitative comparison of solubility parameter approaches. *Eur. Polym. J.* **2007,** *43* (7), 3068-3093.

21. Verma, P. K.; Kundu, A.; Ha, J. H.; Cho, M., Water Dynamics in Cytoplasm-Like Crowded Environment Correlates with the Conformational Transition of the Macromolecular Crowder. *Journal of the American Chemical Society* **2016,** *138* (49), 16081-16088.

22. Huang, K. Y.; Kingsley, C. N.; Sheil, R.; Cheng, C. Y.; Bierma, J. C.; Roskamp, K. W.; Khago, D.; Martin, R. W.; Han, S., Stability of Protein-Specific Hydration Shell on Crowding. *J Am Chem Soc* **2016,** *138* (16), 5392-402.

23. Laage, D.; Stirnemann, G.; Hynes, J. T., Why Water Reorientation Slows without Iceberg Formation around Hydrophobic Solutes. *J. Phys. Chem. B* **2009,** *113* (8), 2428-2435.

24. Laage, D.; Elsaesser, T.; Hynes, J. T., Water Dynamics in the Hydration Shells of Biomolecules. *Chem Rev* **2017**, DOI: 10.1021/acs.chemrev.6b00765.

25. Halle, B., Protein hydration dynamics in solution: a critical survey. *Philosophical Transactions of the Royal Society of London Series B-Biological Sciences* **2004,** *359* (1448), 1207-1223.

26. Qvist, J.; Mattea, C.; Sunde, E. P.; Halle, B., Rotational dynamics in supercooled water from nuclear spin relaxation and molecular simulations. *J Chem Phys* **2012,** *136* (20), 204505.

27. Franck, J. M.; Ding, Y.; Stone, K.; Qin, P. Z.; Han, S., Anomalously Rapid Hydration Water Diffusion Dynamics Near DNA Surfaces. *Journal of the American Chemical Society* **2015,** *137* (37), 12013-12023.

28. Huang, K. Y.; Kingsley, C. N.; Sheil, R.; Cheng, C. Y.; Bierma, J. C.; Roskamp, K. W.; Khago, D.; Martin, R. W.; Han, S., Stability of Protein-Specific Hydration Shell on Crowding. *J. Am. Chem. Soc.* **2016,** *138* (16), 5392-5402.

29. Tielrooij, K. J.; Garcia-Araez, N.; Bonn, M.; Bakker, H. J., Cooperativity in Ion Hydration. *Science* **2010,** *328* (5981), 1006-1009.

30. Kropman, M. F.; Bakker, H. J., Dynamics of water molecules in aqueous solvation shells. *Science* **2001,** *291* (5511), 2118-2120.

31. Dokter, A. M.; Woutersen, S.; Bakker, H. J., Anomalous slowing down of the vibrational relaxation of liquid water upon nanoscale confinement. *Physical Review Letters* **2005,** *94* (17), 178301.

32. Fenn, E. E.; Wong, D. B.; Fayer, M. D., Water dynamics at neutral and ionic interfaces. *P Natl Acad Sci USA* **2009,** *106* (36), 15243-15248.

33. Brookes, J. F.; Slenkamp, K. M.; Lynch, M. S.; Khalil, M., Effect of Solvent Polarity on the Vibrational Dephasing Dynamics of the Nitrosyl Stretch in an Fe-II Complex Revealed by 2D IR Spectroscopy. *J Phys Chem A* **2013,** *117* (29), 6234-6243.

34. Thogersen, J.; Rehault, J.; Odelius, M.; Ogden, T.; Jena, N. K.; Jensen, S. J. K.; Keiding, S. R.; Helbing, J., Hydration Dynamics of Aqueous Nitrate. *Journal of Physical Chemistry B* **2013,** *117* (12), 3376-3388.

35. Okuda, M.; Ohta, K.; Tominaga, K., Comparison of vibrational dynamics between non-ionic and ionic vibrational probes in water: Experimental study with two-dimensional infrared and infrared pump-probe spectroscopies. *J Chem Phys* **2016,** *145* (11), 114503.

36. King, J. T.; Kubarych, K. J., Site-specific coupling of hydration water and protein flexibility studied in solution with ultrafast 2D-IR spectroscopy. *Journal of the American Chemical Society* **2012,** *134* (45), 18705-12.

37. Zhang, L. Y.; Wang, L. J.; Kao, Y. T.; Qiu, W. H.; Yang, Y.; Okobiah, O.; Zhong, D. P., Mapping hydration dynamics around a protein surface. *P Natl Acad Sci USA* **2007,** *104* (47), 18461-18466.

38. Qiu, W. H.; Kao, Y. T.; Zhang, L. Y.; Yang, Y.; Wang, L. J.; Stites, W. E.; Zhong, D. P.; Zewail, A. H., Protein surface hydration mapped by site-specific mutations. *P Natl Acad Sci USA* **2006,** *103* (38), 13979-13984.

39. Li, T. P.; Hassanali, A. A. P.; Kao, Y. T.; Zhong, D. P.; Singer, S. J., Hydration dynamics and time scales of coupled water-protein fluctuations. *Journal of the American Chemical Society* **2007,** *129* (11), 3376-3382.

40. Qin, Y. Z.; Wang, L. J.; Zhong, D. P., Dynamics and mechanism of ultrafast water-protein interactions. *P Natl Acad Sci USA* **2016,** *113* (30), 8424-8429.

41. Bellissent-Funel, M. C.; Hassanali, A.; Havenith, M.; Henchman, R.; Pohl, P.; Sterpone, F.; van der Spoel, D.; Xu, Y.; Garcia, A. E., Water Determines the Structure and Dynamics of Proteins. *Chem Rev* **2016,** *116* (13), 7673-7697.

42. Heugen, U.; Schwaab, G.; Brundermann, E.; Heyden, M.; Yu, X.; Leitner, D. M.; Havenith, M., Solute-induced retardation of water dynamics probed directly by terahertz spectroscopy. *P Natl Acad Sci USA* **2006,** *103* (33), 12301-12306.

43. Ebbinghaus, S.; Kim, S. J.; Heyden, M.; Yu, X.; Heugen, U.; Gruebele, M.; Leitner, D. M.; Havenith, M., An extended dynamical hydration shell around proteins. *P Natl Acad Sci USA* **2007,** *104* (52), 20749-20752.

44. Samanta, N.; Luong, T. Q.; Das Mahanta, D.; Mitra, R. K.; Havenith, M., Effect of Short Chain Poly(ethylene glycol)s on the Hydration Structure and Dynamics around Human Serum Albumin. *Langmuir : the ACS journal of surfaces and colloids* **2016,** *32* (3), 831-7.

45. Palombo, F.; Heisler, I. A.; Hribar-Lee, B.; Meech, S. R., Tuning the Hydrophobic Interaction: Ultrafast Optical Kerr Effect Study of Aqueous Ionene Solutions. *Journal of Physical Chemistry B* **2015,** *119* (29), 8900-8908.

46. Mazur, K.; Heisler, I. A.; Meech, S. R., Water Dynamics at Protein Interfaces: Ultrafast Optical Kerr Effect Study. *J Phys Chem A* **2012,** *116* (11), 2678-2685.

47. Yamamoto, N.; Ohta, K.; Tamura, A.; Tominaga, K., Broadband Dielectric Spectroscopy on Lysozyme in the Sub-Gigahertz to Terahertz Frequency Regions: Effects of Hydration and Thermal Excitation. *Journal of Physical Chemistry B* **2016,** *120* (21), 4743-4755.

48. Groot, C. C. M.; Meister, K.; DeVries, A. L.; Bakker, H. J., Dynamics of the Hydration Water of Antifreeze Glycoproteins. *Journal of Physical Chemistry Letters* **2016,** *7* (23), 4836-4840.

49. Fenn, E. E.; Wong, D. B.; Giammanco, C. H.; Fayer, M. D., Dynamics of Water at the Interface in Reverse Micelles: Measurements of Spectral Diffusion

with Two-Dimensional Infrared Vibrational Echoes. *JOURNAL OF PHYSICAL CHEMISTRY B* **2011,** *115* (40), 11658-11670.

50. Moilanen, D. E.; Fenn, E. E.; Wong, D.; Fayer, M. D., Water dynamics in large and small reverse micelles: From two ensembles to collective behavior. *J Chem Phys* **2009,** *131* (1), 014704.

51. Heyden, M.; Brundermann, E.; Heugen, U.; Niehues, G.; Leitner, D. M.; Havenith, M., Long-range influence of carbohydrates on the solvation dynamics of water-answers from terahertz absorption measurements and molecular modeling simulations. *Journal of the American Chemical Society* **2008,** *130* (17), 5773-5779.

52. Kjellander, R. F., Ebba, Water structure and changes in thermal stability of the system poly(ethylene oxide)-water. *Journal of the Chemical Society, Faraday Transactions 1: Phyiscal Chemistry in Condensed Phases* **1981,** *77* (9), 2053-2077.

53. Fogarty, A. C.; Laage, D., Water Dynamics in Protein Hydration Shells: The Molecular Origins of the Dynamical Perturbation. *Journal of Physical Chemistry B* **2014,** *118* (28), 7715-7729.

54. Stirnemann, G.; Wernersson, E.; Jungwirth, P.; Laage, D., Mechanisms of Acceleration and Retardation of Water Dynamics by Ions. *Journal of the American Chemical Society* **2013,** *135* (32), 11824-11831.

55. Stirnemann, G.; Rossky, P. J.; Hynes, J. T.; Laage, D., Water reorientation, hydrogen-bond dynamics and 2D-IR spectroscopy next to an extended hydrophobic surface. *FARADAY DISCUSSIONS* **2010,** *146*, 263-281.

56. Mukamel, S., *Principles of Nonlinear Optical Spectroscopy*. Oxford University Press: Oxford, U.K. , 1995.

57. Hybl, J. D.; Albrecht Ferro, A.; Jonas, D. M., Two-dimensional Fourier transform electronic spectroscopy. *J. Chem. Phys.* **2001,** *115*, 6606.

58. Khalil, M. D., N.; Tokmakoff, A. , Coherent 2D IR Spectroscopy: Molecular Structure and Dynamics in Solution. *J. Phys. Chem. A* **2003,** *107*, 5258-5279.

59. Krueger, B. P. S., Gregory D.; Fleming, Graham R., Calculation of Couplings and Energy-Transfer Pathways between the Pigments of LH2 by the ab Initio Transition Density Cube Method. *J. Phys. Chem. B* **1998,** *102*, 5378-5386.

60. Khalil, M.; Demirdöven, N.; Tokmakoff, a., Vibrational coherence transfer characterized with Fourier-transform 2D IR spectroscopy. *J. Chem. Phys.* **2004,** *121*, 362-73.

61. Dlott, D. D., Vibrational energy redistribution in polyatomic liquids: 3D infrared–Raman spectroscopy. *Chem. Phys.* **2001,** *266*, 149-166.

62. Anna, J. M.; Baiz, C. R.; Ross, M. R.; McCanne, R.; Kubarych, K. J., Ultrafast equilibrium and non-equilibrium chemical reaction dynamics probed with

multidimensional infrared spectroscopy. *Int. Rev. Phys. Chem.* **2012,** *31*, 367-419.

63. Treuffet, J.; Kubarych, K. J.; Lambry, J.-C.; Pilet, E.; Masson, J.-B.; Martin, J.-L.; Vos, M. H.; Joffre, M.; Alexandrou, A., Direct observation of ligand transfer and bond formation in cytochrome c oxidase by using mid-infrared chirped-pulse upconversion. *Proc. Natl. Acad. Sci. U. S. A.* **2007,** *104*, 15705-10.

64. Nee, M. J.; McCanne, R.; Kubarych, K. J.; Joffre, M., Two-dimensional infrared spectroscopy detected by chirped pulse upconversion. *Opt. Lett.* **2007,** *32*, 713-5.

65. Baiz, C. R.; Nee, M. J.; McCanne, R.; Kubarych, K. J., Ultrafast nonequilibrium Fourier-transform two-dimensional infrared spectroscopy. *Opt. Lett.* **2008,** *33*, 2533-5.

66. Anna, J. M.; Ross, M. R.; Kubarych, K. J., Dissecting enthalpic and entropic barriers to ultrafast equilibrium isomerization of a flexible molecule using 2DIR chemical exchange spectroscopy. *J. Phys. Chem. A* **2009,** *113*, 6544-6547.

67. King, J. T.; Ross, M. R.; Kubarych, K. J., Water-assisted vibrational relaxation of a metal carbonyl complex studied with ultrafast 2D-IR. *J. Phys. Chem. B* **2012,** *116*, 3754-9.

68. Osborne, D. G.; King, J. T.; Dunbar, J. A.; White, A. M.; Kubarych, K. J., Ultrafast 2DIR probe of a host-guest inclusion complex: Structural and dynamical constraints of nanoconfinement. *J. Chem. Phys.* **2013,** *138*, 144501.

69. Hybl, J. D.; Yu, A.; Farrow, D. A.; Jonas, D. M., Polar Solvation Dynamics in the Femtosecond Evolution of Two-Dimensional Fourier Transform Spectra. *J. Phys. Chem. A* **2002,** *106*, 7651-7654.

70. Osborne, D. G.; Kubarych, K. J., Rapid and accurate measurement of the frequency-frequency correlation function. *J. Phys. Chem. A* **2013,** *117*, 5891-8.

71. Roberts, S. T.; Loparo, J. J.; Tokmakoff, A., Characterization of spectral diffusion from two-dimensional line shapes. *J. Chem. Phys.* **2006,** *125*, 084502.

72. Oelmeier, S. A.; Dismer, F.; Hubbuch, J., Molecular dynamics simulations on aqueous two-phase systems - Single PEG-molecules in solution. *Bmc Biophys* **2012,** *5*, 14.

73. Motterlini, R.; Clark, J. E.; Foresti, R.; Sarathchandra, P.; Mann, B. E.; Green, C. J., Carbon monoxide-releasing molecules - Characterization of biochemical and vascular activities. *Circulation Research* **2002,** *90* (2), E17-E24.

74. King, J. T.; Ross, M. R.; Kubarych, K. J., Water-assisted vibrational relaxation of a metal carbonyl complex studied with ultrafast 2D-IR. *The journal of physical chemistry. B* **2012,** *116*, 3754-9.

75. Bruce, M. I.; Stone, F. G. A., Chemistry of Metal Carbonyls .XL. Carbonylation of Ruthenium Trichloride. *Journal of the Chemical Society a - Inorganic Physical Theoretical* **1967,** (8), 1238-1241.

76. Cariati, E.; Dragonetti, C.; Manassero, L.; Roberto, D.; Tessore, F.; Lucenti, E., Efficient catalytic hydration of acetonitrile to acetamide using Os(CO)(3)Cl-2 (2). *Journal of Molecular Catalysis a-Chemical* **2003,** *204*, 279-285.

77. Johnson, B. F. G.; Johnston, R. D.; Lewis, J., Chemistry of Polynuclear Compounds .XV. Halogenocarbonylruthenium Compounds. *Journal of the Chemical Society a -Inorganic Physical Theoretical* **1969**, 792-797.

78. Roberto, D.; Psaro, R.; Ugo, R., Surface Organometallic Chemistry - Reductive Carbonylation of Silica-Supported $RuCl_3 \bullet 3H_2O$. *Journal of Organometallic Chemistry* **1993,** *451* (1-2), 123-131.

79. Cho, B.; Yetzbacher, M. K.; Kitney, K. A.; Smith, E. R.; Jonas, D. M., Propagation and Beam Geometry Effects on Two-Dimensional Fourier Transform Spectra of Multilevel Systems. *J Phys Chem A* **2009,** *113* (47), 13287-13299.

80. Roberts, S. T.; Ramasesha, K.; Tokmakoff, A., Structural Rearrangements in Water Viewed Through Two-Dimensional Infrared Spectroscopy. *Accounts Chem Res* **2009,** *42* (9), 1239-1249.

81. Kirincic, S.; Klofutar, C., Viscosity of aqueous solutions of poly(ethylene glycol)s at 298.15 K. *Fluid Phase Equilibria* **1999,** *155* (2), 311-325.

82. Xu, L. M.; Mallamace, F.; Yan, Z. Y.; Starr, F. W.; Buldyrev, S. V.; Stanley, H. E., Appearance of a fractional Stokes-Einstein relation in water and a structural interpretation of its onset. *Nat Phys* **2009,** *5* (8), 565-569.

83. Turton, D. A.; Wynne, K., Stokes-Einstein-Debye Failure in Molecular Orientational Diffusion: Exception or Rule? *Journal of Physical Chemistry B* **2014,** *118* (17), 4600-4604.

84. Giammanco, C. H.; Yamada, S. A.; Kramer, P. L.; Tamimi, A.; Fayer, M. D., Structural and Rotational Dynamics of Carbon Dioxide in 1-Alkyl-3-methylimidazolium Bis(trifluoromethylsulfonyl)imide Ionic Liquids: The Effect of Chain Length. *Journal of Physical Chemistry B* **2016,** *120* (27), 6698-6711.

85. Kramer, P. L.; Nishida, J.; Fayer, M. D., Separation of experimental 2D IR frequency-frequency correlation functions into structural and reorientation-induced contributions. *J Chem Phys* **2015,** *143* (12).

86. Dormidontova, E. E., Influence of end groups on phase behavior and properties of PEO in aqueous solutions. *Macromolecules* **2004,** *37* (20), 7747-7761.

87. Lusse, S.; Arnold, K., The interaction of poly(ethylene glycol) with water studied by H-1 and H-2 NMR relaxation time measurements. *Macromolecules* **1996,** *29* (12), 4251-4257.

88. Okada, T., Complexation of Poly(Oxyethylene) in Analytical-Chemistry–A Review. *Analyst* **1993,** *118* (8), 959-971.

89. Maltesh, C.; Somasundaran, P., Effect of Binding of Cations to Polyethylene-Glycol on its Interactions with Sodium Dodecyl-Sulfate. *Langmuir : the ACS journal of surfaces and colloids* **1992,** *8* (8), 1926-1930.

90. Kwak, K.; Park, S.; Finkelstein, I.; Fayer, M., Frequency-frequency correlation functions and apodization in two-dimensional infrared vibrational echo spectroscopy: A new approach. *J Chem Phys* **2007,** *127*, 124503.

91. Rubinson, K. A.; Hubbard, J., Experimental compressibilities and average intermolecular distances of poly(ethylene glycol) molecular masses 2000-8000 Da in aqueous solution. *Polymer* **2009,** *50* (12), 2618-2623.

92. Rubinson, K. A.; Krueger, S., Poly(ethylene glycol)s 2000-8000 in water may be planar: A small-angle neutron scattering (SANS) structure study. *Polymer* **2009,** *50* (20), 4852-4858.

93. Rubinson, K. A.; Meuse, C. W., Deep hydration: Poly(ethylene glycol) M-w 2000-8000 Da probed by vibrational spectrometry and small-angle neutron scattering and assignment of Delta G degrees to individual water layers. *Polymer* **2013,** *54* (2), 709-723.

94. Fenn, E. E.; Moilanen, D. E.; Levinger, N. E.; Fayer, M. D., Water Dynamics and Interactions in Water-Polyether Binary Mixtures. *Journal of the American Chemical Society* **2009,** *131* (15), 5530-5539.

95. Laage, D.; Hynes, J. T., A molecular jump mechanism of water reorientation. *SCIENCE* **2006,** *311* (5762), 832-835.

96. Sterpone, F.; Stirnemann, G.; Laage, D., Magnitude and molecular origin of water slowdown next to a protein. *JOURNAL OF THE AMERICAN CHEMICAL SOCIETY* **2012,** *134* (9), 4116-9.

97. Osborne, D. G.; Dunbar, J. A.; Lapping, J. G.; White, A. M.; Kubarych, K. J., Site-Specific Measurements of Lipid Membrane Interfacial Water Dynamics with Multidimensional Infrared Spectroscopy. *Journal of Physical Chemistry B* **2013,** *117* (49), 15407-15414.

98. Chandler, D., Interfaces and the driving force of hydrophobic assembly. *Nature* **2005,** *437* (7059), 640-647.

99. Lum, K.; Chandler, D.; Weeks, J. D., Hydrophobicity at small and large length scales. *Journal of Physical Chemistry B* **1999,** *103* (22), 4570-4577.

100. Costard, R.; Heisler, I. A.; Elsaesser, T., Structural Dynamics of Hydrated Phospholipid Surfaces Probed by Ultrafast 2D Spectroscopy of Phosphate Vibrations. *Journal of Physical Chemistry Letters* **2014,** *5* (3), 506-511.

101. Maron, S. H.; Filisko, F. E., HEATS OF SOLUTION AND DILUTION FOR POLYETHYLENE OXIDE IN SEVERAL SOLVENTS. *Journal of Macromolecular Science-Physics* **1972,** *B 6* (1), 79-&.

102. Daoust, H.; Stcyr, D., MICROCALORIMETRIC STUDY OF POLY(ETHYLENE OXIDE) IN WATER IN WATER ETHANOL MIXED-SOLVENT. *Macromolecules* **1984,** *17* (4), 596-601.

103. Kagemoto, A.; Murakami, S.; Fujishir.R, HEATS OF DILUTION OF POLY(ETHYLENE OXIDE)/WATER SOLUTIONS. *Makromolekulare Chemie* **1967,** *105* (JUL), 154-&.

104. Rowe, R. C.; McKillop, A. G., MOLECULAR-WEIGHT DEPENDENCE OF THE HEATS OF HYDRATION OF SOME OLIGOMERIC ETHYLENE OXIDES AND THEIR METHOXYL DERIVATIVES. *Journal of Applied Polymer Science* **1993,** *50* (2), 321-326.

105. North, A. M.; Pethrick, R. A.; Poh, B. T., ADIABATIC COMPRESSIBILITY STUDIES OF MIXTURES OF POLYETHYLENEOXIDE WITH HYDROPHILIC SOLVENTS. *Advances in Molecular Relaxation and Interaction Processes* **1981,** *19* (2-3), 209-219.

106. Eagland, D.; Crowther, N. J.; Butler, C. J., INTERACTION OF POLY(OXYETHYLENE) WITH WATER AS A FUNCTION OF MOLAR-MASS. *Polymer* **1993,** *34* (13), 2804-2808.

107. Novelli, F.; Pour, S. O.; Tollerud, J.; Roozbeh, A.; Appadoo, D. R. T.; Blanch, E. W.; Davis, J. A., Time-Domain THz Spectroscopy Reveals Coupled Protein-Hydration Dielectric Response in Solutions of Native and Fibrils of Human Lysozyme. *Journal of Physical Chemistry B* **2017,** *121* (18), 4810-4816.

108. Ebbinghaus, S.; Kim, S. J.; Heyden, M.; Yu, X.; Heugen, U.; Gruebele, M.; Leitner, D. M.; Havenith, M., An Extended Dynamical Hydration Shell around Proteins. *Proc. Natl. Acad. Sci. U. S. A.* **2007,** *104* (52), 20749-20752.

109. Stanzione, F.; Jayaraman, A., Hybrid Atomistic and Coarse-Grained Molecular Dynamics Simulations of Polyethylene Glycol (PEG) in Explicit Water. *Journal of Physical Chemistry B* **2016,** *120* (17), 4160-4173.

110. Bailey Jr., F. E.; Koleske, J. V., *Poly(ethylene oxide)*. Academic Press: New York, 1976; p 184.

111. Linegar, K. L.; Adeniran, A. E.; Kostko, A. F.; Anisimov, M. A., Hydrodynamic radius of polyethylene glycol in solution obtained by dynamic light scattering. *Colloid J+* **2010,** *72* (2), 279-281.

112. Jora, M. Z.; Cardoso, M. V. C.; Sabadini, E., Dynamical aspects of water-poly(ethylene glycol) solutions studied by H-1 NMR. *J Mol Liq* **2016,** *222*, 94-100.

Chapter 3 Investigations of Temperature on Aqueous Polymer Solutions

3.1 INTRODUCTION

Traditional biochemical investigations of mechanisms, equilibria, reaction rates, and dynamics are studied under dilute conditions, with concentrations of less than 1 mg/mL of total macromolecule, DNA, or protein. In contrast to such idealized solutions, living systems exist in highly crowded environments containing macromolecules at concentrations of 100s of mg/mL.[1-7] The extent to which crowded macromolecular environments alter structure and dynamics in real biological systems remains an active area of current research. The main thermodynamic considerations driving crowding-induced perturbations were discussed in Chapter 2, but we highlight the key points here since temperature influences these changes in subtle ways.

A typical descriptions of crowding is based on an excluded volume picture. A biomacromolecule, such as a protein, is considered to be stabilized in the folded state due to the limitation of extended conformations due to the volume occupied by crowders. This entropic stabilization would be expected to be responsible for a significant temperature dependence ($-T\Delta S$) to the folding free energy change. The simplicity of the excluded volume argument often obfuscates an alternative, but also highly relevant, countervailing influence: favorable interactions between the protein and the crowding agents. Since so many molecules interact through a variety of noncovalent forces, it is important to keep in mind that favorable interactions with crowders can in fact promote unfolded conformations. This enthalpic destabilization of the folded state therefore contributes a temperature dependence to the overall free energy when these protein-crowder interactions become thermally disrupted. To the extent that these distinct thermodynamic influence may be reinforcing or opposing, it is not sufficient to use temperature to gauge the role of crowding in biochemical

activity. The main consequence of the alternative “chemical” (i.e. enthalpic) and “physical” (i.e. entropic) perturbations is that crowding studies often find significant dependence on the chemical nature of the crowding species. Unfortunately this important complication raises serious questions about the generality of studies performed with one or only a small set of macromolecular crowding agents.

Perhaps the most commonly used molecule used as a crowding agent in these experiments is the synthetic polymer polyethylene glycol (PEG). PEG is also used in many biomedical and biotechnical applications due to its water solubility and biocompatibility over a wide range of molecular weights. For example, PEG has applications in cell separation[8], purification of proteins[9], protein modification[10], and others.[11] PEG is often used to model crowded cellular environments, and how crowded envirnoments might affect protein and enzyme hydration[12-14], protein aggregation[15], conformational properties of intrinsically disordered proteins[16], RNA folding mechanisms[17], DNA-functionalized gold nanoparticles[18], and DNA structure conformations[19-21]. PEG’s appeal in protein crowding studies derives from its apparent inertness to proteins, high solubility, and lack of charges.[7, 22, 23]

Research has started to examine how other aspects of macromolecular crowding must be taken into account for a more complete picture, such as viscosity, soft interactions, perturbed diffusion, and crowder shape, confinement, and concentration, all of which affect the crowded solution. [24-28] There is ample evidence that PEG is possibly not an ideal model for “inert” macromolecular interactions.[29, 30] It is important to understand the interactions PEG has with solvents, like water, first before relying on it as a inert macromolecular crowder. In many of the above-mentioned biologically pertinent crowding studies, experiments are conducted at physiological relevant temperature, which is 37° C (310 K). A recent study of UV-irradiated glycogen phosphorylase b shows that at 37° C, aggregation is irreversible[31], while at 10°C (283 K) it is a reversible process and therefore a good temperature to learn about the initial stages of

protein aggregation.[15] It is therefore necessary to understand the behavior of aqueous PEG solutions through at least this range of temperatures.

Recently, we found that at room temperature and over a wide range of concentration and molecular weights of PEG, the time scale of sensed hydration dynamics differed negligibly from bulk water with an exception of PEG-400, where a dynamical slowdown was observed.[32] The time scale was attributed to the stability of the hydration shell around the long chain PEGs. By looking at thermodynamic trends of aqueous PEG, it was concluded that shorter PEGs promote a less stable hydration shell than do the longer chain polymers, which in turn enables a collective slowdown of hydration dynamics.

Building on that study, using two-dimensional infrared spectroscopy of a water-soluble transition metal complex acting as a vibrational probe, we will report on the hydration dynamics of PEG 400 at low and high concentrations from 283 K to 325 K. We observe how thermodynamics of aqueous PEG solutions may change, and how that affects the hydration dynamics measured. Based on temperature dependent thermodynamic trends of PEG and previous results of PEG crowding at room temperature[32], at increasing temperatures, the hydration shell becomes less stable and we would see a slow down in dynamics. However, the temperature dependence of PEG in D_2O can be more complex than its behavior at room temperature due to entropic, enthalpic, and viscosity effects.

EXPERIMENTAL METHODS

3.1.1 Equilibrium 2DIR Spectroscopy

Two-dimensional infrared spectroscopy (2DIR) is a multidimensional nonlinear optical technique. The 2DIR set up used here has been described in Chapter 2.[33] In its current implementation, an output centered around 800 nm from a regeneratvely amplified Ti:sapphire laser is used. This output has a 1 KHz repetition rate and uses a dual optical parametric amplifier with beta barium borate crystals to generate near IR pulses. These pulses are then used to

generate two mid IR pulses by difference frequency generation in separate $AgGaS_2$ crystals. The mid IR pulses are centered around 2000 cm^{-1} with about 100 cm^{-1} FWHM bandwidth. Using beam splitters, these two beams are then split into three pump pulses, a tracer, and the local oscillator.[33]

The three infrared femtosecond laser pulses interact with the sample and create a third-order nonlinear signal. The three fields are E_1, E_2, or E_3 with corresponding wave vectors k_1, k_2, and k_3. The fields are separated by time delays t_1, t_2 (the so-called waiting time), and t_3. The pulses interact with the sample in a noncollinear box geometry in order to generate a signal in a background free directions during t_3. The phase and amplitude of the signal field are measured directly with a spectrometer via optical heterodyne detection by interference with the local oscillator. [34, 35] During the experiment, the waiting time is incrementally stepped over a range of picoseconds. At each waiting time, the time delay between the first two pulses is scanned continuously. The complex electric field that is collected during this delay is Fourier transformed with respect to the first time delay to yield the excitation frequency axis (ω_1). The spectrometer measures the signal field emitted during t_3 directly in the frequency domain, creating the detection axis directly. The IR signal, the local oscillator, and a chirped 800 nm pulse are combined and upconverted by sum frequency generation to roughly 690 nm and detected using a silicon CCD.[33]

Increasing the waiting time between excitation and detection reveals dynamical changes in the 2D spectral features, which can be related to processes such as solvation dynamics. In this work we will primarily use spectral diffusion.

3.1.2 Variable Temperature Experiment Set Up

A hand built temperature cell was used to control the temperature of the sample cell. A water bath is used as a reservoir for the peltier heat pumps that are attached to the sample cell. The electronics are connected to a personal computer through a USB interface. Labview is used to control the temperature cell. The temperature limits are 276 K to 325 K.

3.1.3 Sample Preparation

A water-soluble variant of $[Ru(CO)_3]_2(\mu\text{-}Cl)_2$ (Strem Chemicals), a carbon monoxide releasing molecule (CORM) commonly referred to as CORM-2, was synthesized for use in these studies. To create the water-soluble variant, the CORM-2 was sonicated in D_2O and heated up to 62°C for 24 minutes until no changes were observed in the FTIR spectrum. CORM-2 has the following IR-active carbonyl stretches: 1972, 2004, 2051, and 2075 cm^{-1}, whereas the water-soluble variant only has 2 observed bands at 1972 and 2051 cm^{-1}. We denote this water-soluble variant as Ru3C.

PEG 400 (FW 400) is a linear macromolecule and an 8-9mer. PEG 400, a liquid, was dissolved in D_2O at increasing concentrations as separate samples with Ru3C. The specific concentrations used for this series of experiments were 5% and 75% PEG 400 by volume.

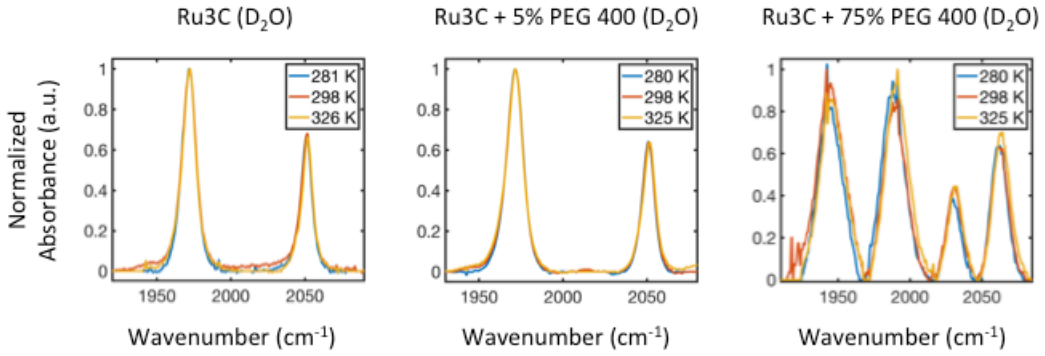

Figure 3.1 Linear FT-IR Spectra of Ru3C in D_2O/PEG-400 mixtures of increasing concentrations and temperatures. (Left) Linear FT-IR of Ru3C in D_2O at increasing temperatures. (Middle) Linear FT-IR of Ru3C and 5% PEG 400 in D_2O at increasing temperatures. (Right) Linear FT-IR of Ru3C and 75% PEG 400 in D_2O at increasing temperatures. There is no significant temperature dependence seen in the spectra.

3.2 RESULTS

Water Soluble Transition Metal Complex Senses 2x Slow Down of Water Dynamics from 325 K to 283 K.

Studying hydration dynamics using metal carbonyl probes is useful because they have an intense vibration in an isolated part of the infrared spectrum. Previously, we synthesized a new water soluble metal complex from $[Ru(CO)_3]_2(\mu\text{-}Cl)_2$, a carbon monoxide releasing complex (CORM-2), that can be

used to sense bulk water dynamics.[32] This new probe, denoted as Ru3C, has an exponential spectral diffusion time constant of 1.76 ±0.2 ps in D_2O (**Fig 3.2 A-C**). This timescale is consistent with the spectral diffusion timescale of an HOD probe in D_2O studied with 2D-IR spectroscopy.[36] Using Ru3C as a vibrational probe, we found that over a wide range of concentration and molecular weights of PEG, the time scale of sensed hydration dynamics differed negligibly from bulk water with an exception of PEG-400, where a dynamical slowdown was observed. The time scales were attributed to the stability of the hydration shell around the long chain PEGs. By looking at thermodynamic trends of aqueous PEG, it was concluded that shorter PEGs promote a less stable hydration shell than do the longer chain polymers, which in turn enables a collective slowdown of hydration dynamics.[32]

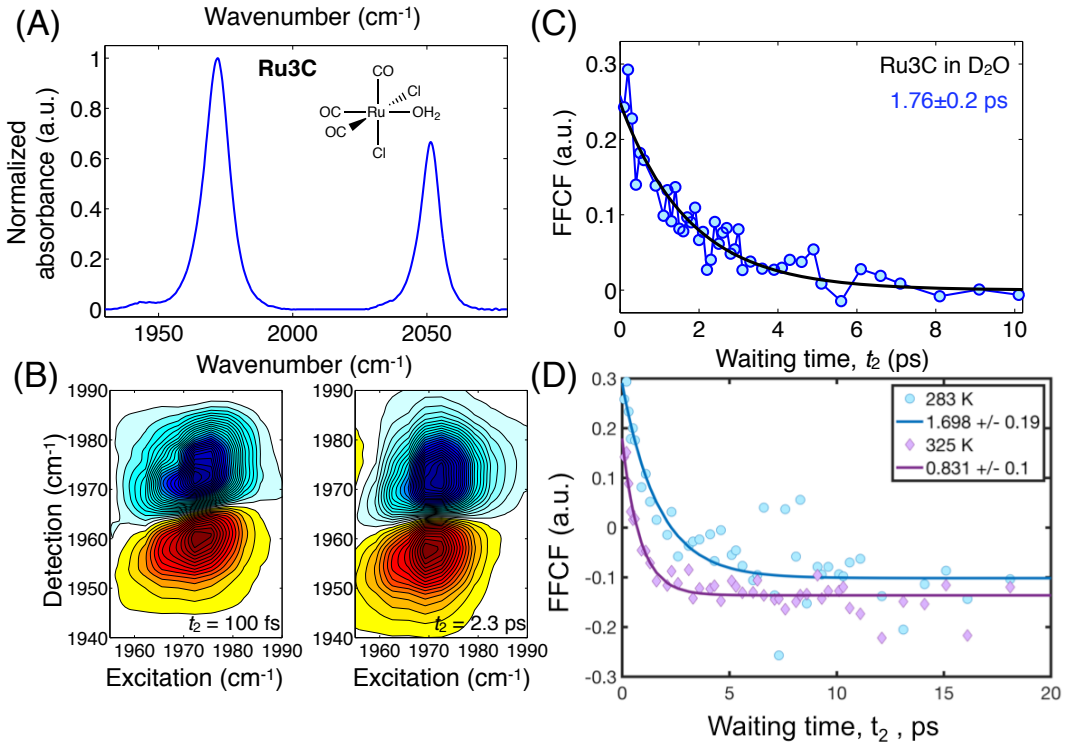

Figure 3.2 A: The FT-IR of Ru3C in D_2O has two peaks consistent with a single tricarbonyl coordination. The asterisk denotes the band shown in (B) and analyzed in (C). B: 2D-IR spectra of Ru3C at early (t_2 = 100 fs) and later (t_2 = 2.3 ps) waiting times. C: The frequency-fluctuation correlation function of Ru3C in D_2O gives a single exponential time constant of 1.76±0.2 ps, which is consistent with bulk D_2O solvation dynamics. (D) FFCFs for the lowest frequency CO stretching mode of Ru3C at increasing temperatures, ranging from 283 K to 325 K.

Using the 1972 cm^{-1} peak of Ru3C to track hydration dynamics of D_2O, we measured the exponential spectral diffusion time constant (**Fig 3.2 D**). It was consistently found that the hydration dynamics of Ru3C slow about by about 2-fold from the measurements taken at 325 K and the measurements taken at 283 K. The maximum t_2 delay collected for all spectra is 20 ps. **Figure 3.1 (left)** shows the FTIR of Ru3C in D_2O at increasing concentrations, with no significant temperature dependence.

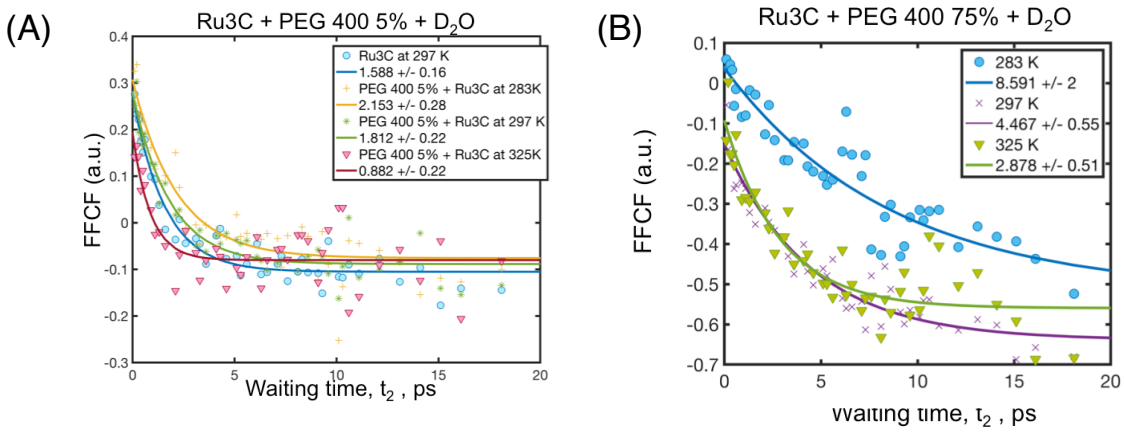

Figure 3.3 Hydration dynamics probed with the 1972 cm^{-1} band of Ru3C in D_2O/PEG 400 mixtures at various temperatures. (A) FFCFs for Ru3C in D_2O/ 5% PEG-400 mixtures, ranging from 283 K to 325 K. (B) FFCFs for Ru3C in D_2O/ 75% PEG-400 mixtures, ranging from 283 K to 325 K. The overall trend is that the probed solvation dynamics are dependent on temperature.

3.2.1 Solutions of PEG 400 Exhibit Increased Hydration Dynamics from 283 K to 325 K. ~2.5 Slow Down From 325 K to 283 K

Ru3C is the metal carbonyl probe used to sense the hydration dynamics in aqueous PEG 400 solutions at varying temperatures. Using 2D-IR, we observed aqueous PEG solutions at increasing concentrations of PEG 400. At the 5% PEG 400 aqueous solution, we measured the hydration dynamics at both 283K, 297 K, and 325 K. Previously we found that the hydration dynamics at low concentrations of aqueous PEG 400 solutions at room temperature were similar to that of Ru3C in D_2O at room temperature.[32] Presently, we consistently find that the hydration dynamics of 5% PEG 400 aqueous solutions slow about by about 2.5-3-fold from the measurements taken at 325 K and the measurements taken at 283 K (**Fig 3.3 A**).

The hydration dynamics of the 75% PEG 400 aqueous solution were also measured at 283 K, 297 K, and 325 K. Previously we found that the hydration dynamics at 75% PEG 400 aqueous solution at room temperature were significantly slower than that of Ru3C probe in D_2O. In this study, we find that is still consistent, and that the hydration dynamics slow about 2.5-3 times from the measurements taken at 325 and the measurements taken at 283 K (**Fig 3.3 B**). The hydration dynamics measured at 283 K are similar to those of 90% PEG 400 aqueous solution at room temperature. **Figure 3.1 (middle and right)** show the FTIR spectra of PEG 400 5% and 75% in D_2O, respectively. There is no significance temperature dependence seen in the spectra.

3.3 DISCUSSION

3.3.1 Ru3C and D_2O solutions

It was observed that the hydration dynamics of Ru3C/D_2O solutions slow as temperature decreases. These results are consistent with temperature dependent 2DIR results of pure water measured previously by Tokmakoff et al..[37, 38] Using 2DIR, they examined dilute HOD in H_2O from 278-345 K, which is a 67 K difference in temperature. It was found that the spectral diffusion time constant decreased from 2.4 ps to 0.7 ps, which is a 3.4-fold increase in time scale and about 0.05-fold increase in dynamics timescale per 1 K increase. We examined Ru3C in D_2O from 283-325 K and 283-318K. Each of these experiments showed a 0.05-fold increase in dynamics timescale per 1 K as well. Hence, it is clear that a solvation dynamics probe is capable of detecting the solvent dynamics even under conditions of varying temperature. This finding has not previously been reported in the literature by any other researchers.

3.3.2 Aqueous PEG 400 Hydration Dynamics at Room Temperature

In order to address the present temperature dependent results, we first review the results from room temperature experiments.[32] There is a lengthy discussion regarding the water-PEG interactions and thermodynamics of solution in Chapter 2. We provide a brief overview here. It was found that as the PEG

lengths decrease, the stability of the hydration shell decreases, with PEG 400 having the least stable hydration shell out of the PEGs studied. It was suggested that by combining the discussed thermodynamic trends described, that shorter PEGs do promote a less stable hydration shell than do the longer chain polymers, which in turn enables a collective slowdown of hydration dynamics leading to a crowding transition.

3.3.3 PEG-Water Structure

When PEG is dissolved in water, the ether oxygens participate in hydrogen bonds with water. The spacing between ethereal oxygens nearly matches water's hydrogen-bonding network. Although the CH_2–O–CH_2–CH_2– units of PEG are chemically inert,[7, 23] the specific structural arrangement of the oxygen atoms, coupled with the hydration shell, imparts remarkable activity to the PEG.[39] This becomes obvious when compared to apparently similar polyethers poly(methylene)glycol (–OCH_2–O–) and poly(trimethylene)glycol (–$OCH_2CH_2CH_2$–O–), neither of which is soluble in water to any extent because the oxygen spacings are incommensurate with the water network.

A highly structured hydration layer exists around PEG molecules, which incorportates the ether oxygens of PEG. This allows for the water network to extend and participate in the hydrogen bond rearrangements of the second hydration shell. According to the extended jump model, which describes a hydrogen reorientation mechanism, extended angular jumps are a major contribution to hydrogen bond rearrangements,[40] and a solute's ability to inhibit these jumps depends on its ability to change the availability of hydrogen bonding partners.[41, 42]

Because it is a short 8-9-mer, the end groups of PEG-400 have the potential to contribute significantly to the concentration dependent hydration dynamics.[39] It has been previously determined that the primary enthalpic contribution was from the hydroxyl end groups.[43] Also, high molecular mass PEGs adopt a helical conformation, while low molecular mass PEGs, which do not form a helix, experience more hydrophobic interactions that control the solution's dynamics.

3.3.4 Thermodynamics of Aqueous PEG Solutions

In general, the enthalpy of solution of PEG in water is negative, indicating that there are more favorable interactions in the solution than in the separated species.[39] The entropy of solution is also negative, indicating that despite the intrinsic entropy increase associated with mixing the constraints on the water overwhelm the net entropy balance. Diluting PEG/water solutions is an exothermic process. At increasing concentrations of PEG, the heat of dilution becomes less exothermic, making the hydration shell less stable. [44, 45] In general, heats of dilution and solution increase in exothermicity with decreased molecular mass, which is consistent with the high solubility of PEG 400 and with the decreased saturation concentrations of larger chain PEGs. [43, 45, 46] As molecular mass increases, the exothermicity of solution is unable to compensate the entropic cost of constraining the hydration water, and the solubility limit decreases.[47]

The Flory-Huggins theory provides a framework to decompose solution thermodynamics into polymer-polymer, polymer-solvent and solvent-solvent interactions using the temperature-dependent interaction parameter χ. Positive values of χ correspond to polymer-polymer or solvent-solvent contacts being favored. Negative values of χ correspond to polymer-solvent contacts being more favored, promoting solvation of the polymer. It was found that the interaction parameter χ decreases with decreasing molecular mass of the PEG polymer chain.[43] Also, short chain PEGs have more negative χ, which correlates to PEG's solubility increases as chain length decreases.[48] In addition to chain length trends, for increasing concentrations, χ becomes less negative,[45] indicating that polymer-polymer and solvent-solvent contacts are more preferred at higher concentrations.

3.3.5 Temperature-Dependent PEG Characteristics

PEG solubility is temperature dependent in water. When heating an aqueous solution of PEG near water's boiling point, the polymer will separate from the water. This is called the lower consolute temperature, lower critical solution temperature, or cloud point. Above 100°C the solution will separate as PEG becomes insoluble. The specific temperature is dependent on molecular weight, concentration and pH.[49] As the length of PEG decreases, the separation temperature increases. For PEG 1900, this is 180°C[50, 51], and for PEG 200,000, it is around 100°C[52], depending on concentration. Looking at this process with the water iceberg structure in mind, as the temperature increases, this layer of water is disturbed in favor of more polymer-polymer and solvent-solvent interactions, and is an entropic process. Salts lower the precipitation temperature of aqueous PEG solutions.[52]

The Flory-Huggins parameter χ is temperature dependent, and generally as temperature increases, χ decreases, but for a hydrogen-bonding pair, χ may increase.[53] A small-angle x-ray scattering experiment confirms this. PEG 4600/D_2O solutions from 1-20 wt% were studied.[54] It was determined that $\chi = \alpha + \beta/T$ was the temperature dependence of χ, where α is the entropic free energy and β is the enthalpic free energy. From this equation, it was determined that the majority of the free energy is entropy related. It was also determined that as temperature increased, χ also increased, which means that as temperature increases, polymer-polymer and solvent-solvent interactions are preferred. Flory-Huggins theory decently describes the data collected. This study also confirms that as the temperature increases, the hydration shell becomes more disordered.

3.3.6 Aqueous PEG 400 Solutions at Varying Temperatures

PEG 400 solutions had hydration dynamics slow as temperature decreased and that the spectral diffusion time constant slowed by ~0.07 x per 1 K. Similarly, PEG 400 75% solutions showed the same change in spectral diffusion. Both the lower critical solution temperature discussion and the temperature-dependent χ indicate that at increasing temperatures, the hydration

shell becomes less stable. Polymer-polymer and solvent-solvent interactions become preferred for both increases in concentration and temperature. In our previous study[32], we argued that a less stable hydration shell leads to slower hydration dynamics experienced by the probe, and a more stable hydration shell led to sensed bulk water dynamics. Here, we see that as the temperature increases and the hydration shell of PEG becomes less stable, the spectral diffusion time constants have a faster decay. As the temperature decreases, the spectral diffusion time constant slows.

What could be happening is that the temperature dependent behavior of D_2O is more prominent than the temperature dependence of χ and other thermodynamics of PEG. While at 283 K PEG's hydration shell should be very stable, the probe is sensing the slowed hydrogen bond reorientation. At increasing temperatures, the barriers to hydrogen bond reconfiguration are low, which could lead to faster spectral diffusion.[37] At higher temperatures, H-bonds are broken, which can cause defects in the hydration water network and disruption in the "iceberg" coating. Such a disruption could induce more collective hydration.

The viscosity of solutions if generally temperature dependent, with increases in temperature leads to a lowering of the shear viscosity.[55, 56] A commonly employed phenomenological model is that of an Arrhenius temperature dependence:

$$\eta(T) = \eta_0 e^{\frac{E_a}{RT}} \tag{3.1}$$

where the sign in the exponent is positive due to the fact that viscosity decreases with increased temperature. If we assume that the time scale for spectral diffusion is viscosity dependent, as it has been found previously in pure water[38, 57], we can estimate the activation barrier from spectral diffusion measurements at two different temperatures similar to how chemical reaction barriers can be determined:

$$\frac{\tau(T_1)}{\tau(T_2)} = \frac{\eta(T_1)}{\eta(T_2)} = \exp\left[\frac{E_a}{R}\left(\frac{1}{T_1} - \frac{1}{T_2}\right)\right] \tag{3.2}$$

which can be rearranged to give E_a:

$$E_a = R \ln \frac{\tau(T_1)}{\tau(T_2)} \left(\frac{1}{T_1} - \frac{1}{T_2} \right)^{-1} \tag{3.3}$$

Table 3.1 shows the results of this Arrhenius analysis using FFCF decays at 283 and 325 K in water (D_2O), PEG 400 (5%), and PEG 400 (75%). For the case of pure D2O, we find an activation energy of 3.1 kcal/mol, which agrees remarkably well with experiments on pure water using 2D-IR spectroscopy. Using all-parallel field polarizations, both Tokmakoff *et al*. and Hamm *et al*. measured apparent activation energies of 3.5 kcal/mol. This agreement with the pure liquid reinforces the fidelity of metal carbonyl probes to access the hydration dynamics of the water solvent, while also serving to confirm that small solutes do not perturb the hydration dynamics appreciably. Repeating the analysis on the PEG solutions, we find a rather weak concentration dependence. At 5% (0.0026 mole fraction) and 75% (0.133 mole fraction), the apparent activation energies are only slightly larger, 3.9 and 4.7 respectively.

Table 3.1 Time constants for spectral diffusion of Ru3C in water (D_2O), and two aqueous PEG solutions (5 and 75% v/v). Activation energies can be obtained using Eq. 3.3. Error bars on the activation energies are obtained by propagating the error bars of the fitted time constants.

	D_2O	PEG-400 (5%)	PEG-400 (75%)
τ (283 K) (ps)	1.7	2.2	8.6
τ (325 K) (ps)	0.83	0.9	2.9
E_a (kJ/mol)	13.1±0.7	16.3±0.6	19.8±1
E_a (kcal/mol)	3.1±0.2	3.9±0.1	4.7±0.2

From measured viscosity data for aqueous PEG solutions[55] (**Fig. 3.4**), we find that although the 5% solution is essentially indistinguishable from neat water, the 75% solution has an activation energy of about 42 kJ/mol (10.0 kcal/mol), which is more than a factor of 2 greater than our experiments would suggest. For such a high activation barrier, the temperature dependence would be much more

pronounced, and would indeed induce a slowdown factor of 10. That is, we would expect the 283 K dynamics to be an order of magnitude slower than the 325 K case, instead of the more modest 3-fold slowdown.

Viewed from the perspective of viscosity-slaved dynamics, the temperature dependent results serve to highlight the degree to which the water dynamics we sense in PEG solutions is bulk-like. Without a temperature dependent set of data, it is difficult to make strong conclusions about the validity of a viscosity dependence to spectral diffusion. Indeed, in many cases, we find that viscosity does not correlate well with spectral diffusion timescales[58], though in other cases, for example, in a series of alcohols, there is a clear linear viscosity dependence.[59, 60] By changing temperature, we can be more confident that spectral diffusion differences do not result from variations in chemical composition, as could occur in a solvent series or even in a concentration series involving a co-solvent. Rather, we expect a more direct readout of the solvation dynamics.

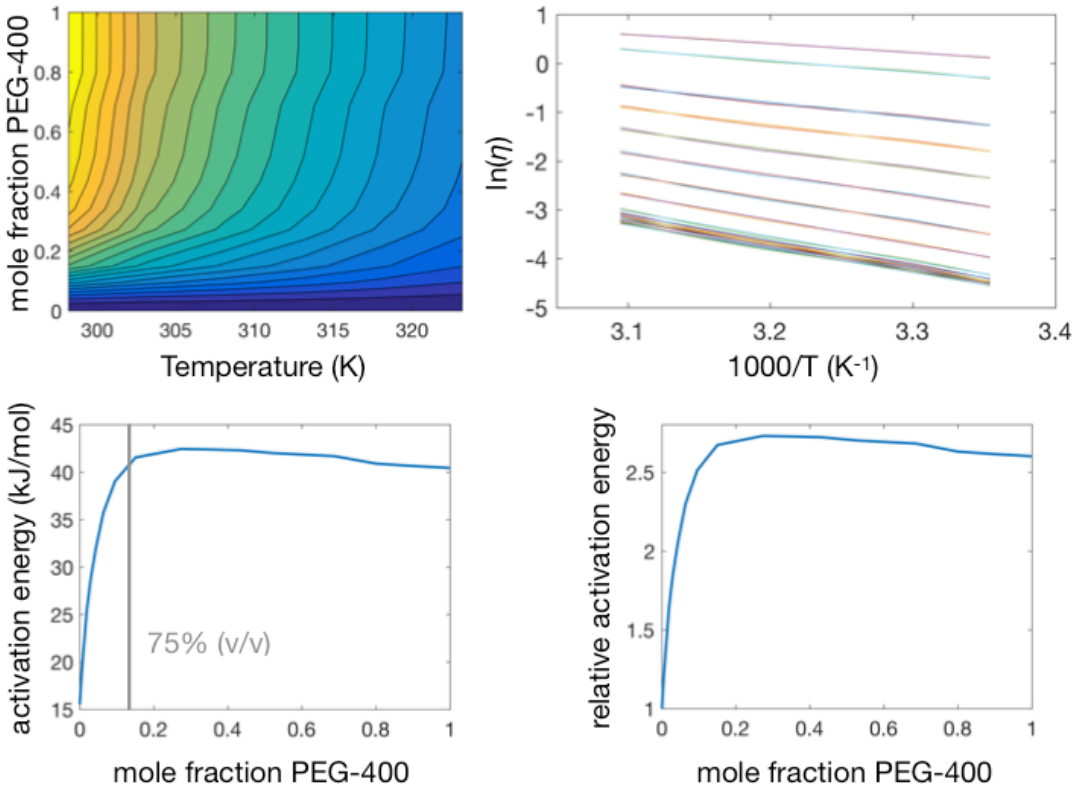

Figure 3.4 Viscosity analysis. (Top Left) Contour plot depicting how as the mole fraction of PEG 400 increases and as temperature decreases, the viscosity increases. (Top Right) Viscosity-dependent

Arrhenius fits for each mol fraction of PEG 400. (Bottom Left) Activation energies calculated from the viscosity-dependent Arrhenius fits for each mole fraction, indicating the activation energy for PEG 400 at 75% in D_2) (Bottom Right) Normalized plot of activation energy versus mole fraction.

3.4 CONCLUSIONS

Temperature dependence adds another dimension to our extensive data set that so far has examined concentration and chain length influences on hydration dynamics. Changing temperature alters both structure and dynamics, and in aqueous PEG solutions is a complex combination of chain length, hydrogen bonding, entropy and transport properties. Our picture, that the bulk-like hydration is promoted by a clathrate-like ice structure of water molecules surrounding the PEG polymer, could have supported a predicted slowdown due to the disruption of this stable hydration shell. Competing influences, however, are significant, and include faster transport reflected in lower viscosity at higher temperatures, as well as an increase in chain extension due to the well-known temperature dependence of the radius of gyration.[61] Increasing the temperature lowers the solubility of PEG in water, and likely leads to changes in the polymer's helicity. This trend is due largely to the breaking of the favorable hydrogen bonds that bear the full cost of decreased entropy of solution.

Despite these complex and often competing effects of temperature, we observe a clear trend in the spectral diffusion results. The Ru3C proves to be capable of reporting the temperature dependent dynamics of neat water, wherein we find a 3.1±0.2 kcal/mol apparent viscosity activation energy, which agrees quantitatively with previous measurements of neat water using 2D-IR spectroscopy without a probe. Comparing the time scales for spectral diffusion measured at two different PEG 400 concentrations, we find in both cases apparent activation energies that are very similar to that of neat water. The results are clearly at odds with a simple solution viscosity dependence, since the literature viscosity values give much larger activation barriers than are consistent with our ultrafast data. We do observe significant, but small, increases in the activation barriers with increased PEG concentration, but the resemblance to

neat water lends further evidence to a picture of bulk-like water hydrating the polymer.

3.5 REFERENCES

1. Minton, A. P., The Influence of Macromolecular Crowding and Macromolecular Confinement on Biochemical Reactions in Physiological Media. *Journal of Biological Chemistry* **2001,** *276*, 10577-10580.

2. Minton, A. P., How can biochemical reactions within cells differ from those in test tubes? *Journal of cell science* **2006,** *119*, 2863-9.

3. Minton, A. P., Macromolecular crowding. *Curr Biol* **2006,** *16* (8), R269-71.

4. Zhou, H.-X.; Rivas, G.; Minton, A. P., Macromolecular crowding and confinement: biochemical, biophysical, and potential physiological consequences. *Annual review of biophysics* **2008,** *37*, 375-397.

5. Rivas, G.; Minton, A. P., Macromolecular Crowding In Vitro, In Vivo, and In Between. *Trends in Biochemical Sciences* **2016,** *41* (11), 970-981.

6. Zimmerman, S. B.; Minton, A. P., MACROMOLECULAR CROWDING: Biochemical, Biophysical, and Physiological Consequences. *Annual review of biophysics and biomolecular structure* **1993,** *22*, 27-65.

7. Ellis, R. J., Macromolecular crowding : obvious but under appreciated. *TRENDS in Biochemical Sciences* **2001,** *26*, 597-604.

8. Brooks, D. E.; Van Alstine, J. M.; Sharp, K. A.; Stocks, S. J., PEG-Derivatized Ligands and Immunological Specificity, Applications in Cell Separation. In *Poly(ethylene glycol) chemistry: Biotechnical and Biomedical Applications*, Harris, J. M., Ed. Plenum Publishing: New York, 1992; Vol. 1.

9. Johansson, G., Affinity Partitioning in PEG-Containtin Two-Phase Systems. In *Poly(ethylene glycol) chemistry: Biotechnical and Biomedical Applications*, Harris, J. M., Ed. Plenum Publishing: New York, 1992; Vol. 1.

10. Yoshinaga, K.; Ishida, H.; Sagawa, T.; Ohkubo, K., PEG-modified Protein Hybrid Catalyst. In *Poly(ethylene glycol) chemistry: Biotechnical and Biomedical Applications*, Harris, J. M., Ed. Plenum Publishing: New York, 1992.

11. *Poly(ethylene glycol) chemistry: Biotechnical and Biomedical Applications*. Plenum Publishing: New York, 1992; Vol. 1.

12. Hospital, A.; Candotti, M.; Gelpí, J. L.; Orozco, M., The Multiple Roles of Waters in Protein Solvation. *Journal of Physical Chemistry B* **2017,** *121* (15), 3636-3643.

13. Samanta, N.; Luong, T. Q.; Das Mahanta, D.; Mitra, R. K.; Havenith, M., Effect of Short Chain Poly(ethylene glycol)s on the Hydration Structure and Dynamics around Human Serum Albumin. *Langmuir* **2016,** *32* (3), 831-7.

14. Verma, P. K.; Rakshit, S.; Mitra, R. K.; Pal, S. K., Role of hydration on the functionality of a proteolytic enzyme alpha-chymotrypsin under crowded environment. *Biochimie* **2011,** *93* (9), 1424-1433.

15. Eronina, T. B.; Mikhaylova, V. V.; Chebotareva, N. A.; Borzova, V. A.; Yudin, I. K.; Kurganov, B. I., Mechanism of aggregation of UV-irradiated glycogen phosphorylase b at a low temperature in the presence of crowders and trimethylamine N-oxide. *Biophysical Chemistry* **2018,** *232*, 12-21.

16. Theillet, F.-x.; Binol, A.; Frembgen-kesner, T.; Hingorani, K.; Sarkar, M.; Kyne, C.; Li, C.; Crowley, P. B.; Gierasch, L.; Pielak, G. J.; Elcock, A. H.; Gershenson, A.; Selenko, P., Physicochemical Properties of Cells and Their Effects on Intrinsically Disordered Proteins (IDPs). *Chem. Rev* **2014,** *114*, 6661-6714.

17. Strulson, C. a.; Boyer, J. a.; Whitman, E. E.; Bevilacqua, P. C., Molecular crowders and cosolutes promote folding cooperativity of RNA under physiological ionic conditions. *RNA* **2014,** *20* (3), 331-347.

18. Shin, J.; Zhang, X.; Liu, J., DNA-functionalized gold nanoparticles in macromolecularly crowded polymer solutions. *Journal of Physical Chemistry B* **2012,** *116* (45), 13396-13402.

19. Petraccone, L.; Malafronte, A.; Amato, J.; Giancola, C., G-quadruplexes from human telomeric DNA: How many conformations in PEG containing solutions? *Journal of Physical Chemistry B* **2012,** *116* (7), 2294-2305.

20. Zhou, J.; Wei, C.; Jia, G.; Wang, X.; Feng, Z.; Li, C., Human telomeric G-quadruplex formed from duplex under near physiological conditions: Spectroscopic evidence and kinetics. *Biochimie* **2009,** *91* (9), 1104-1111.

21. Miyoshi, D.; Matsumura, S.; Nakano, S.-I.; Sugimoto, N., Duplex dissociation of telomere DNAs induced by molecular crowding. *Journal of the American Chemical Society* **2004,** *126* (1), 165-169.

22. Hirano, A.; Shiraki, K.; Arakawa, T., Polyethylene Glycol Behaves Like Weak Organic Solvent Polyethylene Glycol Behaves Like Weak Organic Solvent. *Biopolymers* **2011,** *97*.

23. Reid, C.; Rand, R. P., Probing protein hydration and conformational states in solution. *Biophysical Journal* **1997,** *72* (3), 1022-1030.

24. Weiss, M., *Crowding, diffusion, and biochemical reactions*. 1 ed.; Elsevier Inc.: 2014; Vol. 307, p 383-417.

25. Dix, J. A.; Verkman, A. S., Crowding Effects on Diffusion in Solutions and Cells. *Annual Review of Biophysics* **2008,** *37* (1), 247-263.

26. Giesa, T.; Buehler, M. J., Nanoconfinement and the Strength of Biopolymers. *Annual Review of Biophysics* **2013,** *42* (1), 651-673.

27. Kuznetsova, I. M.; Zaslavsky, B. Y.; Breydo, L.; Turoverov, K. K.; Uversky, V. N., Beyond the excluded volume effects: Mechanistic complexity of the crowded milieu. *Molecules* **2015,** *20* (1), 1377-1409.

28. Shahid, S.; Hassan, M. I.; Islam, A.; Ahmad, F., Size-dependent studies of macromolecular crowding on the thermodynamic stability, structure and functional activity of proteins: in vitro and in silico approaches. *Biochimica et Biophysica Acta - General Subjects* **2017,** *1861* (2), 178-197.

29. Tyrrell, J.; Weeks, K. M.; Pielak, G. J., Challenge of Mimicking the Influences of the Cellular Environment on RNA Structure by PEG-Induced Macromolecular Crowding. *Biochemistry* **2015,** *54* (42), 6447-6453.

30. Israelachvili, J., The different faces of poly(ethylene glycol). *Proceedings of the National Academy of Sciences of the United States of America* **1997,** *94* (16), 8378-8379.

31. Eronina, T. B.; Mikhaylova, V. V.; Chebotareva, N. A.; Makeeva, V. F.; Kurganov, B. I., Checking for reversibility of aggregation of UV-irradiated glycogen phosphorylase b under crowding conditions. *International Journal of Biological Macromolecules* **2016,** *86*, 829-839.

32. Daley, K. R.; Kubarych, K. J., An “Iceberg” Coating Preserves Bulk Hydration Dynamics in Aqueous PEG Solutions. *The Journal of Physical Chemistry B* **2017,** *121* (46), 10574-10582.

33. Nee, M. J.; McCanne, R.; Kubarych, K. J.; Joffre, M., Two-dimensional infrared spectroscopy detected by chirped pulse upconversion. *Optics letters* **2007,** *32*, 713-5.

34. Mukamel, S., Multidimensional Femtosecond Correlation Spectroscopies of Electrionic and Vibrational Excitations. *Annual Review of Physical Chemistry* **2000,** *51*, 691-729.

35. Khalil, M.; Demirdöven, N.; Tokmakoff, a., Coherent 2D IR Spectroscopy: Molecular Structure and Dynamics in Solution. *The Journal of Physical Chemistry A* **2003,** *107*, 5258-5279.

36. Roberts, S. T.; Ramasesha, K.; Tokmakoff, A., Structural Rearrangements in Water Viewed Through Two-Dimensional Infrared Spectroscopy. *ACCOUNTS OF CHEMICAL RESEARCH* **2009,** *42* (9), 1239-1249.

37. Nicodemus, R. A.; Ramasesha, K.; Roberts, S. T.; Tokmakoff, A., Hydrogen bond rearrangements in water probed with temperature-dependent 2D IR. *Journal of Physical Chemistry Letters* **2010,** *1* (7), 1068-1072.

38. Nicodemus, R. A.; Corecelli, S. A.; Skinner, J. L.; Tokmakoff, A., Collective bond reorganization in water studied with temperature-dependent ultrafast infrared spectroscopy. *J. Phys. Chem. B* **2011,** *115*, 5604-5616.

39. Kjellander, R. F., Ebba, Water structure and changes in thermal stability of the system poly(ethylene oxide)-water. *Journal of the Chemical Society, Faraday Transactions 1: Phyiscal Chemistry in Condensed Phases* **1981,** *77* (9), 2053-2077.

40. Laage, D.; Hynes, J. T., A molecular jump mechanism of water reorientation. *SCIENCE* **2006,** *311* (5762), 832-835.

41. Laage, D.; Stirnemann, G.; Hynes, J. T., Why Water Reorientation Slows without Iceberg Formation around Hydrophobic Solutes. *Journal of Physical Chemistry B* **2009,** *113* (8), 2428-2435.

42. Sterpone, F.; Stirnemann, G.; Laage, D., Magnitude and molecular origin of water slowdown next to a protein. *JOURNAL OF THE AMERICAN CHEMICAL SOCIETY* **2012,** *134* (9), 4116-9.

43. Kagemoto, A.; Murakami, S.; Fujishir.R, HEATS OF DILUTION OF POLY(ETHYLENE OXIDE)/WATER SOLUTIONS. *Makromolekulare Chemie* **1967,** *105* (JUL), 154-&.

44. Maron, S. H.; Filisko, F. E., HEATS OF SOLUTION AND DILUTION FOR POLYETHYLENE OXIDE IN SEVERAL SOLVENTS. *Journal of Macromolecular Science-Physics* **1972,** *B 6* (1), 79-&.

45. Daoust, H.; Stcyr, D., MICROCALORIMETRIC STUDY OF POLY(ETHYLENE OXIDE) IN WATER IN WATER ETHANOL MIXED-SOLVENT. *Macromolecules* **1984,** *17* (4), 596-601.

46. Rowe, R. C.; McKillop, A. G., MOLECULAR-WEIGHT DEPENDENCE OF THE HEATS OF HYDRATION OF SOME OLIGOMERIC ETHYLENE OXIDES AND THEIR METHOXYL DERIVATIVES. *Journal of Applied Polymer Science* **1993,** *50* (2), 321-326.

47. North, A. M.; Pethrick, R. A.; Poh, B. T., ADIABATIC COMPRESSIBILITY STUDIES OF MIXTURES OF POLYETHYLENEOXIDE WITH HYDROPHILIC SOLVENTS. *Advances in Molecular Relaxation and Interaction Processes* **1981,** *19* (2-3), 209-219.

48. Eagland, D.; Crowther, N. J.; Butler, C. J., INTERACTION OF POLY(OXYETHYLENE) WITH WATER AS A FUNCTION OF MOLAR-MASS. *Polymer* **1993,** *34* (13), 2804-2808.

49. Harris, J. M., Introduction to Biotechnical and Biomedical Applications of Poly(ethylene glycol). In *Poly(ethylene glycol) chemistry: Biotechnical and Biomedical Applications*, Harris, J. M., Ed. Plenum Publishing: New York, 1992; Vol. 1.

50. Saeki, S.; Kuwahara, N.; Nakata, M.; Kaneko, M., Upper and lower critical solution temperatures in poly (ethylene glycol) solutions. *Polymer* **1976,** *17* (8), 685-689.

51. Golander, C. G.; Herron, J. N.; Lim, K.; Claesson, P.; Stenius, P.; Andrade, J. D., Properties of Immobilized PEG Films and the Interaction with Proteins: Experiments and Modeling. In *Poly(ethylene glycol) chemistry: Biotechnical and Biomedical Applications*, Harris, J. M., Ed. Plenum Publishing: New York, 1992; Vol. 1.

52. Bailey Jr., F. E.; Koleske, J. V., *Poly(ethylene oxide)*. Academic Press: New York, 1976; p 184.

53. Teraoka, I., *Polymer Solutions: An Introduction to Physical Properties*. Wiley-Interscience: Canada, 2002.

54. Pedersen, J. S.; Sommer, C., Temperature dependence of the virial coefficients and the chi parameter in semi-dilute solutions of PEG. *Progress in Colloid and Polymer Science* **2005,** *130*, 70-78.

55. Han, F.; Zhang, J.; Chen, G.; Wei, X., Density , Viscosity , and Excess Properties for Aqueous Poly(ethylene glycol) Solutions from (298.15 to 323.15) K. *Journal of Chemical & Engineering Data* **2008,** *53*, 2598-2601.

56. Bhanot, C.; Trivedi, S.; Gupta, A.; Pandey, S.; Pandey, S., Dynamic viscosity versus probe-reported microviscosity of aqueous mixtures of poly(ethylene glycol). *Journal of Chemical Thermodynamics* **2012,** *45* (1), 137-144.

57. Perakis, F.; Hamm, P., Two-dimensional infrared spectroscopy of supercooled water. *Journal of Physical Chemistry B* **2011,** *115* (18), 5289-5293.

58. Kiefer, L. M.; Kubarych, K. J., Solvent exchange in preformed photocatalyst-donor precursor complexes determines efficiency. *Chemical Science* **2018,** *9* (6), 1527-1533.

59. King, J. T.; Baiz, C. R.; Kubarych, K. J., Solvent-dependent spectral diffusion in a hydrogen bonded "vibrational aggregate". *The journal of physical chemistry. A* **2010,** *114*, 10590-604.

60. Osborne, D. G.; King, J. T.; Dunbar, J. a.; White, A. M.; Kubarych, K. J., Ultrafast 2DIR probe of a host-guest inclusion complex: Structural and dynamical constraints of nanoconfinement. *The Journal of Chemical Physics* **2013,** *138*, 144501.

61. Chudoba, R.; Heyda, J.; Dzubiella, J., Temperature-Dependent Implicit-Solvent Model of Polyethylene Glycol in Aqueous Solution. *Journal of Chemical Theory and Computation* **2017,** *13* (12), 6317-6327.

Chapter 4 CROWDED VERSUS BULK DYNAMICS IN GUAR AND FICOLL SOLUTIONS

4.1 INTRODUCTION

Two-dimensional infrared (2DIR) spectroscopy is an experimental technique that can be used to observe solvent dynamics and provide bond-specific structural resolution.[1] While linear FTIR spectroscopy provides only time-averaged information regarding chemical processes, 2DIR allows for resolution on a picosecond timescale due to the utilization of femtosecond pulses.[2] This technique has been used to study a multitude of subjects such as glass formers,[3] proteins,[4-6] and biological membranes,[7] focusing particularly on aspects of hydration dynamics.

Though 2DIR has been helpful in elucidating a wide array of physical challenges in condensed phases, the fundamental properties of heterogeneous mixtures of polymers remains generally unexplored. Heterogeneous mixtures consist of various components that are either known to or are expected to exhibit complex multiscale dynamics ranging from femtoseconds and picoseconds to much longer timescales.[3] In cases where water is a major component, its role is as both a solvent and as a mediator of dynamical coupling,[5] with likely complicated dependencies on composition, concentration, and other thermodynamic parameters such as temperature, pressure, and strain. Heterogeneous mixtures of polymers have rarely been studied using 2DIR spectroscopy, and little is known about how hydration dynamics are affected by these crowded solutions, which have applications in cell biology, heterogeneous catalysis,[22] and in hydraulic fracturing liquid[8]. Confined liquids also have an important role in the fields of cellular dynamics, lubrication, and microfluidic technology.[9-10]

Hydraulic fracturing liquid (HFL) is a relevant polymer mixture that inspires this study. For more than a decade, the natural gas industry has used hydraulic fracturing to remove natural gas from shale. HFL is a viscous solution typically made of sand, emulsifier (the polymer guar)[11], and water. HFL is injected into a well at high pressures to create fractures in the shale. Guar is used to make the water viscous so that the sand remains in solution.[12] Sand is not water soluble, so the fact that HFL has embedded sand indicates the solution is intrinsically out of equilibrium. Also, during the injection process, HFL exhibits nonlinear and non-equilibrium (i.e. non-Newtonian) dynamics. This leads to properties such as shear thinning, where viscosity becomes a function of shear.[11] Little research has been conducted on the basic chemical dynamics of polymer solutions, like HFL, using the ultrafast spectroscopic techniques that have been so successful in enhancing our understanding of other complex systems such as proteins/peptides and hydrogen bonded liquids.[13-15]

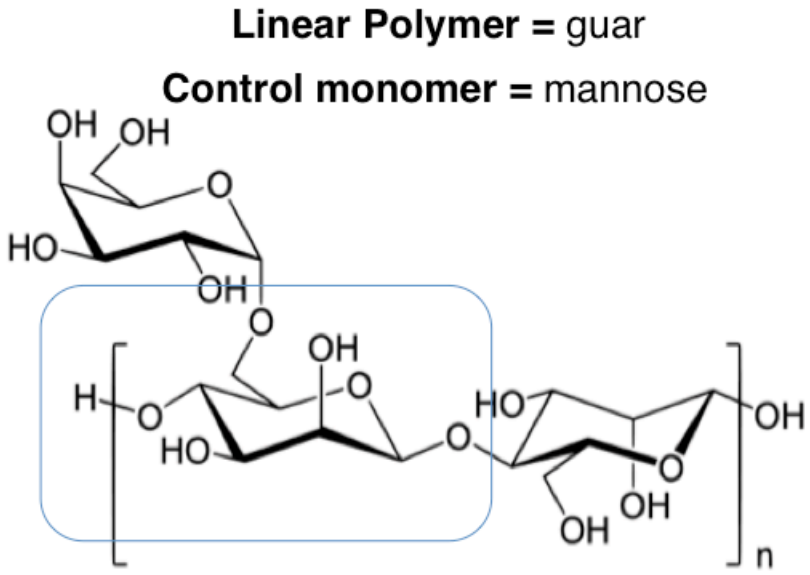

Figure 4.1 Structure of guar and mannose.

Since little is known about the dynamics of HFL,[16] before moving on to model the whole mixture, we first investigate aqueous guar solutions. **Figure 4.1** depicts the structure of guar, and the monomer unit mannose. This model system can provide fundamental information on the hydration dynamics of concentrated polymer solutions, such as how viscosity may relate to the picosecond hydration

dynamics and the effect of macromolecular crowding. We focus on hydration dynamics of polymer solutions and how water behaves as the polymer chains begin to overlap and entangle. We investigate how structural properties, such as branching and size, affect the hydration dynamics. Guar, a linear polymer, and Ficoll (**Figure 4.2**), a hard, spherical polymer, serve as our model macromolecular crowders, while their monomer units will serve as control solutes and allow us to isolate the effects of polymer size and shape.

By studying the fundamental properties of these mixtures, we learn how crowding and confinement affects the structural and dynamical properties of liquids on both a micro- and a macroscale. We explore how hydration dynamics depend on connectivity of the monomer units (i.e. polymerized vs. discrete) and how polymer shape (i.e. linear vs. spherical) affects hydration dynamics of heterogeneous mixtures.

Branched Polymer = Ficoll 400, Ficoll 70

Control monomer = sucrose

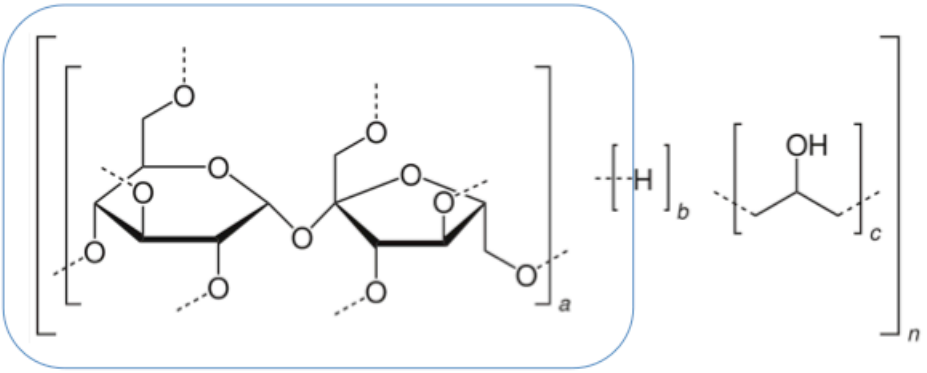

Figure 4.2 Structure of Ficoll and its monomer unit sucrose.

4.2 EXPERIMENTAL METHODS

4.2.1 2DIR Spectroscopy

The experimental set up has been described in full elsewhere.[17] Briefly, 2DIR spectroscopy uses three infrared femtosecond laser pulses to interact with the sample and create a third-order nonlinear signal.[18] There are three time delays in the experiment, which include the evolution period (t_1), the waiting

period (t_2), and the detection period (t_3). Each delay follows the corresponding pulse of E_1, E_2, or E_3. The pulses interact with the sample in the noncollinear box geometry in order to generate the signal in a background free direction.[19] During the experiments, t_1 is scanned using an optical delay line and the signal at each detection frequency ω_3 is Fourier transformed to yield the ω_1 frequency axis. The phase and amplitude of the signal are measured directly with a spectrometer[20] via heterodyne detection by spectral interference with a local oscillator field.[19]

Using 2D-IR, it is possible to extract information about solvent-solute interactions, vibrational dynamics, and molecular structure.[21] We have previously shown that transition metal carbonyl complexes are powerful probes of solution environments, and use one as a probe in this study[22-27] The frequency-fluctuation correlation function (FFCF) is denoted as $C(t) = \langle \delta\omega(0)\delta\omega(t) \rangle$, where $\delta\omega(t)$ is the instantaneous fluctuation from the average frequency.[28] The inhomogeneous index, $I(t)$, which is directly proportional to the FFCF,[29] is extracted from 2DIR spectra and informs on spectral diffusion. At early waiting times (t_2), the excitation and detection frequencies are well correlated because the probe has not had the chance to sample many microscopic environments. As the waiting time (t_2) increases, correlation is lost as the probe samples more solvent environments. The timescale for this loss in correlation is spectral diffusion and can be related to characteristic timescales of the solvent dynamics.[18]

4.2.2 Sample Preparation

$[Ru(CO)_3]_2(\mu\text{-}Cl)_2$ (Strem Chemicals), a carbon monoxide releasing molecule (CORM) commonly referred to as CORM-2, was used in these studies. CORM-2 has the following IR-active carbonyl stretches: 1972, 2004, 2051, and 2075 cm^{-1}. The spectral diffusion time constant of CORM-2 in D_2O is 1.5 +/- 0.4 ps, which is the same value as is obtained from 2DIR studies probing the OH stretch of diluted HOD.[30]

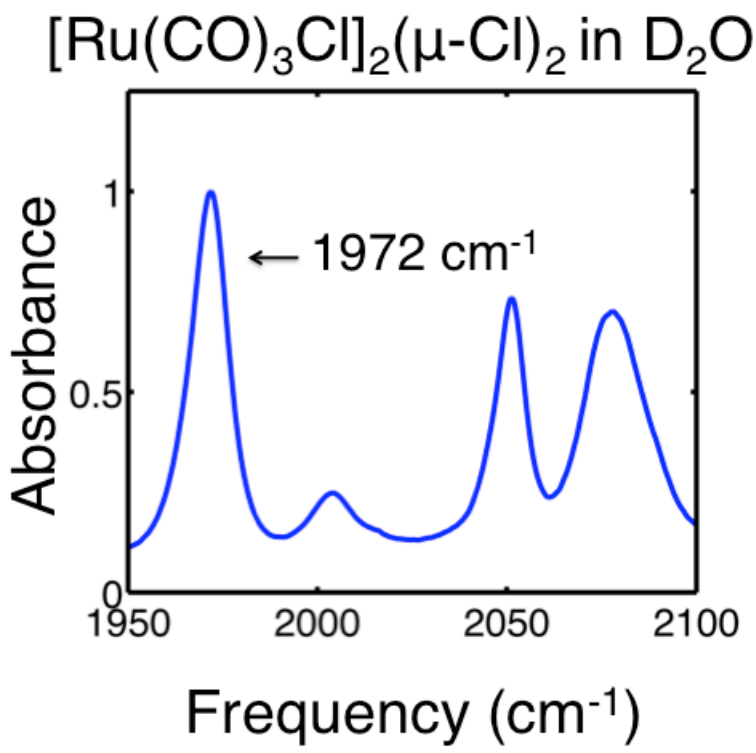

Figure 4.3 CORM-2 FTIR spectrum

Guar is a polymer made of mannose and galactose monomer units. The polymer is linearly shaped and flexible, allowing for polymer strands to become entangled at the molecular level.[31] Guar is naturally occurring, so its molecular weight can vary from 50,000-8,000,000. Ficoll is a highly branched copolymer that is composed of sucrose and epichlorohyrdan. This polymer is a compact, rigid, and spherical molecule.[9] The radius of a single Ficoll-400 molecule ranges from 15-30 nm while the radius of Ficoll-70 ranges from 2-7 nm.[32] The weight of Ficoll 400 is 400,000 Da, and the weight of Ficoll 70 is 70,000 Da. Ficoll-70 is about the size of the lysozyme proteins previously studied with a surface-bound metal carbonyl probe.[5]

CORM-2 was combined with guar at increasing concentrations (0.1-2.7 wt%) in D_2O. CORM-2 FTIR is depicted in **Figure 4.3**. The same was done to prepare samples of mannose, Ficoll, and sucrose. Data collected from each of the samples were analyzed to compare each *C(t)* and see how the spectral diffusion timescales change as a function of composition and concentration.

4.3 RESULTS

4.3.1 Solutions of Guar Experience a Dynamical Transition While Solutions of Mannose Exhibit Bulk-Like Hydration Dynamics

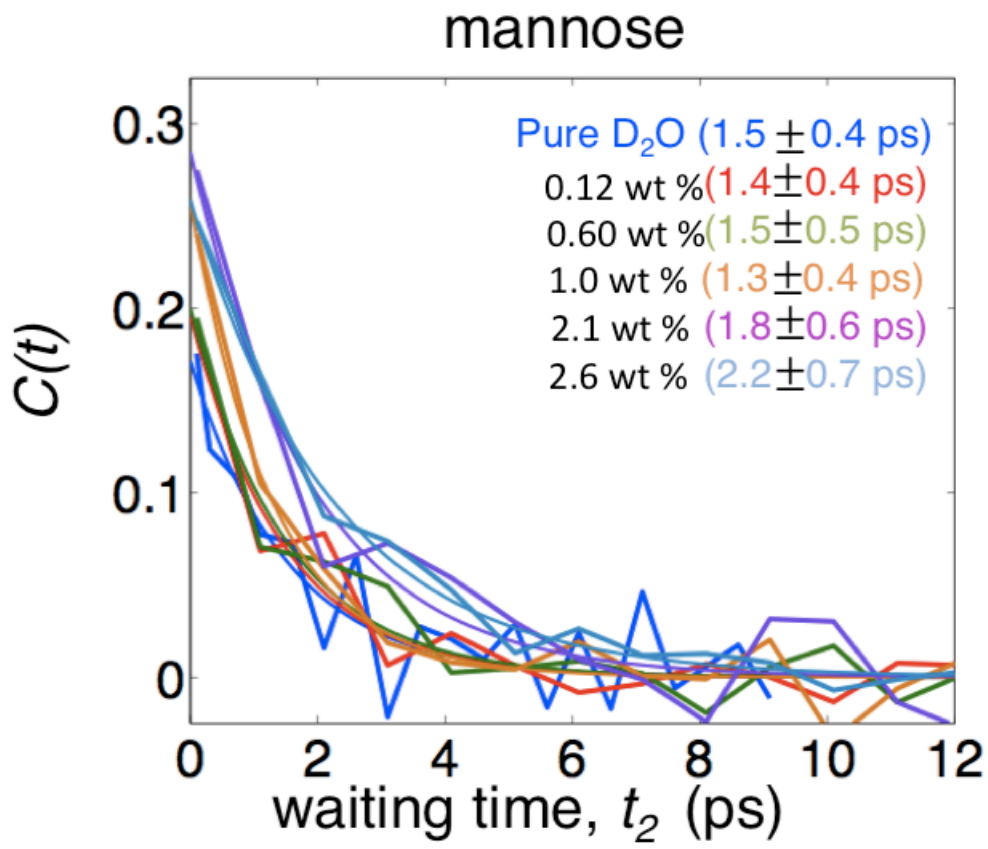

Figure 4.4 Hydration dynamics probed with the 1972 cm^{-1} band of CORM-2 in D_2O/mannose mixtures.

In simple liquids like alcohols, using metal carbonyl probes, several studies show that the decays of the FFCFs are proportional to solvent viscosity.[14-15] In other cases studying complex systems, such as proteins and glass-forming liquids, the group has found highly non-exponential dynamics indicative of a range of relaxation times due to structural and purely dynamical heterogeneity.[3] The linear polymer guar is of particular interest due to its use as an emulsifier in hydraulic fracturing, pharmaceutics, and in other industrial applications. We are particularly interested in understanding how water responds to being crowded by the macromolecular molecule guar and its monomer mannose. This model system can provide fundamental information on the hydration dynamics of concentrated polymer solutions, such as how viscosity or

gel point may relate to the picosecond hydration dynamics of polymer solutions, as well as how water behaves as the polymer chains begin to overlap and become entangled.

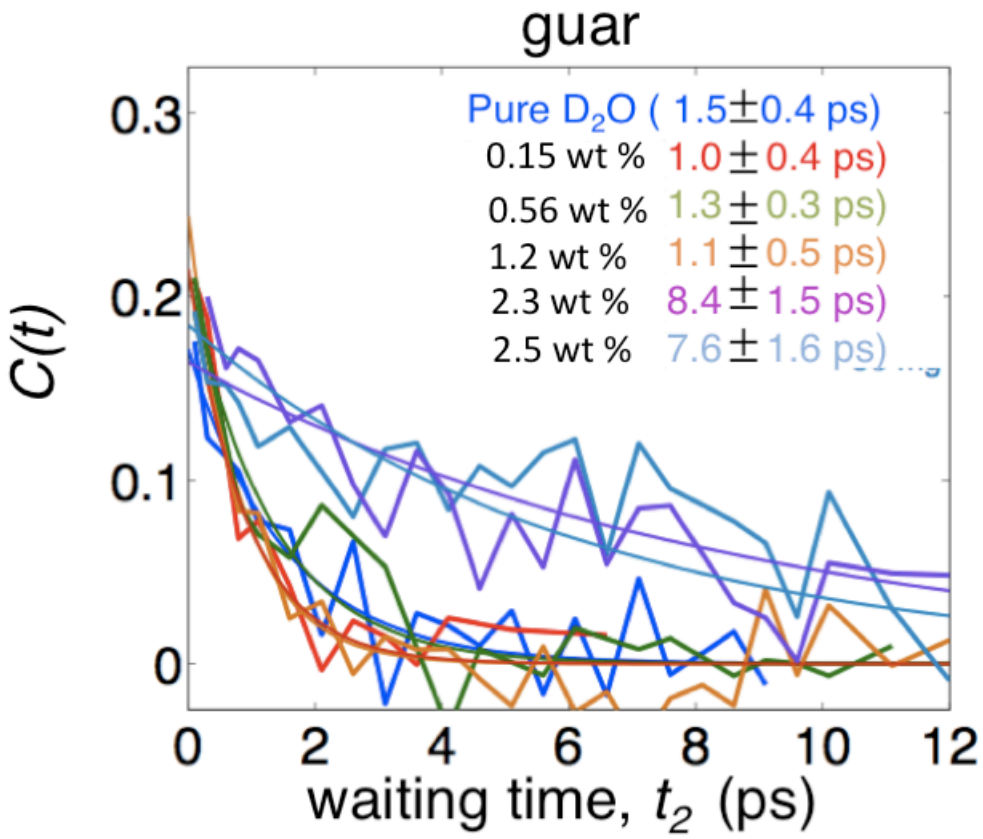

Figure 4.5 FFCFs for the lowest frequency CO stretching mode of CORM-2 in D_2O/guar mixtures, ranging from pure D_2O to 2.5% PEG by volume.

Using CORM-2 as the probe, the hydration dynamics of aqueous guar mixtures were studied, varying the concentration and effective length of the polymer (comparing the monomer to the full polymer). First, we looked at aqueous solutions of mannose (**Figure 4.4**). We looked at the hydration dynamics for increasing approximate concentrations (wt % of monomer in solution): 0.1%, 0.6%, 1.3%, 1.8%, and 2.8%. At low mannose concentrations, the correlation function exponentially decays with a 1.42 +/- 0.4 ps decay time constant, similar. As concentration was increased, the spectral diffusion time constant does not significantly change, revealing bulk hydration dynamics consistent at all concentrations studied. The spectral diffusion time constant for

each mixture of each polymer yielded a similar value to that of CORM-2 in D_2O, within error.

Next, we looked at the hydration dynamics for increasing concentrations of aqueous guar solutions (**Figure 4.5**). We looked at the hydration dynamics for increasing approximate concentrations (wt % of polymer in solution): 0.2%, 0.6%, 1.2%, 2.3%, and 2.5%. As the concentration of guar increased in the aqueous solutions, we find that the spectral dynamics experience an abrupt slow down. At low concentrations of guar, the correlation function exponentially decays with a 1.23 +/- 0.3 ps decay time constant, which is consistent with bulk-like water.[6] At 2.3 % aqueous guar solution, the spectral diffusion shows an abrupt transition and slows to 8.4 +/- 1.5 ps. The decay constant is only weakly coupled with guar concentration on either side of this transition.

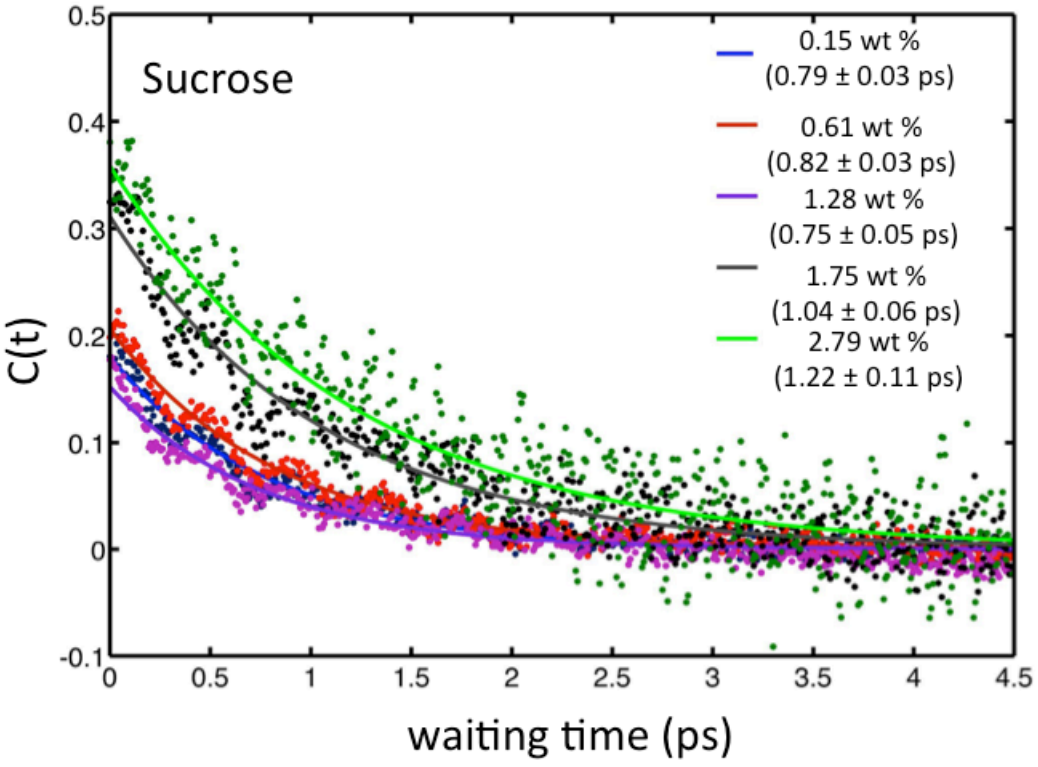

Figure 4.6 FFCFs for the lowest frequency CO stretching mode of CORM-2 in D_2O/sucrose mixtures, ranging from 0.15% to 2.79% sucrose by volume.

4.3.2 Aqueous Ficoll and Sucrose Solutions Reveal Bulk Hydration Dynamics

We also considered the role of polymer shape in hydration dynamics by comparing Ficoll at various sizes. We studied aqueous mixtures of Ficoll-400, Ficoll-70, and one of its monomer units, sucrose. First, we looked at how the hydration dynamics of aqueous solutions of sucrose might change with increased concentration (**Figure 4.6**). We looked at the hydration dynamics for increasing approximate concentrations: 0.1%, 0.6%, 1.3%, 1.8%, and 2.8%. The spectral diffusion time constant for each mixture of each polymer yields a similar value to that of CORM-2 in D_2O, within error. This was consistent with the data we collected for the increasing concentrations of aqueous mannose solutions.

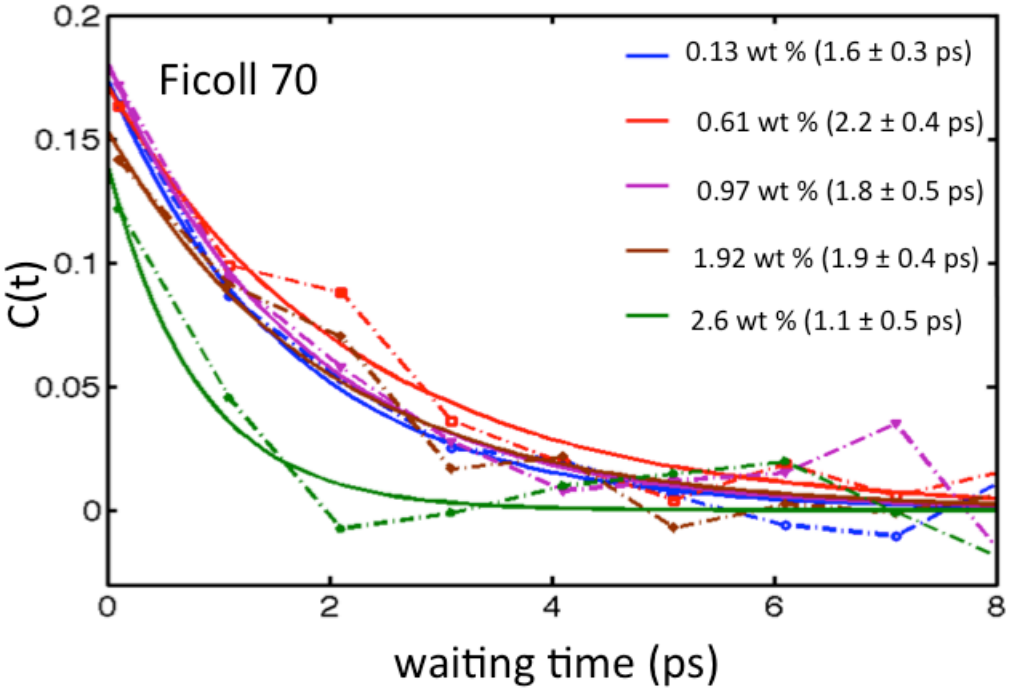

Figure 4.7 FFCFs for the lowest frequency CO stretching mode of CORM-2 in D_2O/Ficoll 70 mixtures, ranging from 0.13% to 2.6% Ficoll 70 by volume.

Next, we conducted experiments with Ficoll-70 (**Figure 4.7**) and Ficoll-400 (**Figure 4.8**), which are bulky polymers. Ficoll-400 is 400,000 Da and Ficoll-70 is 70,000 Da. We looked at the hydration dynamics for increasing approximate concentrations: 0.1%, 0.6%, 1.0%, 2.0%, and 2.7%. The spectral diffusion time constant for each mixture of each polymer yields a similar value to that of CORM-

2 in D_2O, within error. There was no abrupt change in hydration dynamics as we saw with guar.

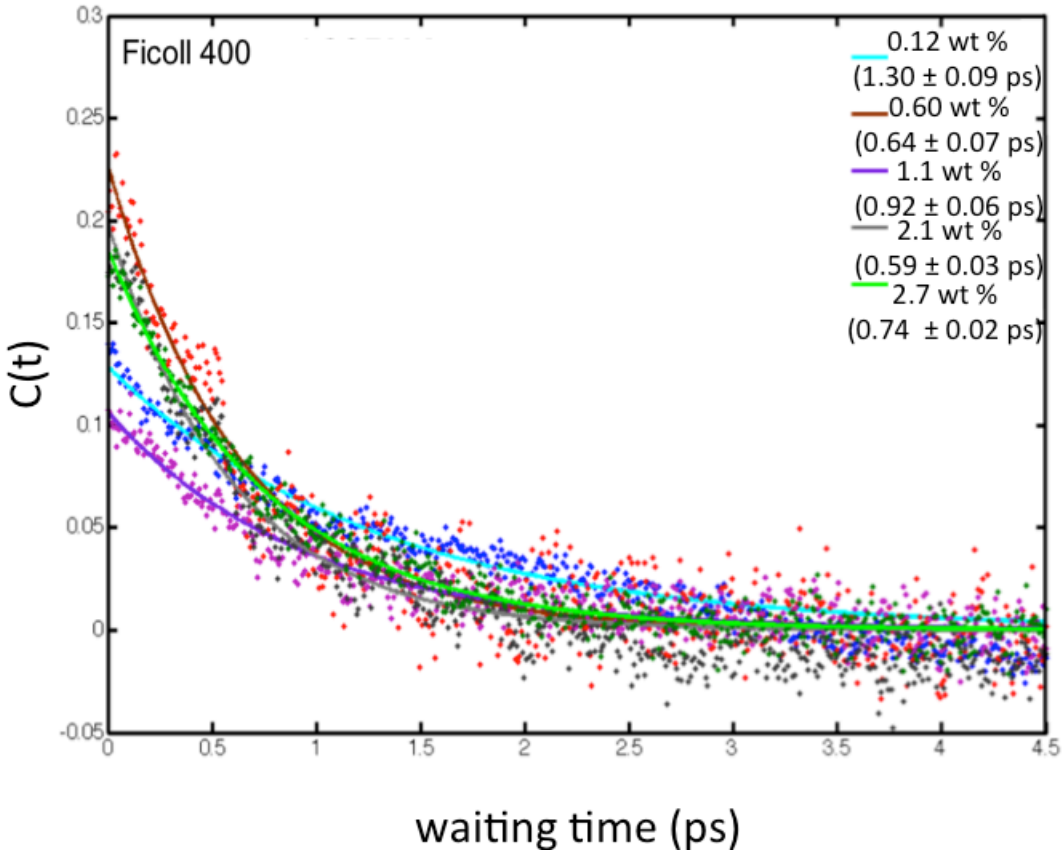

Figure 4.8 FFCFs for the lowest frequency CO stretching mode of CORM-2 in D_2O/Ficoll 400 mixtures, ranging from 0.12% to 2.7% Ficoll 400 by volume.

4.4 DISCUSSION

4.4.1 Aqueous Guar Solutions Experience Slowed Hydration Dynamics at Small Concentrations

At relatively low concentrations of guar, aqueous guar solutions experience an abrupt slow down in hydration dynamics. This abrupt slow down can be compared to results examining PEG 400[33], and also increasing lengths of PEG[34] to gain more insight. In the first example, HEWL was crowded with PEG 400 and it was found that at 50 wt% PEG 400, there was an abrupt slow down in hydration dynamics.[33] This abrupt slow down was attributed to a transition from independent to collective hydration induced by crowding. In the second example, it was found that due to the stability of the hydration shell, aqueous solutions of

PEG 2000, PEG 8000, and PEG 20000 experienced little to no change in hydration dynamics as compared to the probe in D_2O. PEG 400 experienced a linear slow down in hydration dynamics due to a less stable hydration shell experienced by the PEG 400 strands.[34]

Compared to guar, whose molecular weight varies from 50,000-8,000,000 Da, PEG 20,000 has a molecular weight of 20,000 Da. Aqueous solutions of PEG 20,000 did not experience a significant change in hydration dynamics, but aqueous solutions of guar did. Because guar is a naturally occurring polymer, each strand is not a consistent length or weight. Low concentration aqueous guar solutions (2.3 wt%) become extremely viscous as compared to aqueous solutions of PEG 20,000, which only became as viscous as guar solutions at 55 wt%. While there appears to be a similar abrupt slow down in hydration dynamics similar to PEG 400 crowding HEWL, this occurs at a much lower concentration. A possible reason this occurs is that similar to PEG 400, guar may not have a stable hydration shell and due to its inconsistent length and weight of strands, induces a transition from independent to collective hydration in the aqueous solutions. More experiments will need to be completed to confirm this hypothesis.

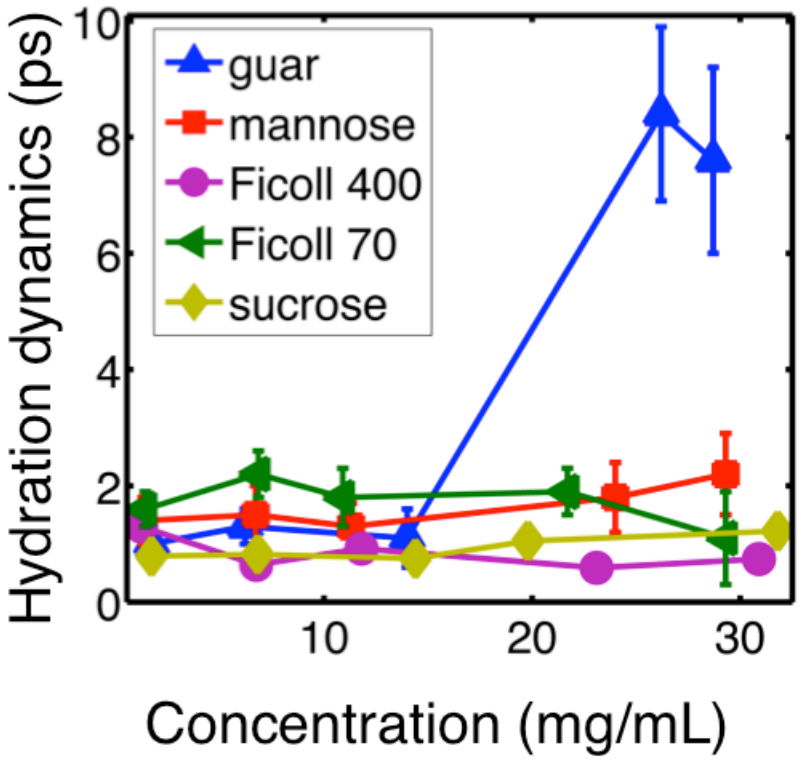

Figure 4.9 Spectral diffusion timescale plotted as a function of mixture concentration. Guar experiences an abrupt slow down, while the other molecules experience consistent hydration dynamics as concentration increases.

4.4.2 Aqueous Mannose, Sucrose, and Ficoll Solutions Experience Bulk-Like Dynamics at Low Concentrations

Figure 4.9 depicts the spectral diffusion plotted as a function of mixture concentration. Sucrose and mannose are monomers of Ficoll and guar, respectively. Variable concentration experiments were done with aqueous solutions of both monomers at increasing concentrations up to about 3 wt %. There were no changes in hydration dynamics across the increasing concentrations. It is possible that at higher concentrations there could be changes in hydration dynamics. However, we wanted to use similar concentration ranges as for Ficoll and guar for comparison purposes. Without doing experiments at higher concentrations, it isn't really possible to draw conclusions about the aqueous mannose and sucrose solutions. Aqueous Ficoll 400 and Ficoll 70 solutions did not exhibit a change in hydration dynamics in solutions up to 3 wt%, as aqueous solutions of guar did. Ficoll 400 and Ficoll 70

are larger in molecular weight per strand than PEG 20,000. Ficoll 400 is closer in molecular weight to guar, so it is possible we might see a change in hydration dynamics at higher concentrations of Ficoll 400 in aqueous solution. Because Ficoll is a synthetic polymer like PEG, it is possible that the strands are more consistent in length and weight than guar, and therefore may follow the same patterns that we saw for longer lengths of PEG: that there are little changes in hydration dynamics for high concentrations of Ficoll. More experiment would need to be conducted in order to test this hypothesis.

4.5 CONCLUSIONS

The description of dynamical molecular interactions in solutions, such as concentrated solutions of polymers, represents a frontier in scientific inquiry. Complex polymer mixtures, such as model HFL, have not been thoroughly investigated by modern spectroscopic techniques. We have undertaken an initial study of mixtures of guar and Ficoll, and the following conclusions have been made: (1) Guar experiences collective hydration at high concentrations, where mannose, its monomer, experiences independent hydration, regardless of concentration. (2) No collective hydration is observed for Ficoll-400 or Ficoll-70 in the same concentration range as guar, possibly due to polymer shape and size.

It is important to increase the concentrations of Ficoll-400 and Ficoll-70 to see if a dynamical transition occurs as predicted above. Further experiments are necessary to expand knowledge of hydration dynamics in polymer solutions. Such studies could include: looking at each aqueous polymer solution at increasing concentrations to saturation. Other experiments with guar indicated its lack of ease for dissolution because it is naturally occurring. To make it easier to work with guar, using a shaker to mix polymers could be useful and letting it mix for longer periods of time.

To better model HFL, experiments will be conducted to see how hydration dynamics are related to pressure and temperature in crowded solutions. Finally, to see if probe dependence exists in the results, anionic, neutral, and cationic probes will be examined. With only two polymers explored here, there is room for much more research on how the nature of crowding agents affect dynamical

transitions. Other polymers of interest include linear polymers, such as poly(N-isopropylacrylamide) due to its known thermoresponsive properties.[35]

4.6 REFERENCES

1. Hamm, P., *Concepts and methods of 2D Infrared Spectroscopy*. Cambridge University Press: New York, 2011.

2. Anna, J. M.; Baiz, C. R.; Ross, M. R.; McCanne, R.; Kubarych, K. J., Ultrafast equilibrium and non-equilibrium chemical reaction dynamics probed with multidimensional infrared spectroscopy. *International Reviews in Physical Chemistry* **2012,** *31*, 367-419.

3. King, J. T.; Ross, M. R.; Kubarych, K. J., Ultrafast α-Like Relaxation of a Fragile Glass-Forming Liquid Measured Using Two-Dimensional Infrared Spectroscopy. *Physical Review Letters* **2012,** *108*, 157401.

4. King, J. T.; Arthur, E. J.; Brooks, C. L.; Kubarych, K. J., Site-Specific Hydration Dynamics of Globular Proteins and the Role of Constrained Water in Solvent Exchange with Amphiphilic Cosolvents. *The journal of physical chemistry. B* **2012**.

5. King, J. T.; Arthur, E. J.; Brooks, C. L.; Kubarych, K. J., Crowding induced collective hydration of biological macromolecules over extended distances. *Journal of the American Chemical Society* **2014,** *136*, 188-94.

6. King, J. T.; Kubarych, K. J., Site-specific coupling of hydration water and protein flexibility studied in solution with ultrafast 2D-IR spectroscopy. *Journal of the American Chemical Society* **2012,** *134*, 18705-12.

7. Osborne, D. G.; Dunbar, J. a.; Lapping, J. G.; White, A. M.; Kubarych, K. J., Site-specific measurements of lipid membrane interfacial water dynamics with multidimensional infrared spectroscopy. *The journal of physical chemistry. B* **2013,** *117*, 15407-14.

8. Tollefson, J., Secrets of fracking fluids pave way for cleaner recipe. *Nature* **2011,** *501*, 146-147.

9. Bohrer, M. P.; Patterson, G. D.; Carroll, P. J., Hindered diffusion of dextran and ficoll in microporous membranes. *Macromolecules* **1984,** *17*, 1170-1173.

10. Farrer, R. a.; Fourkas, J. T., Orientational dynamics of liquids confined in nanoporous sol-gel glasses studied by optical kerr effect spectroscopy. *Accounts Chem Res* **2003,** *36*, 605-12.

11. Xu, B.; Hill, A. D.; Zhu, D.; Texas, A.; Wang, L., Experimental Evaluation of Guar-Fracture-Fluid Filter-Cake Behavior. **2011**, 381-387.

12. Vidic, R. D.; Brantley, S. L.; Vandenbossche, J. M.; Yoxtheimer, D.; Abad, J. D., Impact of shale gas development on regional water quality. *Science (New York, N.Y.)* **2013,** *340*, 1235009.

13. Baiz, C. R.; Kubarych, K. J., Ultrafast vibrational Stark-effect spectroscopy: exploring charge-transfer reactions by directly monitoring the solvation shell response. *Journal of the American Chemical Society* **2010,** *132*, 12784-5.

14. King, J. T.; Baiz, C. R.; Kubarych, K. J., Solvent-dependent spectral diffusion in a hydrogen bonded "vibrational aggregate". *The journal of physical chemistry. A* **2010,** *114*, 10590-604.

15. King, J. T.; Anna, J. M.; Kubarych, K. J., Solvent-hindered intramolecular vibrational redistribution. *Physical chemistry chemical physics : PCCP* **2011,** *13*, 5579-83.

16. Howarth, R. D.; Ingraffea, A., Should fracking stop? *Nature* **2011,** *477*, 271-275.

17. Anna, J. M.; Nee, M. J.; Baiz, C. R.; McCanne, R.; Kubarych, K. J., Measuring absorptive two-dimensional infrared spectra using chirped-pulse upconversion detection. *J. Opt. Soc. Am. B* **2010,** *27* (3), 382-393.

18. Mukamel, S., *Principles of Nonlinear Optical Spectroscopy*. Oxford University Press: Oxford, U.K., 1995.

19. Hybl, J. D.; Albrecht Ferro, A.; Jonas, D. M., Two-dimensional Fourier transform electronic spectroscopy. *The Journal of Chemical Physics* **2001,** *115*, 6606.

20. Dlott, D. D., Vibrational energy redistribution in polyatomic liquids: 3D infrared–Raman spectroscopy. *Chemical Physics* **2001,** *266*, 149-166.

21. Khalil, M. D., N.; Tokmakoff, A. , Coherent 2D IR Spectroscopy: Molecular Structure and Dynamics in Solution. *J. Phys. Chem. A* **2003,** *107*, 5258-5279.

22. Treuffet, J.; Kubarych, K. J.; Lambry, J.-C.; Pilet, E.; Masson, J.-B.; Martin, J.-L.; Vos, M. H.; Joffre, M.; Alexandrou, A., Direct observation of ligand transfer and bond formation in cytochrome c oxidase by using mid-infrared chirped-pulse upconversion. *P Natl Acad Sci USA* **2007,** *104*, 15705-10.

23. Nee, M. J.; McCanne, R.; Kubarych, K. J.; Joffre, M., Two-dimensional infrared spectroscopy detected by chirped pulse upconversion. *Optics letters* **2007,** *32*, 713-5.

24. Baiz, C. R.; Nee, M. J.; McCanne, R.; Kubarych, K. J., Ultrafast nonequilibrium Fourier-transform two-dimensional infrared spectroscopy. *Optics letters* **2008,** *33*, 2533-5.

25. Anna, J. M.; Ross, M. R.; Kubarych, K. J., Dissecting enthalpic and entropic barriers to ultrafast equilibrium isomerization of a flexible molecule using 2DIR chemical exchange spectroscopy. *J. Phys. Chem. A* **2009,** *113*, 6544-6547.

26. King, J. T.; Ross, M. R.; Kubarych, K. J., Water-assisted vibrational relaxation of a metal carbonyl complex studied with ultrafast 2D-IR. *J. Phys. Chem. B* **2012,** *116*, 3754-9.

27. Osborne, D. G.; King, J. T.; Dunbar, J. A.; White, A. M.; Kubarych, K. J., Ultrafast 2DIR probe of a host-guest inclusion complex: Structural and dynamical constraints of nanoconfinement. *J. Chem. Phys.* **2013,** *138*, 144501.

28. Osborne, D. G.; Kubarych, K. J., Rapid and accurate measurement of the frequency-frequency correlation function. *J. Phys. Chem. A* **2013,** *117*, 5891-8.

29. Roberts, S. T.; Loparo, J. J.; Tokmakoff, A., Characterization of spectral diffusion from two-dimensional line shapes. *J. Chem. Phys.* **2006,** *125*, 084502.

30. Fecko, C. J.; Loparo, J. J.; Roberts, S. T.; Tokmakoff, A., Local hydrogen bonding dynamics and collective reorganization in water: ultrafast infrared spectroscopy of HOD/D(2)O. *The Journal of chemical physics* **2005,** *122*, 54506.

31. Dharela, R.; Raj, L.; Chauhan, G. S., Synthesis , Characterization , and Swelling Studies of Guar Gum-Based pH , Temperature , and Salt Responsive Hydrogels. **2012**.

32. Fissell, W. H.; Hofmann, C. L.; Smith, R.; Chen, M. H., Size and conformation of Ficoll as determined by size-exclusion chromatography followed by multiangle light scattering. *American Journal of Physiology - Renal Physiology* **2009,** *298* (1), F205-F208.

33. King, J. T.; Arthur, E. J.; Brooks, C. L.; Kubarych, K. J., Crowding induced collective hydration of biological macromolecules over extended distances. *Journal of the American Chemical Society* **2014,** *136*, 188-194.

34. Daley, K. R.; Kubarych, K. J., An “Iceberg” Coating Preserves Bulk Hydration Dynamics in Aqueous PEG Solutions. *The Journal of Physical Chemistry B* **2017,** *121* (46), 10574-10582.

35. Phillips, D. J.; Gibson, M. I., Biodegradable Poly(disulfide)s Derived from RAFT Polymerization: Monomer Scope, Glutathione Degradation, and Tunable Thermal Responses. *Biomacromolecules* **2012,** *13* (10), 3200-3208.

Chapter 5 Conclusions and Future Direction

5.1 Key Results

This work detailed how hydration dynamics are affected by the interactions with polymers. We find evidence for distinct dynamics sensed by the probe depending on the crowding agent. Polymers used as crowding agents throughout this thesis include PEG, Ficoll, and guar, as well as use of two monomers, sucrose and mannose. We find experimental evidence contributing to the importance of consider both steric effects and chemical effects of a crowding agents on proteins.[1-5]

Using a spectroscopic probe in 2DIR to study macromolecular crowding and confinement of water is useful for several reasons. Biological interfaces are typically in aqueous conditions. Using molecular probes removes the need for really high solute concentration. If –OH stretch was studied directly, at low concentrations the signal would be dominated by bulk water and we wouldn't necessarily see how water affected by the polymer would be different than bulk water. Linear FTIR spectra shown throughout this thesis show, for the most part, little change as concentration, polymer length, and temperature compared to the measure dynamical changes with these changing variable using 2DIR.

At room temperature, the Ru3C spectral diffusion time constant in D_2O is 1.76±0.2 ps, which is consistent with the time scale determined directly using 2D-IR spectroscopy of HOD in D_2O.[6] As a temperature dependent probe, Ru3C measures viscosity dependent activation energy that agrees with previously collected 2D-IR results without a probe.[7, 8] This result indicates that metal carbonyls are useful probes of hydration dynamics, even at varying temperatures.

We focus mainly on PEG and its affects on hydration dynamics of water. PEG is a very widely used polymer for a range of biomedical, pharmaceutical,

and engineering applications, as well as used as an artificial crowding agent to make experimental conditions more physiologically relevant. While PEG is widely used and has been for decades, its interactions with biomolecules do not seem well understood. PEG interesting structural and thermodynamical properties that make its use as a crowding agent questionable.

PEG is very water soluble as compared to other polyethers, and has a very stable hydration shell. The stability of the hydration shell decreases with increasing temperature. PEG solubility is temperature dependent in water and becomes less soluble as the temperature increases. The lower critical solution temperature dependent on molecular weight, concentration and pH.[9] As the length of PEG decreases, the lower critical solution temperature increases. Salts lower the precipitation temperature of aqueous PEG solutions.[10]

High molecular mass PEGs adopt a helical conformation, while low molecular mass PEGs, which do not form a helix, experience more hydrophobic interactions that control the solution's dynamics. Temperature increases of PEG solutions lowers the solubility of PEG in water, and possibly changes the polymer’s helicity. This trend is due largely to the breaking of the favorable hydrogen bonds that bear the full cost of decreased entropy of solution. Generally the entropy of solution for aqueous PEG is negative, indicating constraints on the water overwhelm the net entropy balance, and the enthalpy of solution of PEG in water is negative, indicating that there are more hydrogen bonding in the solution than in the separated species.[11]

PEG has a stable hydration shell at room temperature, so even in very viscous and concentrated solutions, PEG still promotes bulk-like hydration dynamics. This stable hydration shell is able to maintain hydrogen bond acceptors and donors for water, preserving bulk water interactions. We find that as chain length decreases, hydration shell stability also decreases, which in turn enables a collective slowdown of hydration dynamics. At variable temperatures, we find interesting results in terms of activation energy. For PEG 400 at 5% and 75%, activation energies are similar to neat water. If we were to consider typical viscosity dependence in solutions, the results are much different and give a much

larger activation energy. These results (activation energies experimentally determined to be similar to neat water) indicate that it is probably the polymer is hydrated by bulk-like water.

5.2 Future Direction

It is important that more work be done to understand both the chemical and steric effects crowding has on biological systems. There are many directions in which to take this work that can add to its applicability to biological systems. To make these experiments physiologically relevant, higher temperature conditions and multiple crowding agents in one system can be explored. To accomplish this, experimental crowding studies, experimental temperature studies, and computational explorations are proposed:

Crowding experiments from dilute to saturation with commonly used crowding agents: Ficoll, mannose, sucrose can be done to further understand how different shapes and sizes of crowding agents will chemically and sterically effect biological systems. We can begin to do this by determining the time scale of sensed hydration dynamics for these concentration ranges. The logical next step in this investigation is to conduct crowding experiments with two or more different polymers. In general, crowding environments are not crowded by a large concentration of one type of molecule, but smaller concentrations of a variety of molecules, which constitute an overall crowded environment. It is of interest to look at various combinations of smaller and larger crowding agents first to determine how heterogeneity might affect sensed hydration dynamics. Studies of heterogeneous mixtures of crowding agents, which have not been considered at all in ultrafast dynamical experiments, are particularly important since we expect preferential and cooperative interactions to be pronounced. Finally, since there is virtually no neat water in nature, it is imperative to explore how the addition of salts affects the hydration dynamics of crowded polymer mixtures. Ions play an important role in biology, and are always present at physiological conditions. Different ions have been shown to interact with proteins through different mechanisms, but have been generally found to interact with macromolecular solutes.[12-14] Having a deeper understanding of how these ions interact in

solutions of macromolecular crowding agents without proteins will aid in building a more complete understanding in the case where proteins are crowded with macromolecules.

There are several temperature experiments that can be done to explore how more physiological conditions affect hydration dynamics, as well as temperature ranges that are more extreme. In this dissertation, it was discussed that PEG has an interesting temperature dependence from the perspective of thermodynamics of solubility. Conducting further temperature experiments with longer lengths of PEG with a wider temperature range can provide further information regarding PEG's interesting behaviors at higher temperatures. In experiments at temperatures of 100°C or higher at various lengths of PEG, we can learn how the hydration dynamics are affected as PEG becomes less and less soluble. Also, conducting variable temperature experiments with other commonly used crowding agents in a range from below freezing to over 100° C, with a focus around 37° C can provide information for how the hydration dynamics of these solutions changes at a wide range of temperatures, focusing around a biologically similar temperature. Of course, both of these studies will have to confront practical complications that may arise from scattering that make 2D-IR spectra hard to interpret.

Finally, computer simulations can be used to explore and systematically vary specific variables in these crowded solutions. We can use computational methods to specifically study soft interactions, such as how crowding can affect the electrostatics of binding energy.[15] Specific to the previously described temperature experiments, systematically controlling different variables of crowded aqueous mixtures can add to our understanding of how temperature affects the hydration dynamics. Molecular dynamics simulations enable analyses that are impossible experimentally. We can compute structural and dynamical properties of the water as a function of distance from the polymer. Work along this direction is already under way, and will connect directly to the experimental results in this dissertation.

5.3 References

1. Weiss, M., *Crowding, diffusion, and biochemical reactions*. 1 ed.; Elsevier Inc.: 2014; Vol. 307, p 383-417.

2. Dix, J. A.; Verkman, A. S., Crowding Effects on Diffusion in Solutions and Cells. *Annual Review of Biophysics* **2008,** *37* (1), 247-263.

3. Giesa, T.; Buehler, M. J., Nanoconfinement and the Strength of Biopolymers. *Annual Review of Biophysics* **2013,** *42* (1), 651-673.

4. Kuznetsova, I. M.; Zaslavsky, B. Y.; Breydo, L.; Turoverov, K. K.; Uversky, V. N., Beyond the excluded volume effects: Mechanistic complexity of the crowded milieu. *Molecules* **2015,** *20* (1), 1377-1409.

5. Shahid, S.; Hassan, M. I.; Islam, A.; Ahmad, F., Size-dependent studies of macromolecular crowding on the thermodynamic stability, structure and functional activity of proteins: in vitro and in silico approaches. *Biochimica et Biophysica Acta - General Subjects* **2017,** *1861* (2), 178-197.

6. Roberts, S. T.; Ramasesha, K.; Tokmakoff, A., Structural Rearrangements in Water Viewed Through Two-Dimensional Infrared Spectroscopy. *ACCOUNTS OF CHEMICAL RESEARCH* **2009,** *42* (9), 1239-1249.

7. Perakis, F.; Hamm, P., Two-dimensional infrared spectroscopy of supercooled water. *Journal of Physical Chemistry B* **2011,** *115* (18), 5289-5293.

8. Nicodemus, R. A.; Corecelli, S. A.; Skinner, J. L.; Tokmakoff, A., Collective bond reorganization in water studied with temperature-dependent ultrafast infrared spectroscopy. *J. Phys. Chem. B* **2011,** *115*, 5604-5616.

9. Harris, J. M., Introduction to Biotechnical and Biomedical Applications of Poly(ethylene glycol). In *Poly(ethylene glycol) chemistry: Biotechnical and Biomedical Applications*, Harris, J. M., Ed. Plenum Publishing: New York, 1992; Vol. 1.

10. Bailey Jr., F. E.; Koleske, J. V., *Poly(ethylene oxide)*. Academic Press: New York, 1976; p 184.

11. Kjellander, R. F., Ebba, Water structure and changes in thermal stability of the system poly(ethylene oxide)-water. *Journal of the Chemical Society, Faraday Transactions 1: Phyiscal Chemistry in Condensed Phases* **1981,** *77* (9), 2053-2077.

12. Roy, V. P.; Kubarych, K. J., Interfacial Hydration Dynamics in Cationic Micelles Using 2D-IR and NMR. *Journal of Physical Chemistry B* **2017,** *121* (41), 9621-9630.

13. Zhang, Y.; Cremer, P. S., Interactions between macromolecules and ions: the Hofmeister series. *Current Opinion in Chemical Biology* **2006,** *10* (6), 658-663.

14. Schwierz, N.; Horinek, D.; Netz, R. R., Reversed Anionic Hofmeister Series: The Interplay of Surface Charge and Surface Polarity. *Langmuir* **2010,** *26* (10), 7370-7379.

15. Qi, H. W.; Nakka, P.; Chen, C.; Radhakrishnan, M. L., The effect of macromolecular crowding on the electrostatic component of barnase-barstar binding: A computational, implicit solvent-based study. *PLoS ONE* **2014,** *9* (6).

Appendix A

A.1 PEG 1000k Results

Table A.1 Hydration dynamics probed with the 1972 cm^{-1} band of Ru3C in D_2O/PEG 1000k mixtures. Results are similar to PEG 2000, PEG 8000, and PEG 20,000, in that PEG 1000k in viscous solutions still exhibits bulk like water.

mg/mL PEG 1000k in D_2O	Trial 1	Trial 2
0	1.543 +/- 0.309	
4	1.013 +/- 0.34	
9.6	0.8988 +/- 0.47	
14.8	1.159 +/- 0.39	1.464 +/- 0.22
24.3	1.396 +/- 0.27	
29.8	1.411 +/- 0.25	
33.3	1.321 +/- 0.33	
33.5	1.544 +/- 0.306	
37.2	2.144 +/- 0.13	
40.33	1.57 +/- 0.305	
48.7	1.56 +/- 0.301	1.72 +/- 0.285
54.4	1.53 +/- 0.605	
61	1.594 +/- 0.305	